Project title: Inorganic-Organic Molecules and Solids with Nanometer-Sized Pores

DE-FG02-01ER15267

Andrew W. Maverick, PI

Final technical report for the period 09/01/2005-08/31/2008

We are constructing porous inorganic-organic hybrid molecules and solids, many of which contain coordinatively unsaturated metal centers. In this work, we use multifunctional β-diketone ligands as "building blocks" to prepare extended-solid and molecular porous materials that are capable of reacting with a variety of guest molecules.

(a) Extended solids. We have studied the reaction of the trigonal iron(III) complex $Fe(Pyac)_3$ with $AgNO_3$ to produce nanoporous bimetallic crystalline solids, $[Fe(Pyac)_3]_2[AgNO_3]_3(G)_n$, "$Ag_3Fe_2$", as shown in Figure 1 (pores ~18 x 21 Å), with a variety of guests G. We have also demonstrated that the guests can be exchanged in single-crystal-to-single-crystal transformations.

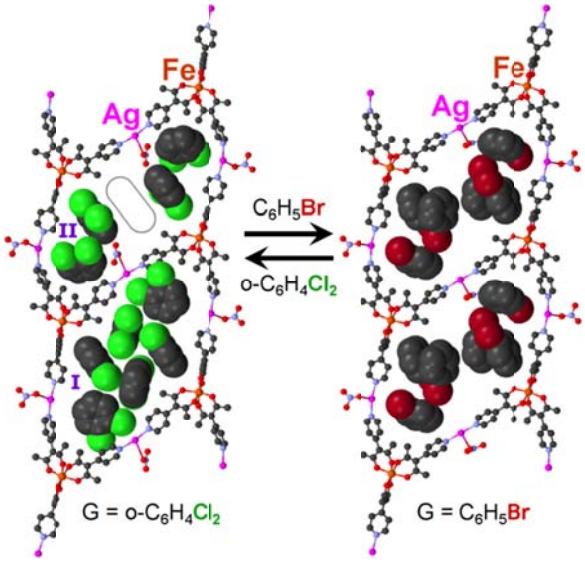

Figure 1. Structures of MOFs $[Fe(Pyac)_3]_2[AgNO_3]_3(G)_n$., and guest exchange reactions. Left: G = 1,2-dichlorobenzene; Right: G = bromobenzene,

We are also preparing building blocks that will be suitable for constructing porous solids with more robust 3D structures. To do this, we are concentrating on the mixed isocyanide–β-diketone ligand HacphNC (see Figure 2). This bifunctional ligand has both "hard" (O) and "soft" (C) moieties. Reaction of this ligand with harder metal ions (Cu^{2+}, Zn^{2+}, Al^{3+}) occurs at the O atoms, generating species such as $Al(acphNC)_3$ (see Figure 3). With softer metal atoms, such as Au, reaction occurs at C. We are now studying the reaction of the free HacphNC ligand and its complexes with softer metals, such as Fe(II), Re(I), and Rh(I)). The goal is 3D structures containing both soft (C-bound) and hard (O-bound) metal ions.

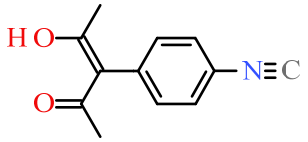

Figure 2. The isocyano-β-diketone HacphNC.

Figure 3. Structure of $Al(acphNC)_3$.

(b) Molecular species. We have made progress with both bis- and tris(β-diketones). In the first area, we previously reported the chemistry of *m*-phenylenebis(β-diketones) (see Figure

4), which react with Cu^{2+} to produce molecular squares.

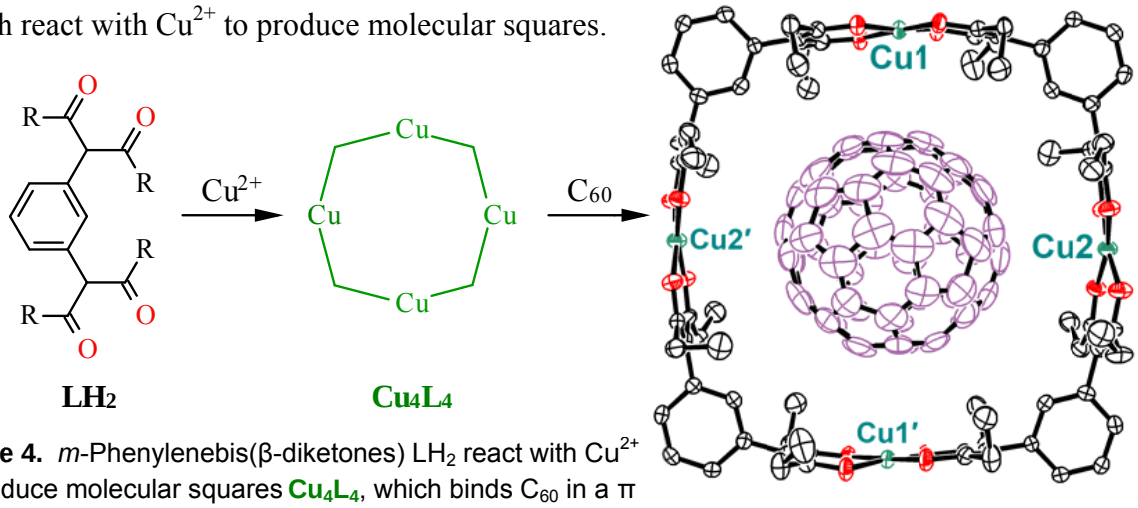

Figure 4. *m*-Phenylenebis(β-diketones) LH_2 react with Cu^{2+} to produce molecular squares **Cu_4L_4**, which binds C_{60} in a π fashion.

A study of σ and π coordination of guest molecules inside and outside these squares is continuing. This includes the following aspects: (a) binding of guests such as 4,4′-bpy, which distorts the squares by bringing two opposite Cu atoms much closer than the remaining unbound Cu atoms; (b) effects of changes in the R groups in the β-diketones on the solubility of the resulting molecular squares (for example, if R = C_5H_{11}, the squares are readily soluble in solvents such as toluene and THF); and (c) effects of *exo* and *endo* substituents on the aromatic ring in LH_2. In the latter experiments, we have recently shown that *endo*-OCH_3 substituents inhibit binding of both σ and π guests.

Meanwhile, we also studied the analogous *ortho* isomer, *o*-$pbaH_2$. Based on the 60° angle between its β-diketone moieties, *o*-$pbaH_2$ was expected to produce trimers, M_3(*o*-pba)$_3$. However, the actual product is the more highly strained dimer Cu_2(*o*-pba)$_2$ (see Figure 5). This dimer is green in solution, but it forms crystals that are either green, orange, blue, or purple, depending on the method of crystallization.

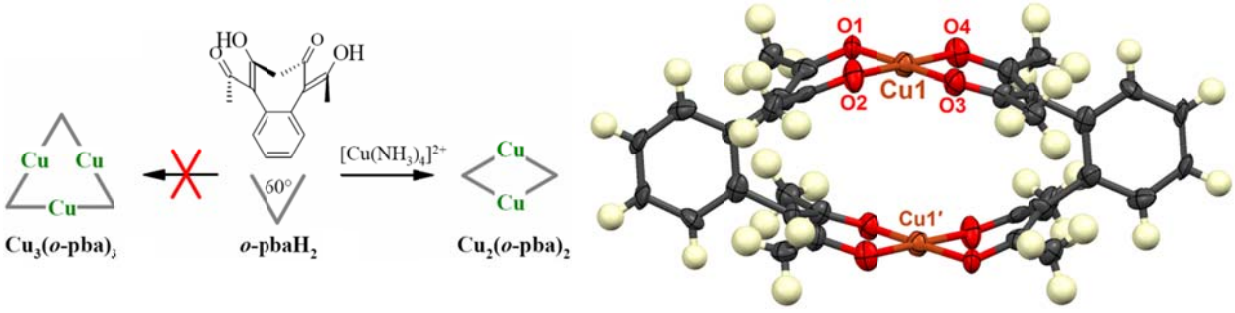

Figure 5. The *o*-phenylenebis(β-diketone) *o*-$pbaH_2$ reacts with Cu^{2+} to produce the strained dimer **Cu_2(o-pba)$_2$**, whose structure is shown at right (and not the expected trimer Cu_3(*o*-pba)$_3$).

We have also prepared tris(β-diketone) ligands, including the silicon-based compounds shown in Figure 6. These ligands yield metal complexes that are soluble in a broader range of solvents (including THF, benzene, and toluene) than species we had previously prepared. A study of Rh and Ir complexes has been published (paper #6), and these are well-behaved. On the other hand, the Cu(II) complexes of these ligands are more complicated. We believe the

products include polyhedral species such as $[Cu_3L_2]_n$ (n = 4, cube; n = 8, decahedron; n = 10, dodecahedron). A study of these compounds utilizing AFM measurements is in progress and will be submitted for publication soon.

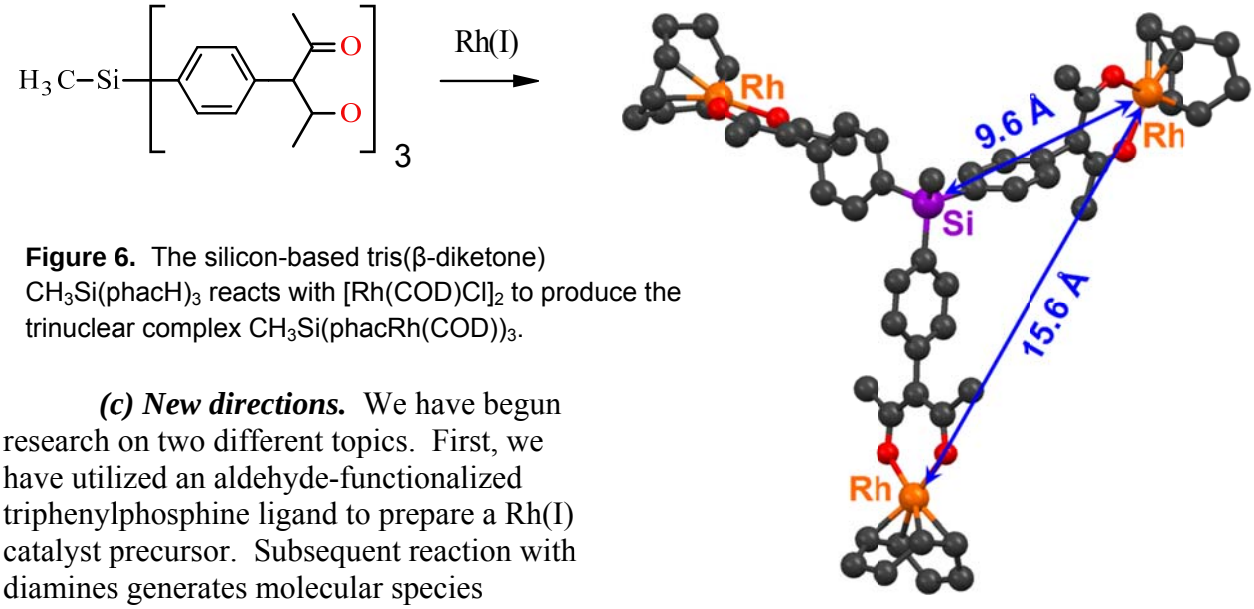

Figure 6. The silicon-based tris(β-diketone) $CH_3Si(phacH)_3$ reacts with $[Rh(COD)Cl]_2$ to produce the trinuclear complex $CH_3Si(phacRh(COD))_3$.

(c) New directions. We have begun research on two different topics. First, we have utilized an aldehyde-functionalized triphenylphosphine ligand to prepare a Rh(I) catalyst precursor. Subsequent reaction with diamines generates molecular species including a Rh-centered supramolecular structure (see Figure 7). We expect that in these compounds, the Rh will serve as a catalyst precursor, while the imine arms (=N–Y–N=) will control access to the catalytic site.

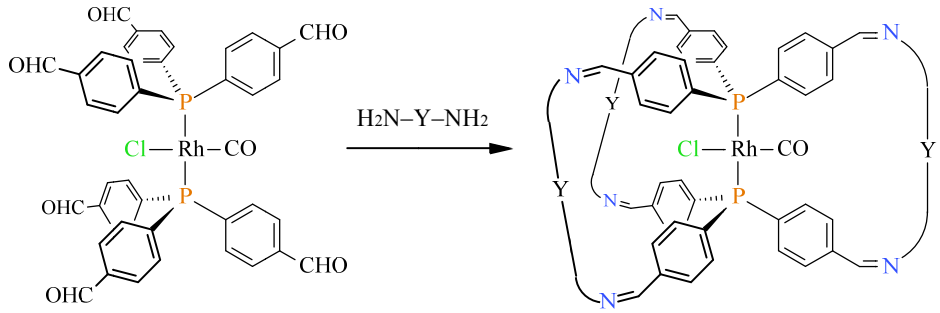

Figure 7. Aldehyde-functionalized $Rh(PPh_3)_2(CO)Cl$ condenses with diamines to make a supramolecular structure that is now being investigated as a catalyst precursor.

The second new direction is based on our structural studies of β-diketonate complexes, which often show coordination in a "bent" fashion, leading to distortions in the complexes and sometimes to the "wrong" product in supramolecular complex formation. Crystal-structure data suggest that N-containing ligands (e.g. 2,2′-bpy) are less likely to coordinate to metals in a distorted manner. Thus, we have explored multifunctional chelating N ligands as supramolecular building blocks. In our preliminary results (Figure 8), a chelating pyridyltriazole ligand yields an undistorted *trans* complex on reaction with Ni^{2+}. We are now extending the work to multifunctional pyridyltriazoles and their coordination polymers.

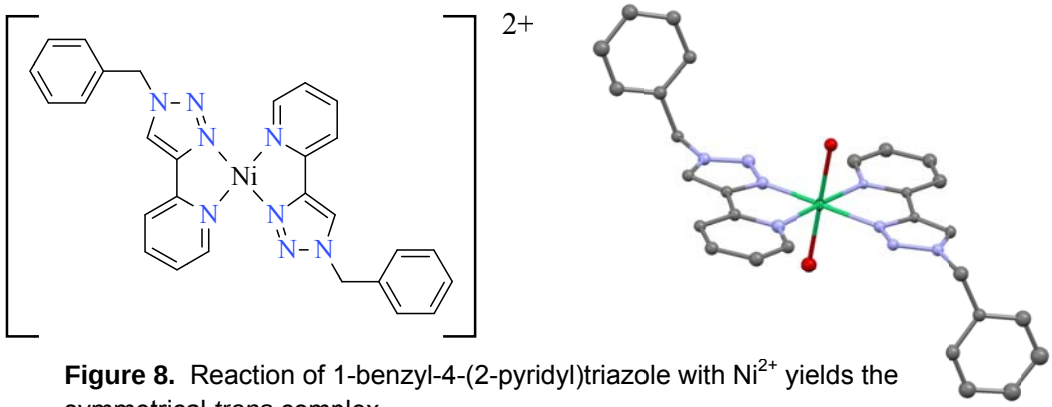

Figure 8. Reaction of 1-benzyl-4-(2-pyridyl)triazole with Ni^{2+} yields the symmetrical *trans* complex.

Publications acknowledging this grant

1. "Copper β-diketonate molecular squares and their host-guest reactions"; Pariya, C.; Sparrow, C. R.; Back, C. K.; Sandí, G.; Fronczek, F. R.; Maverick, A. W. *Angew. Chem., Int. Ed.* **2007,** *46*, 6305-6308.
2. "A molecular corner: *fac*-tricarbonylchlorido-bis[3-(4-pyridyl)pentane-2,4-dione-κ*N*]rhenium(I) chloroform solvate"; Kakoullis, J.; Maverick, A. W.; Fronczek, F. R. *Acta Crystallogr. Sect. E: Struct. Rep. Online* **2007,** *63*, m1360-m1361.
3. "A cofacial binuclear copper(II) complex with a bridging 1,4-dithiane ligand"; Burton, S.; Fronczek, F. R.; Maverick, A. W. *Acta Crystallogr. Sect. E: Struct. Rep. Online* **2007,** *63*, m1977-m1978.
4. "3,5-Diacetyl-2,6-heptanedione"; Burton, S.; Fronczek, F. R.; Maverick, A. W. *Acta Crystallogr. Sect. E: Struct. Rep. Online* **2007,** *63*, o3108.
5. "A nanoporous Ag-Fe mixed-metal-organic framework exhibiting single-crystal-to-single-crystal transformations upon guest exchange"; Zhang, Y.; Chen, B.; Fronczek, F. R.; Maverick, A. W. *Inorg. Chem.* **2008**, *47*, 4433-4435.
6. "Organosilicon-based multifunctional β-diketones and their rhodium and iridium complexes"; Pariya, C.; Marcos, Y. S.; Zhang, Y.; Fronczek, F. R.; Maverick, A. W. *Organometallics*, **2008**, *27*, 4318-4324.
7. "Preparation of an isocyano-β-diketone via its Al, Zn, and Cu complexes, by use of metal ions as protecting groups"; Zhang, Y.; Maverick, A. W. *Inorg. Chem.* **2009**, *48*, 10512-10518.
8. "Bis(*o*-phenylenebis(acetylacetonato))dicopper(II): a Strained Copper(II) Dimer Exhibiting a Wide Range of Colors in the Solid State"; Pariya, C.; Fronczek, F. R.; Maverick, A. W. *Inorg. Chem.* **2011**, *50*, 2748-2753.

(Two additional papers in preparation)

Contents

Supramolecular Chemistry

C. Pariya, C. R. Sparrow, C.-K. Back, G. Sandí, F. R. Fronczek, A. W. Maverick* _____ **6305 – 6308**

Copper β-Diketonate Molecular Squares and Their Host–Guest Reactions

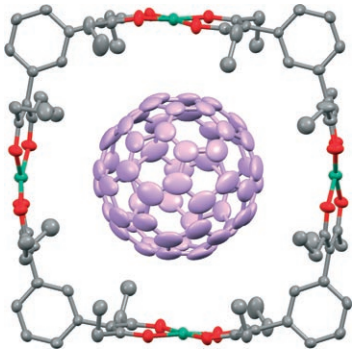

All square: Treatment of *m*-phenylene-bis(β-diketones) with $[Cu(NH_3)_4]^{2+}$ yields molecular squares rather than the expected hexagons. The squares react readily with guests such as C_{60} (see structure) and 4,4′-bipyridine. They are also effective for the storage of H_2 gas, both at 77 K and at room temperature.

Supramolecular Chemistry

DOI: 10.1002/anie.200701252

Copper β-Diketonate Molecular Squares and Their Host–Guest Reactions**

*Chandi Pariya, Christopher R. Sparrow, Chang-Keun Back, Giselle Sandí, Frank R. Fronczek, and Andrew W. Maverick**

In the field of porous supramolecular metal complexes, both molecular[1] and extended-solid[2] materials have been extensively studied in recent years. These materials are attractive due to their applications in gas storage[3] and host–guest chemistry.[4] Among the most often studied of these species are the metal-containing "molecular squares", that is, square-shaped porous tetrameric structures. These have been prepared by several approaches, the most common being the reaction of an organic bridging ligand with a metal complex that has available *cis* coordination sites (Figure 1 a). The bridging ligand is frequently a pyridine derivative (for example, 4,4′-bipyridine (4,4′-bpy)),[5] although bis-chelating ligands have also been used.[6] In these cases, the 90° "corners" in the molecular squares are provided by metal complexes. The resulting metal centers are usually coordinatively saturated, which makes it difficult for guest molecules to interact directly with the metal atoms. Herein we report molecular squares prepared by an alternative approach, in which bifunctional organic moieties serve as the "corners" and join metal atoms in the centers of the "sides" (Figure 1 b).[7] These molecular squares are formed in one step, by reaction of bis(β-diketone) ligands (**1**) with $[Cu(NH_3)_4]^{2+}$ (Scheme 1). The new squares (**2**) are capable of binding guests in both a σ (for example, 4,4′-bpy) and π fashion (for example, C_{60}), and they are also surprisingly effective for hydrogen-gas storage, both at 77 K and at room temperature.

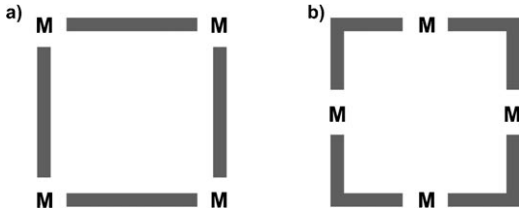

Figure 1. Schematic illustration of metal-organic molecular squares, assembled from: a) linear organic linkers and 90° metal units, or b) linear metal units and organic "corners".

Ligands **1a** and **1b** were synthesized by reaction of isophthalaldehyde with 2,2,2-trimethoxy-4,5-dimethyl-1,3,2-dioxaphospholene and 2,2,2-trimethoxy-4,5-diethyl-1,3,2-dioxaphospholene, respectively, at room temperature and heating the intermediate in methanol under nitrogen.[8] Mixing solutions of **1a** or **1b** in CH_2Cl_2 with aqueous $[Cu(NH_3)_4]^{2+}$ produces **2a** or **2b**, respectively, which can be isolated as dark green solids in approximately 95% yield.

The angles between the two β-diketone moieties in the new ligands **1** are about 120°. Thus, we anticipated that their reaction with metal ions would yield hexamers, for example, $[M_6(m\text{-pba})_6]$. However, X-ray analysis of the crystalline products **2**, which are formed in nearly quantitative yield, shows that they are actually molecular squares, with diameters of about 14 Å (Figure 2).[9] (We explored a variety of conditions for preparing **2**, but found no evidence of other oligomers.) Thus, **2a** and **2b** are unusual examples of molecular squares in which the corners are organic bridging groups, and the metal atoms are in the centers of the sides.

The angles between the β-diketone moieties in the structures of **2a** and **2b** are still approximately 120°. To accommodate this angle within an overall square shape, there must be some distortion elsewhere in the molecule. The two ligands are coplanar with the metal atoms in an undistorted [Cu(β-diketonate)$_2$] complexes,[10] while, in the present squares, the ligands are all bent away from coplanarity.

The formation of squares, despite the "incorrect" angle between the β-diketonate moieties, may be due to two factors. For example, of the reactions shown in Equations (1) and (2)

$$4\,Cu^{2+} + 4\,m\text{-pba}^{2-} \rightleftharpoons [Cu_4(m\text{-pba})_4] \quad (1)$$

$$6\,Cu^{2+} + 6\,m\text{-pba}^{2-} \rightleftharpoons [Cu_6(m\text{-pba})_6] \quad (2)$$

reaction (1) is expected to be favored on entropy grounds. Although self-assembly of *cis* square-planar or octahedral metal coordination units with linear linkers normally yields molecular squares, several examples have been reported in which significant quantities of trimeric products (that is, molecular triangles) form.[11] Studies of supramolecular self-assembly have measured the entropy change that favors the

[*] Dr. C. Pariya, C. R. Sparrow, Dr. F. R. Fronczek, Prof. Dr. A. W. Maverick
Department of Chemistry
Louisiana State University
Baton Rouge, LA 70803-1804 (USA)
Fax: (+1) 225-578-3458
E-mail: maverick@lsu.edu
Homepage: http://chemistry.lsu.edu
Dr. C.-K. Back, Dr. G. Sandí
Chemistry Division
Argonne National Laboratory
9700 South Cass Avenue, Argonne IL 60439 (USA)

[**] We thank the U.S. Department of Energy (DE-FG02-01ER15267, to A.W.M.; DE-AC02-06CH11357, to G.S.) and the ACS-PRF (37234-AC3, to A.W.M.) for support. Additional support was provided by the NSF (CMC-IGERT, DGE-9987603, to C.R.S.) and the Louisiana Board of Regents (LEQSF(1999-2000)-ENH-TR-13, for the X-ray diffractometer). We thank Dr. R. M. Strongin and Dr. K. K. Kim for assistance with synthetic procedures.

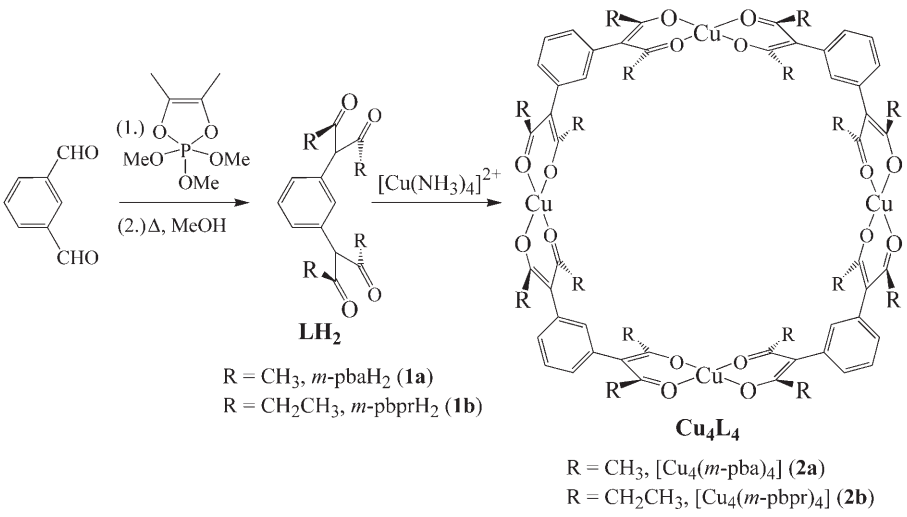

R = CH_3, *m*-pbaH$_2$ (**1a**)
R = CH_2CH_3, *m*-pbprH$_2$ (**1b**)

R = CH_3, [Cu_4(*m*-pba)$_4$] (**2a**)
R = CH_2CH_3, [Cu_4(*m*-pbpr)$_4$] (**2b**)

Scheme 1. Synthesis of *m*-phenylenebis(β-diketones) **1** and their copper(II) molecular squares **2**.

(bringing the *endo*-coordinated Cu atoms closer together, and the *exo*-coordinated ones farther apart), as do the larger Cu–N bond lengths for the internally bound bpy guest. Reaction of **2** with other pyridine derivatives leads to similar color changes, thus indicating Cu–N coordination.

We studied fullerenes as examples of π-binding guests. Numerous hosts have been reported that bind fullerenes, but only a few of these function by wrapping completely around the guest. One such example is the cofacial diporphyrins reported by Tashiro and Aida.[15] The present molecular squares **2** readily bind

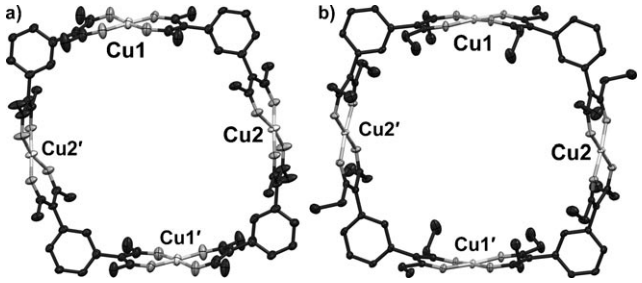

Figure 2. Crystal structure of β-diketonate molecular squares. H atoms and solvent molecules omitted for clarity; ellipsoids shown at 50%. a) [Cu_4(*m*-pba)$_4$] (**2a**), Cu1···Cu1′ 14.317(1) Å; Cu2···Cu2′ 14.647(1) Å. b) [Cu_4(*m*-pbpr)$_4$] (**2b**), Cu1···Cu1′ 14.012(1) Å; Cu2···Cu2′ 14.661(1) Å.

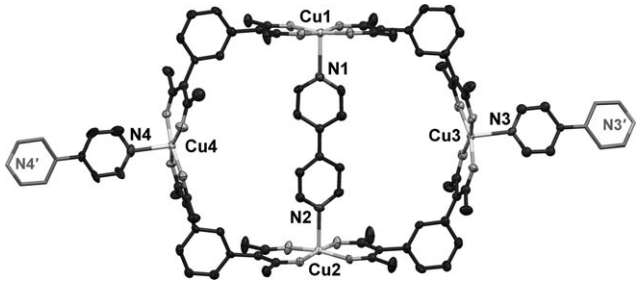

Figure 3. Crystal structure of [Cu_4(*m*-pba)$_4$(4,4′-bpy)$_2$]$_n$ (**3a**). H atoms and solvent molecules omitted for clarity; ellipsoids shown at 50%. Cu1···Cu2 11.807(1), Cu3···Cu4 16.226(1), Cu1-N1 2.360(8), Cu2-N2 2.363(8), Cu3-N3 2.251(7), Cu4-N4 2.250(8) Å. (Inversion-related portions of the 4,4′-bpy molecules at N3 and N4 are shown in a lighter shade, without ellipsoids.)

formation of smaller cyclic oligomers over larger ones.[12] Second, the formation of smaller cyclic products can be favored kinetically: Lehn and co-workers reported that the initial reaction of Cu^I ions with a polypyridine ligand produced a cyclic mononuclear species, followed by rearrangement to the more stable trinuclear supramolecular product.[13] In their case, this was possible because a coordinating solvent was chosen, which permits ligand dissociation/reassociation. In contrast, the compounds reported here are soluble only in noncoordinating solvents such as CH_2Cl_2 and $CHCl_3$. Dissociation in these solvents would lead to unstable ionic intermediates, thus making it difficult for [Cu_4(*m*-pba)$_4$] to rearrange into higher oligomers that might be more stable.

Squares **2** react with several types of guest molecules. For example, **2a** reacts with 4,4′-bpy to produce the turquoise polymeric complex [Cu_4(*m*-pba)$_4$(4,4′-bpy)$_2$]$_n$ (**3a**, Figure 3).[14] In this compound the 4,4′-bpy molecules are intra- and intermolecularly bonded to the molecular square. The Cu···Cu distances in the undistorted squares **2a** are longer than normally observed in 4,4′-bpy-bridged complexes (ca. 10 Å). However, in **3a**, the 4,4′-bpy guest is accommodated by means of smaller distortions at the Cu1 and Cu2 atoms (as compared to those found in **2a** and **2b**) and larger distortions at the Cu3 and Cu4 atoms. The square-pyramidal environment around the Cu atoms favors both changes fullerenes C_{60} and C_{70} in solvents such as chlorobenzene, as evident from UV/Vis spectral changes on mixing. The C_{60} adduct of **2b**, that is, [Cu_4(*m*-pbpr)$_4$·C_{60}] (**4b**), formed crystals that were suitable for X-ray analysis. The structure (Figure 4)[16] shows two interesting features: the ethyl

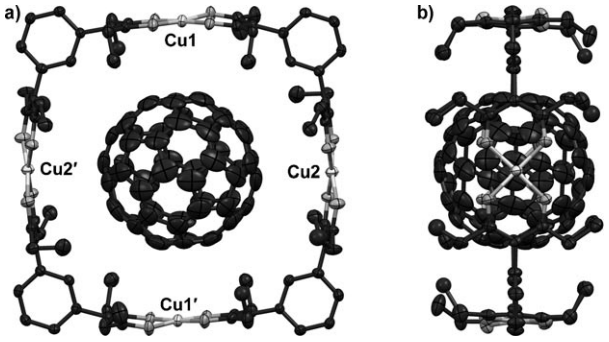

Figure 4. Crystal structure of [Cu_4(*m*-pbpr)$_4$·C_{60}] (**4b**): a) Front view and b) side view. H atoms and solvent molecules omitted for clarity; ellipsoids shown at 50%. Cu1···Cu1′ 13.955(1) Å; Cu2···Cu2′ 14.060(1) Å.

groups from the *m*-pbpr ligands are all oriented toward the C_{60} guest; and the Cu···Cu distances (13.96 and 14.06 Å) are slightly smaller than in the solvated host (**2b**, Figure 2). These structural features suggest that weak attractions between the C_{60} molecule and the C–H bonds and Cu-O-C π systems of the host stabilize the host–guest adduct.

The crystal structures of **2a**, **2b**, and **4b** are all similar, with the Cu_4L_4 squares arranged in parallel so as to create "channels" (see the crystallographic data in the Supporting Information); in **2a** and **2b**, the channels are filled with solvent. This similarity of the structures suggested that it might be possible to remove the solvents from **2** and use the "empty" crystals for gas-storage experiments. However, heating **2** or placing it under vacuum to remove the solvents results in a loss of crystallinity, thus making it impossible to do this experiment directly. Still, even noncrystalline unsolvated **2** cannot pack efficiently and should therefore remain porous; thus, it might serve as a host for gas adsorption. For example, Sudik et al. have recently reported gas-storage properties of "metal-organic polyhedra" as noncrystalline solids.[17] Accordingly, samples of **2a** and **2b** that had been heated to 100 °C under vacuum overnight were used for H_2 adsorption experiments.[18] The results obtained at room temperature and $P_{H_2} = 75$ atm were 0.65 % (**2a**) and 0.56 % w/w (**2b**), which correspond to approximately 4.3 and 4.4 molecules of H_2 per molecule of **2a** and **2b**, respectively. Greater adsorption was observed at 77 K and $P_{H_2} = 43$ atm: 4.3 % (**2a**) and 4.2 % w/w (**2b**). These values are among the best recorded for porous metal-organic compounds,[19] and they demonstrate that noncrystalline, molecular hosts can function effectively in H_2 adsorption.

The present study reports the complexation behavior of the new bis(β-diketone) ligands **1** with copper(II) ions to yield molecular squares **2**. The supramolecular product in these reactions is obtained in high yield in a simple room-temperature reaction. The molecular squares **2** function effectively as hosts for guests that bind through σ- (4,4′-bpy), π- (C_{60}), and van der Waals (H_2) interactions. We are now exploring the reactions of **2** and related hosts in more detail, as well as the assembly of supramolecular hosts from other multidentate β-diketone ligands.

Experimental Section

The preparation of the new bis(β-diketones) **1a** and **1b** is described in the Supporting Information.

2a: A solution of $[Cu(NH_3)_4]^{2+}$ was prepared from $CuSO_4 \cdot 5H_2O$ (0.35 g, 1.4 mmol) in H_2O (10 mL) by slow addition of conc. aqueous NH_3. A solution of **1a** (0.275 g, 1.00 mmol) in CH_2Cl_2 (20 mL), was then added and the mixture was stirred for 6 h. More CH_2Cl_2 (20 mL) was then added, and the organic layer was collected and dried over $MgSO_4$. The residue was washed with hexane (2 × 10 mL) and dried in air. Yield: 0.325 g (96 %). Elemental analysis calcd for $C_{64}H_{64}O_{16}Cu_4$ ($M_r = 1343.40$): C 57.22, H 4.80; found: C 57.43, H 4.69. **2b** was prepared by a similar method; yield: 95 %. Elemental analysis calcd for $C_{80}H_{96}O_{16}Cu_4$ ($M_r = 1567.80$): C 61.29, H 6.17; found: C 61.08, H 6.00. Single crystals of these two compounds suitable for X-ray analysis were obtained by layering solutions in CH_2Cl_2 and $CHCl_3$ with hexane and benzene, respectively.

3a: A solution of **2a** (34 mg, 0.025 mmol) and 4,4′-bpy, (16 mg, 0.102 mmol) in $CHCl_3$ (3 mL) was layered with a mixture of CH_2Cl_2 (5 mL) and toluene (10 mL) at −20 °C. After two days, green crystals appeared. The crystals lost solvent rapidly in air to give a light green powder. Yield: 35 mg (84 %). Elemental analysis calcd for $C_{84}H_{80}N_4Cu_4O_{16}$ ($M_r = 1655.74$): C 60.93, H 4.87, N 3.38; found: C 60.76, H 4.78, N 3.10. Crystals were attached to glass fibers and quickly cooled to 110 K for X-ray analysis.

4b: A solution of **2b** (25 mg, 0.015 mmol) in $CHCl_3$ (2 mL) was layered with a mixture of $CHCl_3$ and 1,2-dichlorobenzene (1:1, 1 mL) and then with a solution of C_{60} (15 mg, 0.021 mmol) in 1,2-dichlorobenzene (5 mL). Dark brown crystals had formed after several days. These crystals also lost solvent rapidly, but they could be mounted quickly and cooled to 110 K for X-ray analysis. The overall yield after drying was 21 mg of dark brown powder, but analytically pure material could not be obtained by this procedure.

X-ray analyses were performed on a Nonius KappaCCD diffractometer (MoK_α radiation, $\lambda = 0.71073$ Å) equipped with an Oxford Cryosystems Cryostream. CCDC-640918–640923 (compounds **1a**, **1b**, **2a**·$2CH_2Cl_2$, **2b**·$6CHCl_3 \cdot 3C_6H_6$, **3a**·$17.26CHCl_3 \cdot 1.74CH_2Cl_2 \cdot 0.5H_2O$, and **4b**·$2CHCl_3 \cdot 3C_6H_4Cl_2$, respectively) contain the supplementary crystallographic data for this paper. These data can be obtained free of charge from The Cambridge Crystallographic Data Centre via www.ccdc.cam.ac.uk/data_request/cif.

Received: March 21, 2007
Published online: July 19, 2007

Keywords: copper · fullerenes · host–guest systems · hydrogen storage · supramolecular chemistry

[1] a) M. Eddaoudi, J. Kim, J. B. Wachter, H. K. Chae, M. O'Keeffe, O. M. Yaghi, *J. Am. Chem. Soc.* **2001**, *123*, 4368; b) S. R. Seidel, P. J. Stang, *Acc. Chem. Res.* **2002**, *35*, 972; c) V. Maurizot, M. Yoshizawa, M. Kawano, M. Fujita, *Dalton Trans.* **2006**, 2750.

[2] a) O. M. Yaghi, M. O'Keeffe, N. W. Ockwig, H. K. Chae, M. Eddaoudi, J. Kim, *Nature* **2003**, *423*, 705; b) C. Janiak, *Dalton Trans.* **2003**, 2781; c) S. Kitagawa, R. Kitaura, S. Noro, *Angew. Chem.* **2004**, *116*, 2388; *Angew. Chem. Int. Ed.* **2004**, *43*, 2334; ; d) C. N. R. Rao, S. Natarajan, R. Vaidhyanathan, *Angew. Chem.* **2004**, *116*, 1490; *Angew. Chem. Int. Ed.* **2004**, *43*, 1466; ; e) D. Bradshaw, J. B. Claridge, E. J. Cussen, T. J. Prior, M. J. Rosseinsky, *Acc. Chem. Res.* **2005**, *38*, 273; f) G. Férey, C. Mellot-Draznieks, C. Serre, F. Millange, *Acc. Chem. Res.* **2005**, *38*, 217.

[3] a) D. N. Dybtsev, H. Chun, K. Kim, *Angew. Chem.* **2004**, *116*, 5143; *Angew. Chem. Int. Ed.* **2004**, *43*, 5033; ; b) L. Pan, M. B. Sander, X. Y. Huang, J. Li, M. Smith, E. Bittner, B. Bockrath, J. K. Johnson, *J. Am. Chem. Soc.* **2004**, *126*, 1308; c) X. B. Zhao, B. Xiao, A. J. Fletcher, K. M. Thomas, D. Bradshaw, M. J. Rosseinsky, *Science* **2004**, *306*, 1012; d) J. L. C. Rowsell, O. M. Yaghi, *Angew. Chem.* **2005**, *117*, 4748; *Angew. Chem. Int. Ed.* **2005**, *44*, 4670; e) S. K. Bhatia, A. L. Myers, *Langmuir* **2006**, *22*, 1688; f) H. Frost, T. Duren, R. Q. Snurr, *J. Phys. Chem. B* **2006**, *110*, 9565.

[4] a) J. A. Whiteford, P. J. Stang, S. D. Huang, *Inorg. Chem.* **1998**, *37*, 5595; b) K. Schlichte, T. Kratzke, S. Kaskel, *Microporous Mesoporous Mater.* **2004**, *73*, 81; c) M. Albrecht, I. Janser, S. Burk, P. Weis, *Dalton Trans.* **2006**, 2875; d) Y. Kobayashi, M. Kawano, M. Fujita, *Chem. Commun.* **2006**, 4377.

[5] a) M. Fujita, J. Yazaki, K. Ogura, *J. Am. Chem. Soc.* **1990**, *112*, 5645; b) P. J. Stang, D. H. Cao, S. Saito, A. M. Arif, *J. Am. Chem. Soc.* **1995**, *117*, 6273; c) R. V. Slone, J. T. Hupp, C. L. Stern, T. E. Albrecht-Schmitt, *Inorg. Chem.* **1996**, *35*, 4096.

[6] a) Y. S. Zhang, S. N. Wang, G. D. Enright, S. R. Breeze, *J. Am. Chem. Soc.* **1998**, *120*, 9398; b) F. A. Cotton, C. Lin, C. A. Murillo, *Inorg. Chem.* **2001**, *40*, 478.

[7] Metal-organic supramolecules have been reported previously in which the organic moieties serve as the "corners"; see, for

example, a) J. R. Hall, S. J. Loeb, G. K. H. Shimizu, G. P. A. Yap, *Angew. Chem.* **1998**, *110*, 130; *Angew. Chem. Int. Ed.* **1998**, *37*, 121; b) M. Roitzsch, B. Lippert, *Angew. Chem.* **2006**, *118*, 153; *Angew. Chem. Int. Ed.* **2006**, *45*, 147; c) H. B. Yang, N. Das, F. H. Huang, A. M. Hawkridge, D. D. Diaz, A. M. Arif, M. G. Finn, D. C. Muddiman, P. J. Stang, *J. Org. Chem.* **2006**, *71*, 6644; d) S. B. Zhao, R. Y. Wang, S. Wang, *J. Am. Chem. Soc.* **2007**, *129*, 3092. However, these metallacycles typically contain square-planar d^8 metals, which have low affinity for the direct binding of guest molecules.

[8] a) F. Ramirez, A. V. Patwardhan, N. Ramanathan, N. B. Desai, C. V. Greco, S. R. Heller, *J. Am. Chem. Soc.* **1965**, *87*, 543; b) F. Ramirez, S. B. Bhatia, A. V. Patwardhan, C. P. Smith, *J. Org. Chem.* **1967**, *32*, 3547.

[9] Crystal data for **2a**·2 CH_2Cl_2 (M_r = 1513.24): Triclinic, space group $P\bar{1}$, T = 105 K, a = 7.577(3), b = 16.419(6), c = 17.423(7) Å; α = 110.17(3), β = 92.57(2), γ = 92.063(15)°; V = 2029.5(14) Å^3; Z = 1; ρ_{calcd} = 1.251 Mg m^{-3}; R = 0.066, wR = 0.193. Crystal data for **2b**·6 $CHCl_3$·3 C_6H_6 (M_r = 2518.26): Triclinic, space group $P\bar{1}$, T = 110 K, a = 9.316(2), b = 16.726(4), c = 18.743(5) Å; α = 78.619(13), β = 86.943(13), γ = 83.472(9)°; V = 2843.1 (12) Å^3; Z = 1; ρ_{calcd} = 1.471 Mg m^{-3}; R = 0.062, wR = 0.183.

[10] a) S. S. Turner, D. Collison, F. E. Mabbs, M. Helliwell, *J. Chem. Soc. Dalton Trans.* **1997**, 1117; b) B. L. Chen, F. R. Fronczek, A. W. Maverick, *Chem. Commun.* **2003**, 2166.

[11] a) M. Fujita, O. Sasaki, T. Mitsuhashi, T. Fujita, J. Yazaki, K. Yamaguchi, K. Ogura, *Chem. Commun.* **1996**, 1535; b) X. Y. Yu, M. Maekawa, M. Kondo, S. Kitagawa, G. X. Jin, *Chem. Lett.* **2001**, 168.

[12] a) T. Yamamoto, A. M. Arif, P. J. Stang, *J. Am. Chem. Soc.* **2003**, *125*, 12309; b) F. A. Cotton, C. A. Murillo, R. M. Yu, *Dalton Trans.* **2006**, 3900.

[13] N. Fatin-Rouge, S. Blanc, A. Pfeil, A. Rigault, A. M. Albrecht-Gary, J.-M. Lehn, *Helv. Chim. Acta* **2001**, *84*, 1694.

[14] Crystal data for **3a**·17.26 $CHCl_3$·1.74 CH_2Cl_2·0.5 H_2O (M_r = 3872.89): Triclinic, space group $P\bar{1}$, T = 110 K, a = 14.824(3), b = 19.384(4), c = 29.616(6) Å; α = 99.043(8), β = 97.751(11), γ = 101.782(9)°; V = 8104(3) Å^3; Z = 2; ρ_{calcd} = 1.587 Mg m^{-3}; R = 0.088, wR = 0.253.

[15] K. Tashiro, T. Aida, *Chem. Soc. Rev.* **2007**, *36*, 189.

[16] Crystal data for **4b**·2 $CHCl_3$·3 $C_6H_4Cl_2$ (M_r = 2968.04): Triclinic, space group $P\bar{1}$, T = 110 K, a = 9.933(3), b = 18.397(7), c = 18.481(6) Å; α = 93.695(15), β = 104.441(18), γ = 92.017(14)°, V = 3259.1(19) Å^3; Z = 1; ρ_{calcd} = 1.512 Mg m^{-3}; R = 0.065, wR = 0.176.

[17] A. C. Sudik, A. R. Millward, N. W. Ockwig, A. P. Cote, J. Kim, O. M. Yaghi, *J. Am. Chem. Soc.* **2005**, *127*, 7110.

[18] C.-K. Back, G. Sandí, J. Prakash, J. Hranisavljevic, *J. Phys. Chem. B* **2006**, *110*, 16225.

[19] a) G. Férey, M. Latroche, C. Serre, F. Millange, T. Loiseau, A. Percheron-Guegan, *Chem. Commun.* **2003**, 2976; b) D. N. Dybtsev, H. Chun, S. H. Yoon, D. Kim, K. Kim, *J. Am. Chem. Soc.* **2004**, *126*, 32; c) B. L. Chen, N. W. Ockwig, A. R. Millward, D. S. Contreras, O. M. Yaghi, *Angew. Chem.* **2005**, *117*, 4823; *Angew. Chem. Int. Ed.* **2005**, *44*, 4745; ; d) M. Dinca, J. R. Long, *J. Am. Chem. Soc.* **2005**, *127*, 9376; e) T. Sagara, J. Ortony, E. Ganz, *J. Chem. Phys.* **2005**, *123*, 214707; f) D. F. Sun, S. Q. Ma, Y. X. Ke, D. J. Collins, H. C. Zhou, *J. Am. Chem. Soc.* **2006**, *128*, 3896; g) B. Xiao, P. S. Wheatley, X. Zhao, A. J. Fletcher, S. Fox, A. G. Rossi, I. L. Megson, S. Bordiga, L. Regli, K. M. Thomas, R. E. Morris, *J. Am. Chem. Soc.* **2007**, *129*, 1203.

Acta Crystallographica Section E
Structure Reports Online
ISSN 1600-5368

A molecular corner: *fac*-tricarbonylchlorido-bis[3-(4-pyridyl)pentane-2,4-dione-κN]rhenium(I) chloroform solvate

James Kakoullis Jr, Andrew W. Maverick and Frank R. Fronczek*

Department of Chemistry, Louisiana State University, Baton Rouge, LA 70803-1804, USA

Correspondence e-mail: ffroncz@lsu.edu

Received 15 March 2007
Accepted 5 April 2007

Key indicators

Single-crystal X-ray study
T = 110 K
Mean σ(C–C) = 0.014 Å
R factor = 0.058
wR factor = 0.151
Data-to-parameter ratio = 16.3

For details of how these key indicators were automatically derived from the article, see http://journals.iucr.org/e.

The title compound, $[ReCl(C_{10}H_{11}NO_2)_2(CO)_3]\cdot CHCl_3$, has Re—N distances of 2.202 (8) and 2.237 (7) Å, an N—Re—N angle of 84.1 (3)° and 2-hydroxy-4-oxopent-2-en-3-yl (acacH) units which are uncoordinated. The acacH units are in the enol tautomeric form, with delocalized single and double bonds.

Comment

The molecule 3-(4-pyridyl)pentane-2,4-dione, PyacH, was first prepared by Nozawa (1986), and has been used in a number of metal complexes (Turner *et al.*, 1997; Mackay *et al.*, 1995; Chen *et al.*, 2003, 2004; Vreshch *et al.*, 2003, 2004, 2005). Here, we describe the title compound (I), which is the first reported PyacH metal complex in which the pyridine unit is bound to the metal atom but the acacH unit is not. This makes (I) suitable as a 'molecular corner' for the construction of metal-organic frameworks or related supramolecular species.

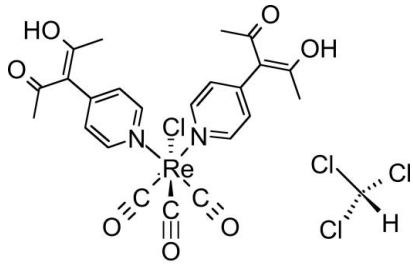

(I)

This molecule (Fig. 1 and Table 1) is similar in structure to the molecules $[Re(CO)_3Cl(py)_2]$, (II), and $[Re(CO)_3Cl(4,4'\text{-bpy})_2]$, (III) (Bélanger *et al.*, 1998). The N1—Re1—N2 angle in (I) is essentially identical to that in (II) [84.2 (2)°], but the corresponding angle in (III) is slightly wider at 87.0 (2)° (Bélanger *et al.*, 1998). The Re—N distances in (I) also agree well with those in (II) and (III).

Both 2-hydroxy-4-oxopent-2-en-3-yl (acacH) units are present in the enol tautomeric form. The similarity of the C—C and C—O distances about the approximately central axes of the acacH units, as well as the somewhat central locations of the refined OH hydrogen positions (Table 2), indicate delocalization of single and double bonds.

Experimental

Compound (I) was prepared by a procedure similar to that used by Zingales *et al.* (1967) for $Re(CO)_3Cl(py)_2$. PyacH was prepared by the method of Mackay *et al.* (1995). A solution of $Re(CO)_5Cl$ (0.0812 g, 2.24×10^{-4} mol) and PyacH (0.105 g, 5.91×10^{-4} mol) in $CHCl_3$ (100 ml) was placed in a flask that was wrapped with Al foil to

protect it from light. The mixture was refluxed for 72 h under N_2, with stirring, during which time it turned from dark yellow to very pale yellow. The solution was concentrated to about 10 ml and added to pentane (80 ml). The resulting white flocculent precipitate was collected, washed with pentane and dried, yielding 0.135 g (91%) of (I) as an off-white powder. Analysis found: C 41.59 H, 3.51, N 4.15%; $C_{23}H_{22}ClN_2O_7Re$ requires: C 41.85, H 3.36, N 4.24%. FT–IR: ν_{CO} 2020, 1908, and 1877 cm^{-1}. Colorless plates of the chloroform solvate of (I) suitable for X-ray analysis were obtained after *ca* 15 days by layering a $CHCl_3$ solution of (I) with hexane.

Crystal data

$[ReCl(C_{10}H_{11}NO_2)_2(CO)_3]\cdot CHCl_3$
M_r = 779.44
Monoclinic, $P2_1/c$
a = 10.889 (4) Å
b = 11.607 (4) Å
c = 24.306 (10) Å
β = 102.477 (14)°
V = 3000 (2) Å^3
Z = 4
Mo $K\alpha$ radiation
μ = 4.45 mm^{-1}
T = 110 K
0.30 × 0.25 × 0.02 mm

Data collection

Nonius KappaCCD diffractometer with Oxford Cryostream
Absorption correction: multi-scan (*SCALEPACK*; Otwinowski & Minor, 1997)
T_{min} = 0.308, T_{max} = 0.907
27300 measured reflections
5749 independent reflections
4148 reflections with $I > 2\sigma(I)$
R_{int} = 0.071

Refinement

$R[F^2 > 2\sigma(F^2)]$ = 0.058
$wR(F^2)$ = 0.151
S = 1.37
5749 reflections
353 parameters
H atoms treated by a mixture of independent and constrained refinement
$\Delta\rho_{max}$ = 1.97 e Å^{-3}
$\Delta\rho_{min}$ = −1.80 e Å^{-3}

Table 1
Selected geometric parameters (Å, °).

Re1—Cl1	2.465 (2)	C12—O5	1.301 (10)
Re1—N1	2.237 (7)	C20—O6	1.309 (14)
Re1—N2	2.202 (8)	C22—O7	1.290 (13)
Re1—C1	1.954 (12)	C10—C11	1.412 (12)
Re1—C2	1.901 (10)	C11—C12	1.402 (11)
Re1—C3	1.915 (12)	C20—C21	1.426 (15)
C10—O4	1.302 (10)	C21—C22	1.369 (14)
Cl1—Re1—N2	86.08 (19)	N1—Re1—N2	84.1 (3)
Cl1—Re1—N1	84.81 (19)		
C3—Re1—N1—C8	−43.5 (7)	C5—C6—C11—C12	−76.2 (12)
C1—Re1—N2—C14	38.7 (7)	C15—C16—C21—C20	69.7 (14)

Table 2
Hydrogen-bond geometry (Å, °).

D—H···A	D—H	H···A	D···A	D—H···A
O5—H5O···O4	1.13 (11)	1.46 (11)	2.459 (9)	144 (8)
O7—H7O···O6	1.06 (15)	1.55 (14)	2.486 (12)	144 (13)

H atoms on C were placed in idealized positions with C—H distances 0.95–1.00 Å and thereafter treated as riding. A torsional parameter was refined for each methyl group. Coordinates of H atoms on O were refined. Isotropic displacement parameters of the H atoms were assigned as 1.2 times U_{eq} of the bonded atoms (1.5 for methyl and OH). The maximum difference map peak was 0.86 Å from Re1 and the deepest hole 0.92 Å from Re1.

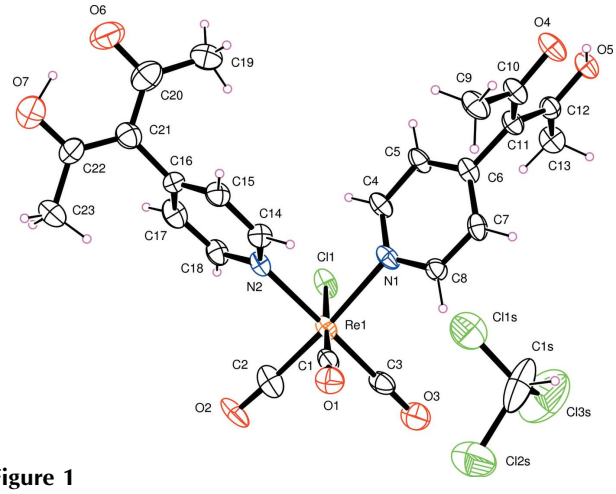

Figure 1
Molecular structure of (I), showing the numbering scheme and displacement ellipsoids at the 50% level. H atoms are represented with an arbitrary radius.

Data collection: *COLLECT* (Nonius, 2000); cell refinement: *SCALEPACK* (Otwinowski & Minor, 1997); data reduction: *SCALEPACK* and *DENZO* (Otwinowski & Minor, 1997); program(s) used to solve structure: *SIR97* (Altomare *et al.*, 1999); program(s) used to refine structure: *SHELXL97* (Sheldrick, 1997); molecular graphics: *ORTEP-3 for Windows* (Farrugia, 1997); software used to prepare material for publication: *SHELXL97*.

This research was supported by the US Department of Energy (DE-FG02–01ER15267). The purchase of the diffractometer was made possible by grant No. LEQSF(1999–2000)-ENH-TR-13, administered by the Louisiana Board of Regents.

References

Altomare, A., Burla, M. C., Camalli, M., Cascarano, G. L., Giacovazzo, C., Guagliardi, A., Moliterni, A. G. G., Polidori, G. & Spagna, R. (1999). *J. Appl. Cryst.* **32**, 115–119.
Bélanger, S., Hupp, J. T. & Stern, C. L. (1998). *Acta Cryst.* C**54**, 1596–1600.
Chen, B., Fronczek, F. R. & Maverick, A. W. (2003). *Chem. Commun.* pp. 2166–2167.
Chen, B., Fronczek, F. R. & Maverick, A. W. (2004). *Inorg. Chem.* **43**, 8209–8211.
Farrugia, L. J. (1997). *J. Appl. Cryst.* **30**, 565.
Mackay, L. G., Anderson, H. L. & Sanders, J. K. M. (1995). *J. Chem. Soc. Perkin Trans. 1*, pp. 2269–2273.
Nonius (2000). *COLLECT*. Nonius BV, Delft, The Netherlands.
Nozawa, M. (1986). JP 61 69, 760; *Chem. Abstr.* **105**, 97336m.
Otwinowski, Z. & Minor, W. (1997). *Methods in Enzymology*, Vol. 276, *Macromolecular Crystallography*, Part A, edited by C. W. Carter Jr & R. M. Sweet, pp. 307–326. New York: Academic Press.
Sheldrick, G. M. (1997). *SHELXL97*. University of Göttingen, Germany.
Turner, S. S., Collison, D., Mabbs, F. E. & Helliwell, M. (1997). *J. Chem. Soc. Dalton Trans.* pp. 1117–1118.
Vreshch, V. D., Chernega, A. N., Howard, J. A. K., Sieler, J. & Domasevitch, V. K. (2003). *Dalton Trans.* pp. 1707–1711.
Vreshch, V. D., Lysenko, A. B., Chernega, A. N., Howard, J. A. K., Krautscheid, H., Sieler, J. & Domasevitch, V. K. (2004). *Dalton Trans.* pp. 2899–2903.
Vreshch, V. D., Lysenko, A. B., Chernega, A. N., Sieler, J. & Domasevitch, V. K. (2005). *Polyhedron*, **24**, 917–926.
Zingales, F., Sartorelli, U. & Trovati, A. (1967). *Inorg. Chem.* **6**, 1246–1248.

Acta Crystallographica Section E
Structure Reports Online
ISSN 1600-5368

A cofacial binuclear copper(II) complex with a bridging 1,4-dithiane ligand

Sylvester Burton,‡ Frank R. Fronczek* and Andrew W. Maverick

Department of Chemistry, Louisiana State University, Baton Rouge, LA 70803-1804, USA
Correspondence e-mail: ffroncz@lsu.edu

Received 30 May 2007; accepted 15 June 2007

Key indicators: single-crystal X-ray study; T = 120 K; mean σ(C–C) = 0.005 Å; R factor = 0.050; wR factor = 0.110; data-to-parameter ratio = 12.7.

The molecule of (μ-1,4-dithiane-κ^2S:S')bis{μ-3,3′-[naphthalene-2,7-diylbis(methylene)]bis(pentane-2,4-dionato)-κ^4O,O':O'',O'''}dicopper(II), $[Cu_2(C_{22}H_{22}O_4)(C_4H_8S_2)]$, lies on an inversion center, with a Cu···Cu distance of 8.130 (1) Å. The Cu^{II} centers have square-pyramidal coordination geometry, with Cu—O distances in the range 1.905 (2)–1.925 (2) Å and a Cu—S distance of 2.8088 (10) Å. The host binuclear complex is distorted from a rectangular shape. The inversion symmetry of the molecule requires that the two coordination planes be parallel. However, they are 'slipped': the normals to the two coordination planes at the Cu atoms are 1.865 (1) Å apart. Another measure of this 'slipping' is provided by the four CH_2 groups, whose C atoms form a parallelogram with interior angles of 87.2 (3) and 92.8 (3)°. The two chelate rings tilt differently from the coordination plane, with one Cu atom lying only 0.0131 (5) Å out of one C_3O_2 mean plane, but 0.4416 (5) Å out of the other. Those two chelate planes form a dihedral angle of 11.2 (4)°. This relatively large deviation is believed to be due to the large size of the 1,4-dithiane guest.

Related literature

$Cu_2(NBA)_2$ {$NBAH_2$ is 3,3′-[naphthalene-2,7-diylbis(methylene)]bis(pentane-2,4-dione)} forms a crystalline solvate with two $CHCl_3$ molecules, in which the Cu···Cu distance is 7.349 (1) Å at room temperature (Maverick *et al.*, 1986) and 7.298 (1) Å at 100 K (Burton *et al.*, 2002). With μ-Dabco (1,4-diazabicyclo[2.2.2]octane), the Cu···Cu distance is 7.403 (4) Å (Maverick *et al.*, 1986), with μ-2,5-dimethylpyrazine it is 7.559 (2) and 7.596 (2) Å (Maverick *et al.*, 1990), and with μ-2-methylpyrazine it is 7.4801 (8) Å (Maverick *et al.*, 2001). For related literature, see: Martin *et al.* (1959).

‡ Current address: Department of Chemistry, Southern University, Baton Rouge, LA 70813, USA.

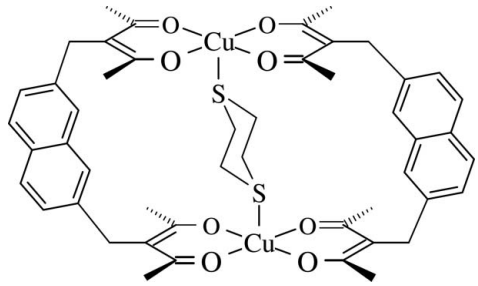

Experimental

Crystal data

$[Cu_2(C_{22}H_{22}O_4)(C_4H_8S_2)]$
M_r = 948.10
Monoclinic, $P2_1/c$
a = 7.758 (2) Å
b = 28.981 (7) Å
c = 9.640 (3) Å
β = 97.840 (15)°
V = 2147.1 (10) Å^3
Z = 2
Mo $K\alpha$ radiation
μ = 1.14 mm^{-1}
T = 120 K
0.15 × 0.08 × 0.07 mm

Data collection

Nonius KappaCCD diffractometer with an Oxford Cryosystems Cryostream cooler
Absorption correction: multi-scan (*SCALEPACK*; Otwinowski & Minor, 1997)
T_{min} = 0.878, T_{max} = 0.924
10982 measured reflections
3491 independent reflections
2598 reflections with $I > 2\sigma(I)$
R_{int} = 0.046

Refinement

$R[F^2 > 2\sigma(F^2)]$ = 0.050
$wR(F^2)$ = 0.110
S = 1.06
3491 reflections
275 parameters
H-atom parameters constrained
$\Delta\rho_{max}$ = 0.30 e Å^{-3}
$\Delta\rho_{min}$ = −0.44 e Å^{-3}

Data collection: *COLLECT* (Nonius, 2000); cell refinement: *SCALEPACK* (Otwinowski & Minor, 1997); data reduction: *SCALEPACK* and *DENZO* (Otwinowski & Minor, 1997); program(s) used to solve structure: *SIR97* (Altomare *et al.*, 1999); program(s) used to refine structure: *SHELXL97* (Sheldrick, 1997); molecular graphics: *ORTEP-3 for Windows* (Farrugia, 1997); software used to prepare material for publication: *SHELXL97*.

This research was supported by the Petroleum Research Fund (American Chemical Society) and by the US Department of Energy. The purchase of the diffractometer was made possible by grant No. LEQSF(1999–2000)-ENH-TR-13, administered by the Louisiana Board of Regents.

Supplementary data and figures for this paper are available from the IUCr electronic archives (Reference: FJ2036).

References

Altomare, A., Burla, M. C., Camalli, M., Cascarano, G. L., Giacovazzo, C., Guagliardi, A., Moliterni, A. G. G., Polidori, G. & Spagna, R. (1999). *J. Appl. Cryst.* **32**, 115–119.
Burton, S., Maverick, A. W. & Fronczek, F. R. (2002). Private communication (refcode FAGKED01). CCDC, Union Road, Cambridge, England.
Farrugia, L. J. (1997). *J. Appl. Cryst.* **30**, 565.

 doi:10.1107/S1600536807029583

Martin, D. F., Fernelius, W. C. & Shamma, M. (1959). *J. Am. Chem. Soc.* **81**, 130–133.
Maverick, A. W., Billodeaux, D. R., Ivie, M. L., Fronczek, F. R. & Maverick, E. F. (2001). *J. Incl. Phenom. Macrocyclic Chem.* **39**, 19–26.
Maverick, A. W., Buckingham, S. C., Yao, Q., Bradbury, J. R. & Stanley, G. G. (1986). *J. Am. Chem. Soc.* **108**, 7430–7431.
Maverick, A. W., Ivie, M. L., Waggenspack, J. H. & Fronczek, F. R. (1990). *Inorg. Chem.* **29**, 2403–2409.
Nonius (2000). *COLLECT*. Nonius BV, Delft, The Netherlands.
Otwinowski, Z. & Minor, W. (1997). *Methods in Enzymology*, Vol. 276, *Macromolecular Crystallography*, Part A, edited by C. W. Carter Jr & R. M. Sweet, pp. 307–326. New York: Academic Press.
Sheldrick, G. M. (1997). *SHELXL97*. University of Göttingen, Germany.

supplementary materials

Acta Cryst. (2007). E**63**, m1977-m1978 [**doi:10.1107/S1600536807029583**]

A cofacial binuclear copper(II) complex with a bridging 1,4-dithiane ligand

S. Burton, F. R. Fronczek and A. W. Maverick

Comment

Our group has previously prepared binuclear metal complexes derived from polydentate liands, which have been shown to intramolecularly bind bridging substrate molecules, similar to those produced by several other flexible binucleating macrocycles. This work was undertaken in an attempt to associate and quantify the binding between di-sulfur bases and their previously studied nitrogen analogues, see Related Literature section.

The molecule is centrosymmetric, and inclusion of the 1,4-dithiane molecule organizes the host such that the Cu···Cu distance, 8.130 (1) Å, is longer than in complexes with other guests, see Related Literature section. Several distortions take place in this organization. The $Cu_2(NBA)_2$ unit is not rectangular, but slipped such that the four CH_2 groups (C6, C17 and their inversion equivalents) form a parallelogram with sides 7.578 (5) and 9.570 (5) Å, and interior angles differing from orthogonality by 2.8 (3)°. This involves a slippage of the coordination planes horizontally by 1.865 (1) Å.

The coordination sphere is square pyramidal, with distances given in the Abstract and geometric details table. The two chelate rings tilt differently from the coordination plane, with Cu1 lying only 0.0131 (5) Å out of the best plane O1/O2/C2/C3/C4, but 0.4416 (5) Å out of the best plane O3/O4/C19/C20/C21. Those two planes form a dihedral angle of 11.2 (4)°. The Cu—S bond is tilted away from O1 and O2 (O—Cu—S angles 98.91 (8) and 96.32 (7)°) and toward O3 and O4 (angles 86.77 (7) and 87.66 (7)°), and forms an angle of 20.15 (5)° with the Cu···Cu vector.

Experimental

The $NBAH_2$, (2,7-naphthalenediylbis(methylene)bis(acetylacetone)) ligand was prepared previously by the general nucleophilic substitution method outlined by Martin *et al.* (1959). The $Cu_2(NBA)_2$ was also prepared by previously published procedures, see Related Literature section. Bis(3,3'-(naphthalene-2,7-diylbis(methylene)bis(2,4-pentanedionato)))\ dicopper(μ-1,4-dithiane) was prepared by combining a 5.05 mMolar chloroform solution of $Cu_2(NBA)_2$ with a 1.02 Molar chloroform solution of 1,4-dithiane. The resulting mixture was layered with acetonitrile and afforded light blue (turquoise) crystals of $Cu_2(NBA)_2$(μ-1,4-dithiane) after standing for 5 days.

Refinement

H atoms were placed in idealized positions with C—H distances 0.95 − 0.99 Å and thereafter treated as riding. U_{iso} for H was assigned as 1.2 times U_{eq} of the attached C atoms (1.5 for methyl). A torsional parameter was refined for each methyl group.

Figures

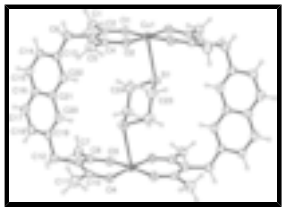

Fig. 1. Numbering scheme and ellipsoids at the 50% level. H atoms are represented with arbitrary radius.

(μ-1,4-Dithiane-κ^2*S*:*S*')bis[μ-3,3'-(naphthalene-2,7- diyldimethylene)bis(pentane-2,4-dionato)-κ^4*O*,*O*':*O*'',*O*''']dicopper,

Crystal data

$[Cu_2(C_{22}H_{22}O_4)(C_4H_8S_2)]$	F_{000} = 988
M_r = 948.10	D_x = 1.466 Mg m^{-3}
Monoclinic, $P2_1/c$	Mo $K\alpha$ radiation λ = 0.71073 Å
Hall symbol: -P 2ybc	Cell parameters from 6304 reflections
a = 7.758 (2) Å	θ = 2.5–25.0º
b = 28.981 (7) Å	μ = 1.14 mm^{-1}
c = 9.640 (3) Å	T = 120 K
β = 97.840 (15)º	Prism, light blue
V = 2147.1 (10) Å^3	0.15 × 0.08 × 0.07 mm
Z = 2	

Data collection

Nonius KappaCCD diffractometer with an Oxford Cryosystems Cryostream cooler	3491 independent reflections
Radiation source: fine-focus sealed tube	2598 reflections with $I > 2\sigma(I)$
Monochromator: graphite	R_{int} = 0.046
T = 120 K	θ_{max} = 25.0º
ω scans with κ offsets	θ_{min} = 2.5º
Absorption correction: multi-scan (SCALEPACK; Otwinowski & Minor, 1997)	h = −9→9
T_{min} = 0.878, T_{max} = 0.924	k = −33→34
10982 measured reflections	l = −11→11

Refinement

Refinement on F^2	Secondary atom site location: difference Fourier map
Least-squares matrix: full	Hydrogen site location: inferred from neighbouring sites
$R[F^2 > 2\sigma(F^2)]$ = 0.050	H-atom parameters constrained
$wR(F^2)$ = 0.110	$w = 1/[\sigma^2(F_o^2) + (0.0425P)^2 + 2.9798P]$

	where $P = (F_o^2 + 2F_c^2)/3$
$S = 1.06$	$(\Delta/\sigma)_{max} < 0.001$
3491 reflections	$\Delta\rho_{max} = 0.30$ e Å^{-3}
275 parameters	$\Delta\rho_{min} = -0.44$ e Å^{-3}
Primary atom site location: structure-invariant direct methods	Extinction correction: none

Special details

Geometry. All e.s.d.'s (except the e.s.d. in the dihedral angle between two l.s. planes) are estimated using the full covariance matrix. The cell e.s.d.'s are taken into account individually in the estimation of e.s.d.'s in distances, angles and torsion angles; correlations between e.s.d.'s in cell parameters are only used when they are defined by crystal symmetry. An approximate (isotropic) treatment of cell e.s.d.'s is used for estimating e.s.d.'s involving l.s. planes.

Refinement. Refinement of F^2 against ALL reflections. The weighted *R*-factor *wR* and goodness of fit S are based on F^2, conventional *R*-factors *R* are based on F, with F set to zero for negative F^2. The threshold expression of $F^2 > 2\text{sigma}(F^2)$ is used only for calculating *R*-factors(gt) *etc*. and is not relevant to the choice of reflections for refinement. *R*-factors based on F^2 are statistically about twice as large as those based on F, and R– factors based on ALL data will be even larger.

Fractional atomic coordinates and isotropic or equivalent isotropic displacement parameters (Å^2)

	x	*y*	*z*	U_{iso}*/U_{eq}
Cu1	0.88337 (6)	0.458966 (15)	0.80517 (5)	0.02939 (16)
S1	0.66505 (12)	0.46085 (3)	0.54758 (10)	0.0331 (3)
O1	1.0347 (3)	0.50850 (8)	0.7737 (2)	0.0290 (6)
O2	0.7427 (3)	0.49798 (8)	0.9033 (2)	0.0291 (6)
O3	0.2550 (3)	0.59178 (8)	0.1455 (2)	0.0300 (6)
O4	−0.0323 (3)	0.58236 (8)	0.2801 (2)	0.0291 (6)
C1	1.1720 (4)	0.58089 (13)	0.7810 (4)	0.0356 (10)
H1A	1.2465	0.5895	0.8676	0.053*
H1B	1.1232	0.6088	0.7336	0.053*
H1C	1.2411	0.5642	0.7194	0.053*
C2	1.0269 (5)	0.55050 (12)	0.8153 (4)	0.0289 (9)
C3	0.8971 (4)	0.56851 (12)	0.8897 (4)	0.0280 (9)
C4	0.7629 (4)	0.54102 (13)	0.9297 (4)	0.0285 (9)
C5	0.6320 (4)	0.56102 (12)	1.0147 (4)	0.0340 (10)
H5A	0.5341	0.5396	1.0141	0.051*
H5B	0.5897	0.5906	0.9740	0.051*
H5C	0.6871	0.5659	1.1112	0.051*
C6	0.9059 (4)	0.61985 (11)	0.9282 (4)	0.0293 (9)
H6A	0.8458	0.6243	1.0114	0.035*
H6B	1.0296	0.6282	0.9556	0.035*
C7	0.3945 (5)	0.66348 (12)	0.1506 (4)	0.0393 (10)
H7A	0.5020	0.6625	0.2171	0.059*
H7B	0.3499	0.6951	0.1435	0.059*
H7C	0.4187	0.6531	0.0585	0.059*
C8	0.2612 (4)	0.63233 (13)	0.2010 (4)	0.0296 (9)
C9	0.1539 (4)	0.64831 (12)	0.2977 (4)	0.0257 (9)

C10	0.0089 (4)	0.62301 (13)	0.3266 (4)	0.0294 (9)
C11	−0.1178 (5)	0.64297 (13)	0.4144 (4)	0.0398 (10)
H11A	−0.2097	0.6204	0.4234	0.060*
H11B	−0.1695	0.6710	0.3699	0.060*
H11C	−0.0570	0.6505	0.5076	0.060*
C12	0.1908 (4)	0.69621 (12)	0.3596 (4)	0.0317 (9)
H12A	0.1820	0.7187	0.2817	0.038*
H12B	0.0985	0.7039	0.4173	0.038*
C13	0.8278 (4)	0.65323 (12)	0.8151 (4)	0.0282 (9)
C14	0.9166 (5)	0.69515 (11)	0.7956 (4)	0.0317 (9)
H14	1.0252	0.7011	0.8511	0.038*
C15	0.8490 (5)	0.72711 (12)	0.6989 (4)	0.0324 (9)
H15	0.9119	0.7547	0.6881	0.039*
C16	0.6881 (4)	0.71991 (12)	0.6148 (4)	0.0285 (9)
C17	0.6175 (4)	0.75160 (12)	0.5128 (4)	0.0305 (9)
H17	0.6788	0.7793	0.4998	0.037*
C18	0.4621 (5)	0.74330 (12)	0.4318 (4)	0.0323 (9)
H18	0.4176	0.7652	0.3626	0.039*
C19	0.3664 (4)	0.70273 (12)	0.4493 (4)	0.0288 (9)
C20	0.4350 (4)	0.67094 (12)	0.5462 (4)	0.0285 (9)
H20	0.3729	0.6432	0.5565	0.034*
C21	0.5968 (4)	0.67833 (12)	0.6320 (4)	0.0271 (9)
C22	0.6716 (4)	0.64566 (12)	0.7320 (4)	0.0303 (9)
H22	0.6117	0.6175	0.7420	0.036*
C23	0.4616 (5)	0.46546 (13)	0.6187 (4)	0.0360 (10)
H23A	0.4343	0.4351	0.6577	0.043*
H23B	0.4763	0.4879	0.6968	0.043*
C24	0.6918 (5)	0.51949 (12)	0.4876 (4)	0.0369 (10)
H24A	0.7030	0.5407	0.5688	0.044*
H24B	0.8002	0.5215	0.4444	0.044*

Atomic displacement parameters (Å^2)

	U^{11}	U^{22}	U^{33}	U^{12}	U^{13}	U^{23}
Cu1	0.0288 (3)	0.0309 (3)	0.0285 (3)	−0.0002 (2)	0.00385 (19)	−0.0009 (2)
S1	0.0315 (6)	0.0372 (6)	0.0301 (6)	0.0030 (5)	0.0023 (4)	0.0026 (5)
O1	0.0273 (14)	0.0293 (15)	0.0310 (16)	−0.0012 (11)	0.0069 (11)	−0.0013 (12)
O2	0.0309 (15)	0.0271 (15)	0.0299 (16)	−0.0005 (11)	0.0066 (12)	−0.0040 (13)
O3	0.0332 (15)	0.0310 (15)	0.0260 (16)	−0.0016 (12)	0.0053 (12)	−0.0006 (12)
O4	0.0316 (14)	0.0269 (14)	0.0281 (15)	0.0012 (12)	0.0008 (12)	−0.0017 (13)
C1	0.036 (2)	0.038 (2)	0.034 (2)	−0.0012 (19)	0.0103 (19)	−0.004 (2)
C2	0.026 (2)	0.036 (2)	0.022 (2)	0.0000 (18)	−0.0056 (17)	0.0004 (19)
C3	0.025 (2)	0.033 (2)	0.025 (2)	0.0034 (18)	0.0019 (17)	−0.0008 (19)
C4	0.030 (2)	0.034 (2)	0.019 (2)	0.003 (2)	−0.0028 (16)	−0.001 (2)
C5	0.030 (2)	0.036 (2)	0.036 (2)	0.0006 (18)	0.0068 (19)	−0.001 (2)
C6	0.030 (2)	0.031 (2)	0.026 (2)	−0.0019 (17)	0.0003 (17)	−0.0024 (19)
C7	0.044 (3)	0.034 (2)	0.041 (3)	−0.0044 (19)	0.011 (2)	0.001 (2)
C8	0.031 (2)	0.033 (2)	0.023 (2)	−0.0018 (18)	−0.0048 (18)	0.0065 (19)

C9	0.022 (2)	0.026 (2)	0.027 (2)	0.0017 (17)	−0.0013 (17)	0.0027 (18)
C10	0.030 (2)	0.038 (2)	0.018 (2)	0.0090 (19)	−0.0032 (17)	0.0033 (19)
C11	0.037 (2)	0.041 (2)	0.043 (3)	−0.004 (2)	0.010 (2)	−0.002 (2)
C12	0.032 (2)	0.029 (2)	0.034 (2)	0.0052 (17)	0.0032 (18)	0.0004 (19)
C13	0.030 (2)	0.030 (2)	0.025 (2)	−0.0011 (18)	0.0009 (18)	−0.0041 (19)
C14	0.036 (2)	0.026 (2)	0.031 (2)	−0.0062 (19)	−0.0021 (19)	−0.005 (2)
C15	0.038 (2)	0.027 (2)	0.032 (2)	−0.0063 (18)	0.0036 (19)	−0.005 (2)
C16	0.027 (2)	0.032 (2)	0.025 (2)	0.0016 (19)	0.0014 (18)	0.0009 (19)
C17	0.031 (2)	0.027 (2)	0.034 (2)	−0.0059 (18)	0.0080 (19)	0.001 (2)
C18	0.036 (2)	0.031 (2)	0.029 (2)	0.0044 (19)	0.0024 (19)	0.0053 (19)
C19	0.030 (2)	0.030 (2)	0.026 (2)	0.0016 (18)	0.0029 (18)	−0.0034 (19)
C20	0.031 (2)	0.024 (2)	0.030 (2)	−0.0033 (17)	0.0058 (19)	−0.0018 (19)
C21	0.031 (2)	0.024 (2)	0.025 (2)	0.0025 (17)	0.0016 (18)	−0.0039 (18)
C22	0.038 (2)	0.024 (2)	0.029 (2)	−0.0057 (18)	0.0058 (19)	−0.0019 (19)
C23	0.033 (2)	0.043 (2)	0.032 (2)	−0.005 (2)	0.0045 (18)	0.008 (2)
C24	0.035 (2)	0.043 (2)	0.033 (2)	−0.0076 (19)	0.0058 (19)	0.001 (2)

Geometric parameters (Å, °)

Cu1—O1	1.905 (2)	C9—C10	1.402 (5)
Cu1—O2	1.910 (2)	C9—C12	1.523 (5)
Cu1—O3^{i}	1.918 (2)	C10—C11	1.499 (5)
Cu1—O4^{i}	1.925 (2)	C11—H11A	0.9800
Cu1—S1	2.8088 (10)	C11—H11B	0.9800
S1—C23	1.809 (4)	C11—H11C	0.9800
S1—C24	1.816 (4)	C12—C19	1.522 (5)
O1—C2	1.286 (4)	C12—H12A	0.9900
O2—C4	1.278 (4)	C12—H12B	0.9900
O3—C8	1.289 (4)	C13—C22	1.376 (5)
O3—Cu1^{i}	1.918 (2)	C13—C14	1.422 (5)
O4—C10	1.285 (4)	C14—C15	1.367 (5)
O4—Cu1^{i}	1.925 (2)	C14—H14	0.9500
C1—C2	1.502 (5)	C15—C16	1.408 (5)
C1—H1A	0.9800	C15—H15	0.9500
C1—H1B	0.9800	C16—C17	1.401 (5)
C1—H1C	0.9800	C16—C21	1.419 (5)
C2—C3	1.413 (5)	C17—C18	1.365 (5)
C3—C4	1.406 (5)	C17—H17	0.9500
C3—C6	1.533 (5)	C18—C19	1.413 (5)
C4—C5	1.505 (4)	C18—H18	0.9500
C5—H5A	0.9800	C19—C20	1.367 (5)
C5—H5B	0.9800	C20—C21	1.422 (5)
C5—H5C	0.9800	C20—H20	0.9500
C6—C13	1.520 (5)	C21—C22	1.418 (5)
C6—H6A	0.9900	C22—H22	0.9500
C6—H6B	0.9900	C23—C24^{i}	1.525 (5)
C7—C8	1.502 (5)	C23—H23A	0.9900
C7—H7A	0.9800	C23—H23B	0.9900

C7—H7B	0.9800	C24—C23^{i}	1.525 (5)
C7—H7C	0.9800	C24—H24A	0.9900
C8—C9	1.410 (5)	C24—H24B	0.9900
O1—Cu1—O2	92.23 (10)	O4—C10—C11	113.5 (3)
O1—Cu1—O3^{i}	174.31 (10)	C9—C10—C11	121.1 (3)
O2—Cu1—O3^{i}	87.38 (10)	C10—C11—H11A	109.5
O1—Cu1—O4^{i}	88.97 (10)	C10—C11—H11B	109.5
O2—Cu1—O4^{i}	175.62 (10)	H11A—C11—H11B	109.5
O3^{i}—Cu1—O4^{i}	91.01 (10)	C10—C11—H11C	109.5
O1—Cu1—S1	98.91 (8)	H11A—C11—H11C	109.5
O2—Cu1—S1	96.32 (7)	H11B—C11—H11C	109.5
O3^{i}—Cu1—S1	86.77 (7)	C19—C12—C9	116.2 (3)
O4^{i}—Cu1—S1	87.66 (7)	C19—C12—H12A	108.2
C23—S1—C24	101.26 (17)	C9—C12—H12A	108.2
C23—S1—Cu1	96.79 (13)	C19—C12—H12B	108.2
C24—S1—Cu1	102.62 (13)	C9—C12—H12B	108.2
C2—O1—Cu1	127.4 (2)	H12A—C12—H12B	107.4
C4—O2—Cu1	127.8 (2)	C22—C13—C14	117.6 (3)
C8—O3—Cu1^{i}	126.0 (2)	C22—C13—C6	123.3 (3)
C10—O4—Cu1^{i}	125.7 (2)	C14—C13—C6	119.1 (3)
C2—C1—H1A	109.5	C15—C14—C13	121.4 (3)
C2—C1—H1B	109.5	C15—C14—H14	119.3
H1A—C1—H1B	109.5	C13—C14—H14	119.3
C2—C1—H1C	109.5	C14—C15—C16	121.3 (3)
H1A—C1—H1C	109.5	C14—C15—H15	119.4
H1B—C1—H1C	109.5	C16—C15—H15	119.4
O1—C2—C3	125.1 (3)	C17—C16—C15	122.5 (3)
O1—C2—C1	114.7 (3)	C17—C16—C21	119.0 (3)
C3—C2—C1	120.2 (3)	C15—C16—C21	118.4 (3)
C4—C3—C2	122.4 (3)	C18—C17—C16	121.0 (3)
C4—C3—C6	119.6 (3)	C18—C17—H17	119.5
C2—C3—C6	118.0 (3)	C16—C17—H17	119.5
O2—C4—C3	125.0 (3)	C17—C18—C19	121.1 (3)
O2—C4—C5	114.2 (3)	C17—C18—H18	119.5
C3—C4—C5	120.7 (3)	C19—C18—H18	119.5
C4—C5—H5A	109.5	C20—C19—C18	118.7 (3)
C4—C5—H5B	109.5	C20—C19—C12	122.6 (3)
H5A—C5—H5B	109.5	C18—C19—C12	118.7 (3)
C4—C5—H5C	109.5	C19—C20—C21	121.8 (3)
H5A—C5—H5C	109.5	C19—C20—H20	119.1
H5B—C5—H5C	109.5	C21—C20—H20	119.1
C13—C6—C3	116.3 (3)	C22—C21—C16	118.8 (3)
C13—C6—H6A	108.2	C22—C21—C20	122.8 (3)
C3—C6—H6A	108.2	C16—C21—C20	118.4 (3)
C13—C6—H6B	108.2	C13—C22—C21	122.4 (3)
C3—C6—H6B	108.2	C13—C22—H22	118.8
H6A—C6—H6B	107.4	C21—C22—H22	118.8

C8—C7—H7A	109.5	$C24^{i}$—C23—S1	114.1 (3)
C8—C7—H7B	109.5	$C24^{i}$—C23—H23A	108.7
H7A—C7—H7B	109.5	S1—C23—H23A	108.7
C8—C7—H7C	109.5	$C24^{i}$—C23—H23B	108.7
H7A—C7—H7C	109.5	S1—C23—H23B	108.7
H7B—C7—H7C	109.5	H23A—C23—H23B	107.6
O3—C8—C9	125.5 (3)	$C23^{i}$—C24—S1	111.7 (3)
O3—C8—C7	113.7 (3)	$C23^{i}$—C24—H24A	109.3
C9—C8—C7	120.7 (3)	S1—C24—H24A	109.3
C10—C9—C8	121.4 (3)	$C23^{i}$—C24—H24B	109.3
C10—C9—C12	120.8 (3)	S1—C24—H24B	109.3
C8—C9—C12	117.5 (3)	H24A—C24—H24B	107.9
O4—C10—C9	125.4 (3)		
O1—Cu1—S1—C23	−125.86 (14)	C12—C9—C10—O4	−179.5 (3)
O2—Cu1—S1—C23	−32.59 (14)	C8—C9—C10—C11	−171.8 (3)
$O3^{i}$—Cu1—S1—C23	54.41 (14)	C12—C9—C10—C11	2.4 (5)
$O4^{i}$—Cu1—S1—C23	145.55 (14)	C10—C9—C12—C19	121.8 (4)
O1—Cu1—S1—C24	−22.68 (15)	C8—C9—C12—C19	−63.8 (4)
O2—Cu1—S1—C24	70.59 (14)	C3—C6—C13—C22	43.2 (5)
$O3^{i}$—Cu1—S1—C24	157.59 (15)	C3—C6—C13—C14	−138.7 (3)
$O4^{i}$—Cu1—S1—C24	−111.27 (15)	C22—C13—C14—C15	0.5 (5)
O2—Cu1—O1—C2	1.7 (3)	C6—C13—C14—C15	−177.6 (3)
$O4^{i}$—Cu1—O1—C2	−174.1 (3)	C13—C14—C15—C16	0.3 (5)
S1—Cu1—O1—C2	98.4 (3)	C14—C15—C16—C17	−178.6 (3)
O1—Cu1—O2—C4	−0.5 (3)	C14—C15—C16—C21	−0.3 (5)
$O3^{i}$—Cu1—O2—C4	173.8 (3)	C15—C16—C17—C18	179.2 (3)
S1—Cu1—O2—C4	−99.7 (3)	C21—C16—C17—C18	0.9 (5)
Cu1—O1—C2—C3	−2.6 (5)	C16—C17—C18—C19	0.7 (5)
Cu1—O1—C2—C1	176.5 (2)	C17—C18—C19—C20	−2.1 (5)
O1—C2—C3—C4	1.9 (5)	C17—C18—C19—C12	177.8 (3)
C1—C2—C3—C4	−177.1 (3)	C9—C12—C19—C20	−43.3 (5)
O1—C2—C3—C6	−178.6 (3)	C9—C12—C19—C18	136.8 (3)
C1—C2—C3—C6	2.4 (5)	C18—C19—C20—C21	1.9 (5)
Cu1—O2—C4—C3	0.1 (5)	C12—C19—C20—C21	−178.0 (3)
Cu1—O2—C4—C5	−177.7 (2)	C17—C16—C21—C22	177.9 (3)
C2—C3—C4—O2	−0.6 (6)	C15—C16—C21—C22	−0.5 (5)
C6—C3—C4—O2	179.9 (3)	C17—C16—C21—C20	−1.1 (5)
C2—C3—C4—C5	177.1 (3)	C15—C16—C21—C20	−179.5 (3)
C6—C3—C4—C5	−2.4 (5)	C19—C20—C21—C22	−179.2 (3)
C4—C3—C6—C13	−97.4 (4)	C19—C20—C21—C16	−0.3 (5)
C2—C3—C6—C13	83.1 (4)	C14—C13—C22—C21	−1.4 (5)
$Cu1^{i}$—O3—C8—C9	−7.1 (5)	C6—C13—C22—C21	176.7 (3)
$Cu1^{i}$—O3—C8—C7	174.3 (2)	C16—C21—C22—C13	1.4 (5)
O3—C8—C9—C10	−10.2 (6)	C20—C21—C22—C13	−179.7 (3)
C7—C8—C9—C10	168.3 (3)	C24—S1—C23—$C24^{i}$	59.9 (3)

O3—C8—C9—C12	175.4 (3)	Cu1—S1—C23—C24^{i}	164.3 (2)
C7—C8—C9—C12	−6.1 (5)	C23—S1—C24—C23^{i}	−58.2 (3)
Cu1^{i}—O4—C10—C9	14.3 (5)	Cu1—S1—C24—C23^{i}	−157.9 (2)
Cu1^{i}—O4—C10—C11	−167.5 (2)	S1—C24—C23^{i}—S1^{i}	66.0 (3)
C8—C9—C10—O4	6.3 (5)		

Symmetry codes: (i) −*x*+1, −*y*+1, −*z*+1.

Fig. 1

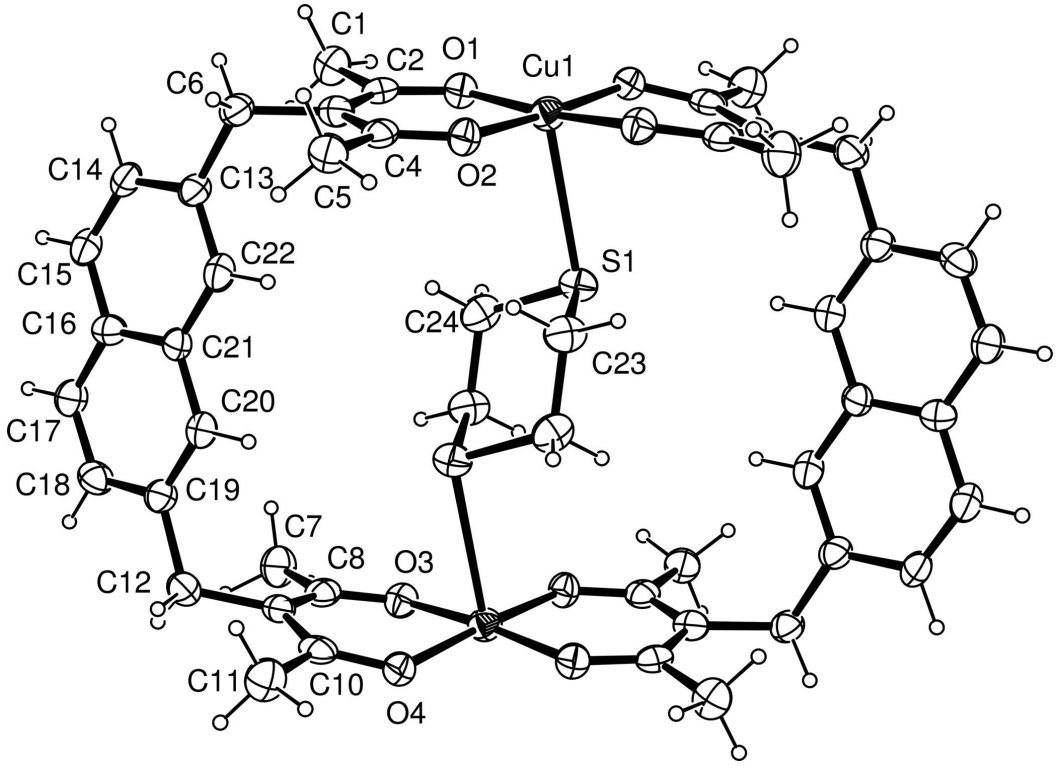
C1
C2
O1
Cu1
C6
C14
C13
C5
C4
O2
C15
C22
S1
C16
C24
C21
C23
C20
C17
C18
C19
C7
C8
O3
C12
C11
C10
O4

Acta Crystallographica Section E
Structure Reports Online
ISSN 1600-5368

3,5-Diacetylheptane-2,6-dione

Sylvester Burton,‡ Frank R. Fronczek* and Andrew W. Maverick

Department of Chemistry, Louisiana State University, Baton Rouge, LA 70803-1804, USA
Correspondence e-mail: ffroncz@lsu.edu

Received 25 May 2007; accepted 29 May 2007

Key indicators: single-crystal X-ray study; T = 100 K; mean σ(C–C) = 0.002 Å; R factor = 0.041; wR factor = 0.113; data-to-parameter ratio = 18.9.

The title compound, $C_{11}H_{16}O_4$, was produced when pentane-2,4-dione (acacH) was treated with formaldehyde in a *ca* 2.16:1 molar ratio. The compound exists in the solid state as the keto tautomer, although the enol tautomer also exists in solution. The C=O distances are in the range 1.2097 (18)–1.2169 (18) Å. Intermolecular C=O···C=O interactions exist, the shortest having a C···O distance of 3.378 (2) Å.

Related literature

The title compound was described over 100 years ago (Scholtz, 1897; Knoevenagel *et al.*, 1903). We have recently reported the structure of 1,1′,1″-[(5*R*,6*R*)-6-hydroxy-6-methyltetrahydro-2*H*-pyran-3,3,5-triyl]triethanone (Burton *et al.*, 2007), which is formed when excess formaldehyde is used in the synthesis. For related literature, see: Allen *et al.* (1998); Wilson (1963).

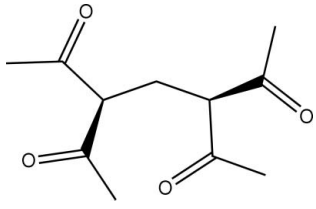

Experimental

Crystal data

$C_{11}H_{16}O_4$
M_r = 212.24
Orthorhombic, $P2_12_12_1$
a = 7.810 (2) Å
b = 8.611 (2) Å
c = 17.431 (4) Å
V = 1172.3 (5) Å^3
Z = 4
Mo $K\alpha$ radiation
μ = 0.09 mm^{-1}
T = 100 K
0.47 × 0.43 × 0.40 mm

Data collection

Nonius KappaCCD diffractometer (with Oxford Cryostream)
Absorption correction: none
15692 measured reflections
2647 independent reflections
2352 reflections with $I > 2\sigma(I)$
R_{int} = 0.016

Refinement

$R[F^2 > 2\sigma(F^2)]$ = 0.041
$wR(F^2)$ = 0.113
S = 1.04
2647 reflections
140 parameters
H-atom parameters constrained
$\Delta\rho_{max}$ = 0.29 e Å^{-3}
$\Delta\rho_{min}$ = −0.18 e Å^{-3}

Table 1
Selected geometric parameters (Å, °).

O1—C2	1.2145 (15)	C2—C3	1.5256 (17)
O2—C4	1.2097 (18)	C3—C4	1.5284 (17)
O3—C8	1.2169 (18)	C8—C9	1.5256 (18)
O4—C10	1.2158 (17)	C9—C10	1.5301 (17)
O1—C2—C3—C6	−15.71 (16)	O3—C8—C9—C6	−15.27 (16)
C6—C3—C4—O2	103.37 (14)	C6—C9—C10—O4	112.32 (14)

Data collection: *COLLECT* (Nonius, 2000); cell refinement: *SCALEPACK* (Otwinowski & Minor, 1997); data reduction: *DENZO* (Otwinowski & Minor, 1997) and *SCALEPACK*; program(s) used to solve structure: *SIR97* (Altomare *et al.*, 1999); program(s) used to refine structure: *SHELXL97* (Sheldrick, 1997); molecular graphics: *ORTEP-3 for Windows* (Farrugia, 1997); software used to prepare material for publication: *SHELXL97*.

The purchase of the diffractometer was made possible by grant No. LEQSF(1999–2000)-ENH-TR-13, administered by the Louisiana Board of Regents. This research was supported by grants from the Department of Energy (DE-FG02–01ER15267) and the ACS Petroleum Research Fund (37234-AC3).

Supplementary data and figures for this paper are available from the IUCr electronic archives (Reference: BQ2022).

References

Allen, F. H., Baalham, C. A., Lommerse, J. P. M. & Raithby, P. R. (1998). *Acta Cryst.* B**54**, 320–329.
Altomare, A., Burla, M. C., Camalli, M., Cascarano, G. L., Giacovazzo, C., Guagliardi, A., Moliterni, A. G. G., Polidori, G. & Spagna, R. (1999). *J. Appl. Cryst.* **32**, 115–119.
Burton, S., Fronczek, F. R. & Maverick, A. W. (2007). *Acta Cryst.* E**63**, o2661–o2662.
Farrugia, L. J. (1997). *J. Appl. Cryst.* **30**, 565.
Knoevenagel, E., Bialon, K., Ruschhaupt, W., Schneider, G., Croner, F. & Sanger, W. (1903). *Chem. Ber.* **36**, 2136–2180.
Nonius (2000). *COLLECT*. Nonius BV, Delft, The Netherlands.
Otwinowski, Z. & Minor, W. (1997). *Methods in Enzymology*, Vol. 276, *Macromolecular Crystallography*, Part A, edited by C. W. Carter Jr & R. M. Sweet, pp. 307–326. New York: Academic Press.
Scholtz, M. (1897). *Chem. Ber.* **30**, 2295–2299.
Sheldrick, G. M. (1997). *SHELXL97*. University of Göttingen, Germany.
Wilson, B. D. (1963). *J. Org. Chem.* **28**, 314–320.

‡ Current Address: Department of Chemistry, Southern University, Baton Rouge, LA 70813, USA.

  doi:10.1107/S1600536807026323

supplementary materials

Acta Cryst. (2007). E**63**, o3108 [**doi:10.1107/S1600536807026323**]

3,5-Diacetylheptane-2,6-dione

S. Burton, F. R. Fronczek and A. W. Maverick

Comment

The title compound, (I), was first explored by Scholtz (1897) and Knoevenagel *et al.* (1903). Our goal was to utilize the title compound (I) in the preparation of polynuclear metal complexes.

Solutions of (I) in $CHCl_3$ show evidence in ^1H NMR spectra for both keto and enol tautomers, but the crystal contains only the keto form. C3 and C9 (Fig. 1) are protonated and tetrahedral, all the C—C bond lengths to them are typical of single bonds, and the four C═O distances (Table 1) are typical of double bonds.

Allen *et al.* (1998) have shown that intermolecular carbonyl···carbonyl interactions in ketones can significantly influence the packing of such molecules, and have identified three major geometric types. The shortest such contact in (I), O3···C10 ($1-x, y-1/2, 3/2-z$) resembles their perpendicular interaction, and its O···C distance 3.387 (2)Å is near the mean distance they report. However, the O atom in this interaction is actually nearer the methyl C [O3···C11 = 3.267 (2) Å].

Experimental

In accordance with previously described preparative methods (Knoevenagel *et al.*, 1903; Wilson, 1963), a mixture of 40 ml acetylacetone (0.39 mol) and 13.5 ml of formaldehyde (37% aqueous solution; 0.18 mol) was stirred for 5 days. The product separated on standing into a gold-colored organic bottom layer (40 ml) and a pale-yellow aqueous top layer (10 ml). The organic layer was dried over $MgSO_4$ and an equal volume of diethyl ether was added. The resulting solution was cooled in a dry ice-acetone bath to produce a white solid. After repeatedly taking up the viscous portions in a minimum of diethyl ether and cooling in the dry ice-acetone bath, a total of 11.0 g (0.052 mole, 26% yield) of crystalline solid, mp 39.5–41.0 °C, was isolated. X-ray quality crystals were obtained by cooling a solution in diethyl ether in a dry ice-acetone bath.

Refinement

H atoms were placed in idealized positions with C—H distances 0.98 − 1.00 Å and thereafter treated as riding. U_{iso} for H was assigned as 1.2 times U_{eq} of the attached C atoms (1.5 for methyl). A torsional parameter was refined for each methyl group. The absolute structure could not be determined, and Friedel pairs were averaged.

Figures

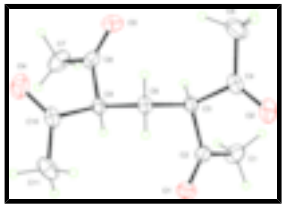

Fig. 1. Numbering scheme and ellipsoids at the 50% level. H atoms are represented with arbitrary radius.

3,5-Diacetylheptane-2,6-dione

Crystal data

$C_{11}H_{16}O_4$	$D_x = 1.203$ Mg m^{-3}
$M_r = 212.24$	Melting point: 313.5-314.0 K
Orthorhombic, $P2_12_12_1$	Mo $K\alpha$ radiation $\lambda = 0.71073$ Å
Hall symbol: P 2ac 2ab	Cell parameters from 2556 reflections
$a = 7.810$ (2) Å	$\theta = 2.5$–33.7º
$b = 8.611$ (2) Å	$\mu = 0.09$ mm^{-1}
$c = 17.431$ (4) Å	$T = 100$ K
$V = 1172.3$ (5) Å^3	Fragment, colourless
$Z = 4$	0.47 × 0.43 × 0.40 mm
$F_{000} = 456$	

Data collection

Nonius KappaCCD (with Oxford Cryostream) diffractometer	2352 reflections with $I > 2\sigma(I)$
Radiation source: fine-focus sealed tube	$R_{int} = 0.016$
Monochromator: graphite	$\theta_{max} = 33.7$º
$T = 100$ K	$\theta_{min} = 2.8$º
ω scans with κ offsets	$h = -11\rightarrow11$
Absorption correction: none	$k = -13\rightarrow13$
15692 measured reflections	$l = -27\rightarrow27$
2647 independent reflections	

Refinement

Refinement on F^2	H-atom parameters constrained
Least-squares matrix: full	$w = 1/[\sigma^2(F_o^2) + (0.0668P)^2 + 0.1309P]$ where $P = (F_o^2 + 2F_c^2)/3$
$R[F^2 > 2\sigma(F^2)] = 0.041$	$(\Delta/\sigma)_{max} = 0.006$
$wR(F^2) = 0.113$	$\Delta\rho_{max} = 0.29$ e Å^{-3}
$S = 1.04$	$\Delta\rho_{min} = -0.18$ e Å^{-3}
2647 reflections	Extinction correction: none
140 parameters	
Primary atom site location: structure-invariant direct methods	
Secondary atom site location: difference Fourier map	
Hydrogen site location: inferred from neighbouring sites	

Special details

Geometry. All e.s.d.'s (except the e.s.d. in the dihedral angle between two l.s. planes) are estimated using the full covariance matrix. The cell e.s.d.'s are taken into account individually in the estimation of e.s.d.'s in distances, angles and torsion angles; correlations between e.s.d.'s in cell parameters are only used when they are defined by crystal symmetry. An approximate (isotropic) treatment of cell e.s.d.'s is used for estimating e.s.d.'s involving l.s. planes.

Refinement. Refinement of F^2 against ALL reflections. The weighted *R*-factor *wR* and goodness of fit S are based on F^2, conventional *R*-factors *R* are based on F, with F set to zero for negative F^2. The threshold expression of $F^2 > 2\text{sigma}(F^2)$ is used only for calculating *R*-factors(gt) *etc*. and is not relevant to the choice of reflections for refinement. *R*-factors based on F^2 are statistically about twice as large as those based on F, and R– factors based on ALL data will be even larger.

Fractional atomic coordinates and isotropic or equivalent isotropic displacement parameters (Å^2)

	x	*y*	*z*	U_{iso}*/U_{eq}
O1	0.05730 (14)	0.48942 (13)	0.67423 (5)	0.0284 (2)
O2	−0.06423 (14)	0.21860 (16)	0.54715 (7)	0.0388 (3)
O3	0.52584 (15)	0.07629 (14)	0.65558 (6)	0.0346 (3)
O4	0.45874 (17)	0.10347 (15)	0.84527 (6)	0.0383 (3)
C1	0.1592 (2)	0.53906 (18)	0.54771 (8)	0.0296 (3)
H1A	0.0884	0.6328	0.5508	0.044*
H1B	0.1286	0.4802	0.5016	0.044*
H1C	0.2803	0.5686	0.5452	0.044*
C2	0.12923 (16)	0.44037 (15)	0.61741 (7)	0.0212 (2)
C3	0.19679 (15)	0.27436 (14)	0.61312 (6)	0.0184 (2)
H3	0.3141	0.2768	0.5901	0.022*
C4	0.08071 (18)	0.17786 (17)	0.56105 (7)	0.0246 (2)
C5	0.1554 (2)	0.03050 (19)	0.52954 (9)	0.0366 (3)
H5A	0.0644	−0.0469	0.5234	0.055*
H5B	0.2423	−0.0092	0.5650	0.055*
H5C	0.2082	0.0514	0.4796	0.055*
C6	0.20811 (15)	0.19736 (15)	0.69250 (6)	0.0195 (2)
H6A	0.1052	0.2245	0.7228	0.023*
H6B	0.2105	0.0831	0.6863	0.023*
C7	0.69870 (18)	0.2565 (2)	0.72430 (11)	0.0348 (3)
H7A	0.7860	0.1755	0.7298	0.052*
H7B	0.6838	0.3103	0.7734	0.052*
H7C	0.7351	0.3310	0.6851	0.052*
C8	0.53220 (16)	0.18388 (16)	0.70076 (7)	0.0231 (2)
C9	0.36884 (15)	0.24996 (14)	0.73593 (6)	0.0182 (2)
H9	0.3751	0.3659	0.7337	0.022*
C10	0.36087 (17)	0.20085 (16)	0.82022 (7)	0.0236 (2)
C11	0.22526 (19)	0.27536 (18)	0.86857 (7)	0.0294 (3)
H11A	0.2417	0.2456	0.9223	0.044*
H11B	0.1122	0.2407	0.8512	0.044*
H11C	0.2332	0.3885	0.8638	0.044*

Atomic displacement parameters (Å^2)

	U^{11}	U^{22}	U^{33}	U^{12}	U^{13}	U^{23}
O1	0.0318 (5)	0.0291 (5)	0.0243 (4)	0.0065 (4)	0.0051 (4)	−0.0015 (4)
O2	0.0300 (5)	0.0493 (7)	0.0371 (6)	0.0006 (5)	−0.0138 (5)	−0.0062 (5)
O3	0.0336 (5)	0.0348 (6)	0.0354 (5)	0.0123 (5)	−0.0005 (4)	−0.0080 (5)
O4	0.0445 (7)	0.0436 (6)	0.0269 (5)	0.0058 (6)	−0.0062 (5)	0.0120 (4)
C1	0.0315 (6)	0.0299 (6)	0.0275 (6)	0.0059 (5)	0.0050 (5)	0.0104 (5)
C2	0.0197 (5)	0.0237 (5)	0.0201 (4)	0.0015 (4)	−0.0005 (4)	0.0018 (4)
C3	0.0182 (5)	0.0219 (5)	0.0152 (4)	0.0000 (4)	−0.0008 (4)	−0.0002 (4)
C4	0.0287 (6)	0.0280 (6)	0.0169 (4)	−0.0038 (5)	−0.0027 (4)	−0.0007 (4)
C5	0.0404 (8)	0.0341 (7)	0.0353 (7)	−0.0033 (7)	−0.0031 (6)	−0.0142 (6)
C6	0.0203 (5)	0.0220 (5)	0.0163 (4)	−0.0024 (4)	−0.0024 (4)	0.0018 (4)
C7	0.0203 (6)	0.0335 (7)	0.0506 (9)	−0.0010 (6)	−0.0019 (6)	0.0075 (7)
C8	0.0211 (5)	0.0231 (5)	0.0250 (5)	0.0033 (5)	−0.0009 (4)	0.0053 (4)
C9	0.0197 (4)	0.0184 (4)	0.0165 (4)	−0.0011 (4)	−0.0014 (4)	0.0012 (4)
C10	0.0283 (6)	0.0249 (5)	0.0175 (4)	−0.0066 (5)	−0.0043 (4)	0.0018 (4)
C11	0.0338 (7)	0.0348 (7)	0.0198 (5)	−0.0117 (6)	0.0050 (5)	−0.0036 (5)

Geometric parameters (Å, °)

O1—C2	1.2145 (15)	C5—H5C	0.9800
O2—C4	1.2097 (18)	C6—C9	1.5343 (16)
O3—C8	1.2169 (18)	C6—H6A	0.9900
O4—C10	1.2158 (17)	C6—H6B	0.9900
C1—C2	1.5011 (18)	C7—C8	1.500 (2)
C1—H1A	0.9800	C7—H7A	0.9800
C1—H1B	0.9800	C7—H7B	0.9800
C1—H1C	0.9800	C7—H7C	0.9800
C2—C3	1.5256 (17)	C8—C9	1.5256 (18)
C3—C4	1.5284 (17)	C9—C10	1.5301 (17)
C3—C6	1.5370 (16)	C9—H9	1.0000
C3—H3	1.0000	C10—C11	1.498 (2)
C4—C5	1.501 (2)	C11—H11A	0.9800
C5—H5A	0.9800	C11—H11B	0.9800
C5—H5B	0.9800	C11—H11C	0.9800
C2—C1—H1A	109.5	C9—C6—H6B	109.4
C2—C1—H1B	109.5	C3—C6—H6B	109.4
H1A—C1—H1B	109.5	H6A—C6—H6B	108.0
C2—C1—H1C	109.5	C8—C7—H7A	109.5
H1A—C1—H1C	109.5	C8—C7—H7B	109.5
H1B—C1—H1C	109.5	H7A—C7—H7B	109.5
O1—C2—C1	122.37 (12)	C8—C7—H7C	109.5
O1—C2—C3	121.72 (11)	H7A—C7—H7C	109.5
C1—C2—C3	115.90 (10)	H7B—C7—H7C	109.5
C2—C3—C4	109.48 (10)	O3—C8—C7	121.98 (13)
C2—C3—C6	112.33 (10)	O3—C8—C9	120.65 (12)

C4—C3—C6	109.52 (10)	C7—C8—C9	117.37 (12)
C2—C3—H3	108.5	C8—C9—C10	108.47 (10)
C4—C3—H3	108.5	C8—C9—C6	112.08 (10)
C6—C3—H3	108.5	C10—C9—C6	111.04 (10)
O2—C4—C5	122.38 (14)	C8—C9—H9	108.4
O2—C4—C3	121.09 (13)	C10—C9—H9	108.4
C5—C4—C3	116.53 (12)	C6—C9—H9	108.4
C4—C5—H5A	109.5	O4—C10—C11	122.55 (12)
C4—C5—H5B	109.5	O4—C10—C9	120.66 (12)
H5A—C5—H5B	109.5	C11—C10—C9	116.78 (11)
C4—C5—H5C	109.5	C10—C11—H11A	109.5
H5A—C5—H5C	109.5	C10—C11—H11B	109.5
H5B—C5—H5C	109.5	H11A—C11—H11B	109.5
C9—C6—C3	111.34 (9)	C10—C11—H11C	109.5
C9—C6—H6A	109.4	H11A—C11—H11C	109.5
C3—C6—H6A	109.4	H11B—C11—H11C	109.5
O1—C2—C3—C4	106.19 (14)	O3—C8—C9—C10	107.67 (13)
C1—C2—C3—C4	−74.56 (13)	C7—C8—C9—C10	−72.17 (14)
O1—C2—C3—C6	−15.71 (16)	O3—C8—C9—C6	−15.27 (16)
C1—C2—C3—C6	163.54 (11)	C7—C8—C9—C6	164.88 (12)
C2—C3—C4—O2	−20.20 (17)	C3—C6—C9—C8	−70.39 (13)
C6—C3—C4—O2	103.37 (14)	C3—C6—C9—C10	168.12 (10)
C2—C3—C4—C5	160.62 (12)	C8—C9—C10—O4	−11.25 (17)
C6—C3—C4—C5	−75.80 (14)	C6—C9—C10—O4	112.32 (14)
C2—C3—C6—C9	−79.56 (12)	C8—C9—C10—C11	170.22 (11)
C4—C3—C6—C9	158.56 (10)	C6—C9—C10—C11	−66.21 (14)

Fig. 1

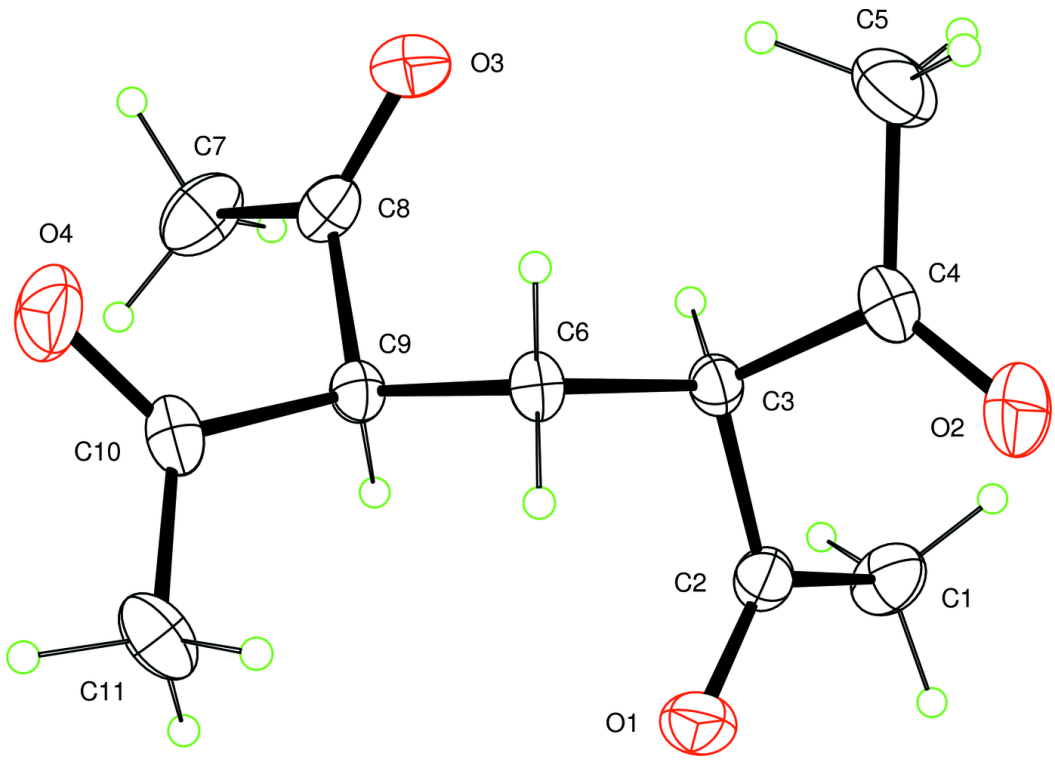

Inorg. Chem. **2008**, *47*, 4433−4435

A Nanoporous Ag−Fe Mixed-Metal−Organic Framework Exhibiting Single-Crystal-to-Single-Crystal Transformations upon Guest Exchange

Yixun Zhang, Banglin Chen,† Frank R. Fronczek, and Andrew W. Maverick*

Department of Chemistry, Louisiana State University, Baton Rouge, Louisiana 70803

Received January 29, 2008

The reaction of solutions of $Fe(Pyac)_3$ [PyacH = 3-(4-pyridyl)-2,4-pentanedione] and $AgNO_3$ produces two types of porous mixed-metal−organic frameworks (M′MOFs). With lower $AgNO_3$ concentrations, the product (**M′MOF1**) has a 2D honeycomb structure with Ag:Fe = 1:1 and pores of ca. 12 × 16 Å. When a higher concentration of $AgNO_3$ is employed, however, the product (**M′MOF2**) has Ag:Fe = 3:2 and a porous 1D ladder structure. A variety of nonpolar solvents serve as guests in **M′MOF2**: with 1,2-$C_6H_4Cl_2$, $[AgNO_3]_3[Fe(Pyac)_3]_2(1,2\text{-}C_6H_4Cl_2)_{5.5}$ (**M′MOF2a**); with C_6H_5Br, $[AgNO_3]_3[Fe(Pyac)_3]_2(C_6H_5Br)_6$ (**M′MOF2b**). M′MOFs **2a** and **2b** can be interconverted by treatment with the appropriate solvent, in *single-crystal-to-single-crystal transformations*.

Porous metal−organic frameworks (MOFs) that are stable upon guest removal and exchange are being studied for a variety of applications.[1] The most stable of such frameworks retain their crystallinity upon guest exchange, as demonstrated by single-crystal X-ray analysis.[2,3] The majority of these robust MOFs are three-dimensional (3D) networks linked by coordination bonds; only a few are based on one-dimensional (1D) frameworks.[3]

Recently, we have applied the emerging preconstructed building block approach[4] to the syntheses of porous mixed-metal−organic frameworks (M′MOFs).[5,6] For example, we have successfully incorporated $Cu(Pyac)_2$ {bis-[3-(4-pyridyl)pentane-2,4-dionato]copper(II)} into porous Cd−Cu M′MOFs that contain unsaturated metal sites in their pores.[5b] However, their 1D and two-dimensional (2D) networks are not stable under guest/solvent exchange. Herein we report the syntheses and crystal structures of two different M′MOFs by the reaction of the tridentate preconstructed building block $Fe(Pyac)_3$ with $AgNO_3$.[7] The new M′MOFs have Ag:Fe ratios of 1:1 (**M′MOF1**, $[AgNO_3][Fe(Pyac)_3](G)_m$, with a 2D trigonal grid structure) and 3:2 (**M′MOF2**, $[AgNO_3]_3[Fe(Pyac)_3]_2(G)_n$, with a 1D ladder structure). Surprisingly, the 1D **M′MOF2**, reinforced by weak Ag···Ag and Ag−nitrate−Ag interactions, is robust and exhibits reversible single-crystal-to-single-crystal transformations upon guest exchange. Also, although M′MOFs **2a** and **2b** contain the same framework, they have slightly different crystal symmetry and their channels have different shapes. This indicates that the framework is not only sufficiently robust to withstand guest exchange but also flexible enough to accommodate variations in guest size and packing.

Domasevitch et al. found that $Fe(Pyac)_3$ shows a substantial deviation from regular trigonal symmetry in the solid state (N···Fe···N 71.7, 135.3, 152.9°). In coordination assemblies of $Fe(Pyac)_3$ with metal ions such as Cd^{2+}, they found a similarly wide range of N···Fe···N angles.[6b] We were interested in M′MOFs constructed from $Fe(Pyac)_3$ because of this compatibility with a variety of site symmetries.

* To whom correspondence should be addressed. E-mail: maverick@lsu.edu.
† Present address: Department of Chemistry, The University of Texas-Pan American, Edinburg, TX 78541.

(1) (a) Eddaoudi, M.; Moler, D. B.; Li, H. L.; Chen, B. L.; Reineke, T. M.; O'Keeffe, M.; Yaghi, O. M. *Acc. Chem. Res.* **2001**, *34*, 319–330. (b) Janiak, C. *Dalton Trans.* **2003**, 2781–2804. (c) Yaghi, O. M.; O'Keeffe, M.; Ockwig, N. W.; Chae, H. K.; Eddaoudi, M.; Kim, J. *Nature* **2003**, *423*, 705–714. (d) Kitagawa, S.; Kitaura, R.; Noro, S. *Angew. Chem., Int. Ed.* **2004**, *43*, 2334–2375.
(2) (a) Choi, H. J.; Suh, M. P. *J. Am. Chem. Soc.* **2004**, *126*, 15844–15851. (b) Dybtsev, D. N.; Chun, H.; Kim, K. *Angew. Chem., Int. Ed.* **2004**, *43*, 5033–5036. (c) Ohmori, O.; Kawano, M.; Fujita, M. *J. Am. Chem. Soc.* **2004**, *126*, 16292–16293. (d) Zeng, M. H.; Feng, X. L.; Chen, X. M. *Dalton Trans.* **2004**, 2217–2223. (e) Halder, G. J.; Kepert, C. J. *J. Am. Chem. Soc.* **2005**, *127*, 7891–7900. (f) Ohmori, O.; Kawano, M.; Fujita, M. *CrystEngComm* **2005**, *7*, 255–259.
(3) (a) Takamizawa, S.; Nakata, E.; Yokoyama, H.; Mochizuki, K.; Mori, W. *Angew. Chem., Int. Ed.* **2003**, *42*, 4331–4334. (b) Lee, E. Y.; Suh, M. P. *Angew. Chem., Int. Ed.* **2004**, *43*, 2798–2801. (c) Wu, C. D.; Lin, W. B. *Angew. Chem., Int. Ed.* **2005**, *44*, 1958–1961.
(4) This is sometimes called the "metalloligand" approach. See, for example, ref 1d and: (a) Garibay, S.; Stork, J. R.; Cohen, S. M. *Prog. Inorg. Chem.* **2008**, in press. (b) Smithenry, D. W.; Wilson, S. R.; Suslick, K. S. *Inorg. Chem.* **2003**, *42*, 7719–7721.
(5) (a) Chen, B. L.; Fronczek, F. R.; Maverick, A. W. *Chem. Commun.* **2003**, 2166–2167. (b) Chen, B. L.; Fronczek, F. R.; Maverick, A. W. *Inorg. Chem.* **2004**, *43*, 8209–8211.
(6) Domasevitch and co-workers have also assembled supramolecular material from $M(Pyac)_n$ complexes: (a) Vreshch, V. D.; Chernega, A. N.; Howard, J. A. K.; Sieler, J.; Domasevitch, K. V. *Dalton Trans.* **2003**, *170*, 7–1711. (b) Vreshch, V. D.; Lysenko, A. B.; Chernega, A. N.; Howard, J. A. K.; Krautscheid, H.; Sieler, J.; Domasevitch, K. V. *Dalton Trans.* **2004**, 2899–2903.
(7) For an early example of the use of $M(Pyac)_3$ in the preparation of supramolecular structures, see: Mackay, L. G.; Anderson, H. L.; Sanders, J. K. M. *Chem. Commun.* **1992**, 43–44.

10.1021/ic800183v CCC: $40.75
Published on Web 05/03/2008

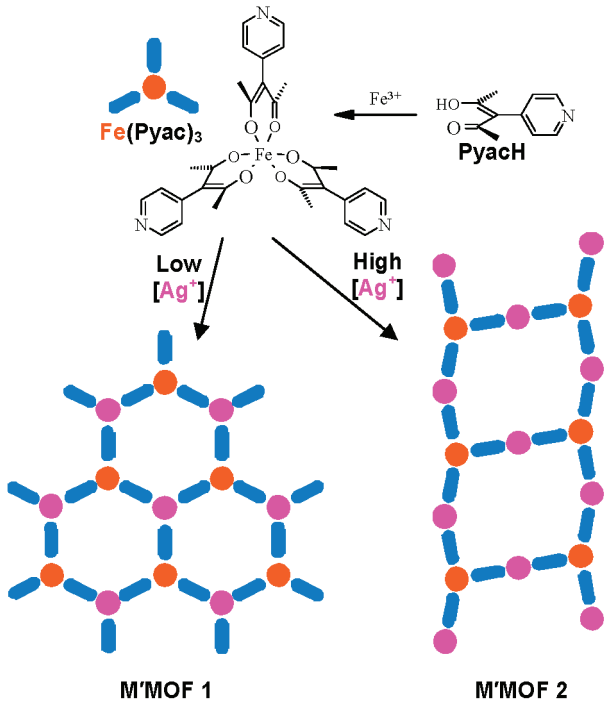

Figure 1. Reaction of the trigonal building block $Fe(Pyac)_3$ with Ag^+ produces two frameworks: 2D honeycomb **M′MOF1** and 1D ladder **M′MOF2**.

We prepared the two new M′MOFs[8] by the reaction of solutions of $Fe(Pyac)_3$ (in nonpolar organic solvents) and $AgNO_3$ (in a small amount of CH_3CN), as shown schematically in Figure 1.

Figure 2 shows a portion of one 2D layer from the crystal structure of **M′MOF1**. The pores in this structure are approximately hexagonal in shape, ca. 11.7 × 16.0 Å.

Crystals of **M′MOF1** become opaque within a few minutes when they are immersed in other solvents. This indicates that the lattice is not stable under solvent (guest) exchange. However, the second type of framework is much more robust: **M′MOF2** ($[AgNO_3]_3[Fe(Pyac)_3]_2(G)_n$), with Ag:Fe = 3:2, forms when a higher concentration of Ag^+ is used. It crystallizes with a variety of guest molecules; the products with 1,2-dichlorobenzene (**M′MOF2a**) and bromobenzene (**M′MOF2b**) are discussed in detail here.

In the **M′MOF2** structure (see Figures 1 and 3), $AgNO_3$ nodes are bridged by tridentate $Fe(Pyac)_3$ building blocks to form a 1D porous ladder with Fe···Fe distances of ca. 19 Å.

When the $Fe(Pyac)_3$ reactant is dissolved in 1,2-$C_6H_4Cl_2$, the product is **M′MOF2a**, $[AgNO_3]_3[Fe(Pyac)_3]_2$(1,2-$C_6H_4Cl_2)_{5.5}$. In this structure, the Fe···Fe distances are 19.50 Å (across the "rungs" of the ladder) and 18.35 and 19.01 Å (along the "uprights"). This framework encloses two crystallographically independent, centrosymmetric pores, labeled **I** and **II** in Figure 3, with cross-sectional areas of ca. 189 and 154 Å^2, respectively.[9] The larger pores (**I**) accommodate six guest molecules, and the smaller pores (**II**) five, for a total of 5.5 guest molecules per $[AgNO_3]_3[Fe(Pyac)_3]_2$ formula unit. These 1D ladders are further interconnected

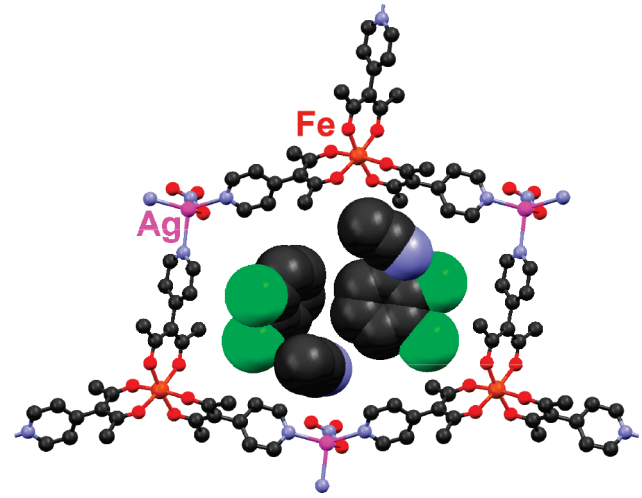

Figure 2. Portion of one 2D layer in the crystal structure of **M′MOF1**, $[AgNO_3][Fe(Pyac)_3](CH_3CN)_2$(1,2-$C_6H_4Cl_2)_2$. H atoms are omitted for clarity.

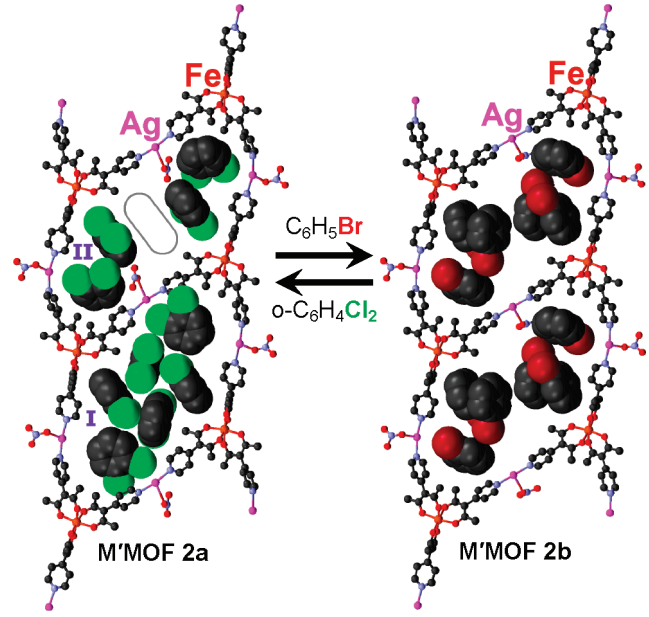

Figure 3. Crystal structures of **M′MOF2a**, $[AgNO_3]_3[Fe(Pyac)_3]_2$(1,2-$C_6H_4Cl_2)_{5.5}$, and **M′MOF2b**, $[AgNO_3]_3[Fe(Pyac)_3]_2(C_6H_5Br)_6$, and reactions representing their single-crystal-to-single-crystal transformation. H atoms and minor components of disordered guest molecules are omitted for clarity. The gray oval in **M′MOF2a** shows the location of the disordered fifth guest molecule in pore **II**.

(8) Crystal data for **M′MOF1**: $[AgNO_3][C_{30}H_{30}FeN_3O_6](C_6H_4Cl_2)_2(CH_3CN)_2$, M = 1130.39, T = 100 K, triclinic, $P\bar{1}$, a = 10.474(2) Å, b = 15.215(3) Å, c = 17.051(4) Å, α = 109.691(10)°, β = 98.453(10)°, γ = 90.388(12)°, V = 2526.0(9) Å^3, Z = 2, D_c = 1.486 g cm^{-3}, μ = 0.944 mm^{-1}, $R1$ [$I > 2\sigma(I)$] = 0.068, $wR2$ (all data) = 0.196. Crystal data for **M′MOF2a**: $[AgNO_3]_3[C_{30}H_{30}FeN_3O_6]_2(C_6H_4Cl_2)_{5.5}$, M = 2487.00, T = 100 K, triclinic, $P\bar{1}$, a = 7.606(2) Å, b = 22.397(6) Å, c = 31.296(11) Å, α = 83.892(10)°, β = 85.753(11)°, γ = 82.90(2)°, V = 5250(3) Å^3, Z = 2, D_c = 1.583 g cm^{-3}, μ = 1.171 mm^{-1}, $R1$ [$I > 2\sigma(I)$] = 0.111, $wR2$ (all data) = 0.346. Crystal data for **M′MOF2b**: $[AgNO_3]_3[C_{30}H_{30}FeN_3O_6]_2(C_6H_5Br)_6$, M = 2620.54, T = 110 K, triclinic, $P\bar{1}$, a = 7.788(4) Å, b = 15.728(9) Å, c = 22.439(15) Å, α = 94.37(3)°, β = 95.32(3)°, γ = 100.51(2)°, V = 2679(3) Å^3, Z = 1, D_c = 1.625 g cm^{-3}, μ = 3.109 mm^{-1}, $R1$ [$I > 2\sigma(I)$] = 0.139, $wR2$ (all data) = 0.382.

(9) The areas of the pores in these structures were estimated by using graphical space-filling models generated by the program *Mercury* (version 1.4.1, Cambridge Crystallographic Data Centre, Cambridge, U.K., 2005; http://www.ccdc.cam.ac.uk/mercury/), with the view perpendicular to the least-squares plane of the 1D ladder framework. The "slice" feature of this program was also used to estimate the perpendicular distances between adjacent layers.

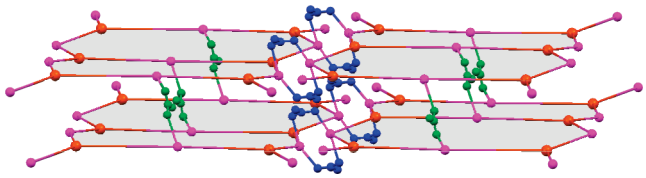

Figure 4. Schematic illustration of the structure of **M′MOF2a**, showing only Ag, Fe, and nitrates. Pores within the 1D ladders are shaded for clarity. Nitrate ions joining one 1D ladder to the next one in the same layer are shown in blue, and those joining one layer to the next in green.

by weak Ag···Ag interactions (3.29 Å) and accompanying bridging nitrate anions (Ag−O 2.61 and 2.72 Å) to form infinite 2D sheets that are separated by ca. 5.9 Å; see Figure 4. Also, the "rung" Ag atoms in adjacent 2D layers are linked by nitrate ions (Ag···O−N−O···Ag 7.61 Å; also shown in Figure 4) to produce an overall 3D network. In this nanoporous Ag−Fe M′MOF (**2a**), 43.1% of the volume is "solvent-accessible".[10]

When the $Fe(Pyac)_3$ reactant is dissolved in bromobenzene instead, the product is $[AgNO_3]_3[Fe(Pyac)_3]_2(C_6H_5Br)_6$, **M′MOF2b** (Figure 3). The structure of **2b** is similar to that of **2a**, with Fe···Fe distances of 19.53 Å (rung) and 18.78 Å (edge), except that all pores in **2b** have the same dimensions and contain six bromobenzene guest molecules. Contacts between the 1D ladders are Ag···Ag (3.25 Å) and Ag−O (2.57 and 2.77 Å). In **2b**, the interlayer separation is ca. 5.7 Å (with Ag···O−N−O···Ag 7.79 Å) and 43.6% of the volume is "solvent-accessible".

M′MOFs **2a** and **2b** can also be prepared when methanol is used as the solvent for $AgNO_3$ (rather than CH_3CN), though in lower yield. Details of this preparation are available as Supporting Information.

The ladder-type M′MOFs **2a** and **2b** are soluble in CH_3CN, *N*,*N*-dimethylformamide, and dimethyl sulfoxide, and cannot be recovered from their solutions easily; this indicates that the framework dissociates in these coordinating solvents. This was surprising at first because CH_3CN is used as a solvent in the synthesis of **2a** and **2b**. However, it is only a minor fraction of the synthesis solvent mixture; see the Supporting Information for details. In contrast, crystals of **2a** and **2b** are insoluble and remain transparent in noncoordinating solvents such as diethyl ether, C_6H_6, chlorobenzene, and 1,2-dichlorobenzene. This observation led us to examine the possibility of guest exchange reactions in these solvents by single-crystal diffraction studies. We find that **2a** and **2b** can be interconverted in single-crystal-to-single-crystal transformations, as illustrated in Figure 3.

As an example of these interconversions, we prepared crystalline **M′MOF2a** directly from $Fe(Pyac)_3$ in a 1,2-dichlorobenzene solution. We chose one single crystal of **2a** from this batch, converted it into **2b** by immersion in bromobenzene, and then converted it back to **2a** by immersion in 1,2-dichlorobenzene again. The transformations were essentially complete in 24 h in both directions, as judged by the successful solution of structures **2a**, **2b**, and **2a** again (after both exchange processes) on the same single crystal, including resolved solvent/guest molecules. This experiment clearly establishes that the nanoporous Ag−Fe **M′MOF2** is robust upon solvent exchange. In other words, **M′MOF2** retains its framework connectivity despite the fact that the different guests lead to noticeable changes in the pore geometry and symmetry, Fe···Fe and Ag···Ag distances, and interlayer separations.

Compounds **2a** and **2b** are unusual examples in which shorter- and longer-range Ag···Ag interactions[11] serve to connect 1D units in the second and third dimensions. These interactions may contribute to the stability of the lattice under guest exchange. Taking advantage of the richness of the preconstructed building block approach and interactions such as Ag···Ag, we expect that a variety of porous M′MOFs will be possible. We are now studying the range of guest molecules that can be accommodated within the framework of **M′MOF2** and exploring the potential applications of these M′MOFs in sensors, gas storage, and catalysis.

Acknowledgment. This work was supported by the Department of Energy (Grant DE-FG02-01ER15267) and by the American Chemical Society Petroleum Research Fund (37234-AC3).

Supporting Information Available: X-ray structure data in CIF format and details of experimental procedures. This material is available free of charge via the Internet at http://pubs.acs.org.

IC800183V

(10) Spek, A. L. *J. Appl. Crystallogr.* **2003**, *36*, 7–13.

(11) (a) Pyykkö, P. *Chem. Rev.* **1997**, *97*, 597–636. (b) Wang, Q. M.; Mak, T. C. W. *J. Am. Chem. Soc.* **2001**, *123*, 7594–7600.

Organosilicon-Based Multifunctional β-Diketones and their Rhodium and Iridium Complexes

Chandi Pariya,* Yoseph S. Marcos, Yixun Zhang, Frank R. Fronczek, and Andrew W. Maverick*

Department of Chemistry, Louisiana State University, Baton Rouge, Louisiana 70803

Received December 9, 2007

Six new organosilicon-based bis-, tris-, and tetrakis(β-diketones) and their Rh^I(COD) and Ir^I(COD) (COD = 1,5-cyclooctadiene) complexes have been prepared and characterized. The β-diketones, $(CH_3)_{4-n}Si(4\text{-}C_6H_4CH(COR)_2)_n$ (n = 2, 3, 4; R = Me, Et), were prepared from the corresponding aldehydes $(CH_3)_{4-n}Si(4\text{-}C_6H_4CHO)_n$ by reaction with trimethyl phosphite-α-diketone adducts. Reaction with $[M(COD)(\mu\text{-}Cl)]_2$ (M = Rh and Ir) produces the Rh and Ir complexes, three of which have been characterized by X-ray analysis. The β-diketone moieties are ca. 13.3 Å apart, which leads to intramolecular M···M distances in the complexes averaging ca. 15.6 Å. The present organosilicon-based route is expected to be useful for the construction of a variety of polytopic molecules containing either β-diketone or other functional groups and polygonal or polyhedral metal complexes based on them.

Introduction

The design and synthesis of metal-organic compounds is a rapidly growing area of study because there are many promising fragments available for the construction of supramolecular materials.[1−6] These materials are most often prepared by first synthesizing multifunctional organic ligands (sometimes called "linkers" or "building blocks") and then treating them with metal ions. We are interested in building blocks based on β-diketonate ligands, because they offer the stability of chelation as well as the opportunity for symmetrical placement of substituents.[7]

We now report a family of tetrahedral building blocks that have two, three, and four β-diketone moieties; these react further with metal salts to form polynuclear metal complexes as shown in Figure 1. The building blocks are designed for the synthesis of structurally defined metal-organic frameworks (MOFs), including both molecular and network-solid materials. The present work represents the first steps toward achieving that goal. We used organosilicon chemistry because it provides a simple and efficient synthetic route to multifunctional β-diketones. We also converted the new β-diketones into their polynuclear Rh and Ir complexes, which are stable in the solid state. Three of the Rh complexes have also been characterized by X-ray crystallography, which reveals intramolecular Si···Rh and Rh···Rh distances averaging 9.6 and 15.6 Å, respectively, and Rh···Si···Rh angles averaging ca. 109°, as expected for approximately tetrahedral structures. The approach outlined here is expected to be valuable for the preparation of molecules containing both β-diketone and other functional groups at well-defined distances and orientations and for their subsequent conversion to polynuclear metal complexes.

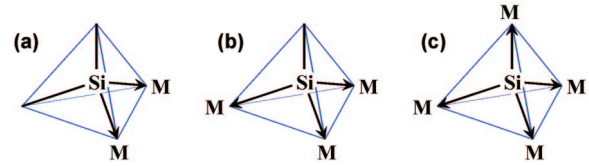

Figure 1. Sketch of the polynuclear metal complexes that can form when tetrahedral organosilicon-based (a) bis-, (b) tris-, and (c) tetrakis(β-diketones) react with metal ions.

Experimental Section

General Considerations. Reagents were used as received: 4-bromobenzaldehyde dimethyl acetal and $SiCl_4$ (Aldrich), dimethyldichlorosilane and methyltrichlorosilane (Gelest Inc.), $CDCl_3$ (Fisher), $[Rh(COD)(\mu\text{-}Cl)]_2$ (Strem), and $[Ir(COD)(\mu\text{-}Cl)]_2$ (COD = 1,5-cyclooctadiene) (Pressure Chemicals). Column chromatography was carried out with Sorbent Technologies silica gel (230−450 mesh). NMR spectra were recorded on Bruker (250, 300, or 400 MHz) or Varian (500 MHz) spectrometers, with $CDCl_3$ as solvent unless otherwise noted. Elemental analyses were performed by M-H-W Laboratories, Phoenix, AZ. The phospholenes 2,2,2-trimethoxy-4,5-dimethyl-[8] and 2,2,2-trimethoxy-4,5-diethyl-1,3,2-dioxaphospholene,[9] and bis(4-formylphenyl)dimethylsilane ($(CH_3)_2Si(4\text{-}C_6H_4CHO)_2$),[10] were prepared by literature methods.

Tris(4-formylphenyl)methylsilane ($CH_3Si(4\text{-}C_6H_4CHO)_3$). 4-Bromobenzaldehyde dimethyl acetal (12.02 g, 52.0 mmol) was dissolved in dry THF (150 mL) under nitrogen. n-BuLi solution in hexane (1.6 M, 32.5 mL, 52 mmol) was added at −78 °C over 40 min. After stirring for an additional 90 min at −78 °C, methyl-

* Corresponding author. E-mail: maverick@lsu.edu.

(1) Kajitani, H.; Tanabe, Y.; Kuwata, S.; Iwasaki, M.; Ishii, Y. *Organometallics* **2005**, *24*, 2251–2254.
(2) Grote, Z.; Scopelliti, R.; Severin, K. *J. Am. Chem. Soc.* **2004**, *126*, 16959–16972.
(3) Kraft, S.; Beckhaus, R.; Haase, D.; Saak, W. *Angew. Chem., Int. Ed.* **2004**, *43*, 1583–1587.
(4) Swiegers, G. F.; Malefetse, T. J. *Coord. Chem. Rev.* **2002**, *225*, 91–121.
(5) Leininger, S.; Olenyuk, B.; Stang, P. J. *Chem. Rev.* **2000**, *100*, 853–907.
(6) Klausmeyer, K. K.; Rauchfuss, T. B.; Wilson, S. R. *Angew. Chem., Int. Ed.* **1998**, *37*, 1694–1696.
(7) Chen, B.; Fronczek, F. R.; Maverick, A. W. *Inorg. Chem.* **2004**, *43*, 8209–8211.
(8) Ramirez, F.; Ramanathan, N.; Desai, N. B. *J. Am. Chem. Soc.* **1962**, *84*, 1317–1318.
(9) Pariya, C.; Sparrow, C. R.; Back, C. K.; Sandí, G.; Fronczek, F. R.; Maverick, A. W. *Angew. Chem., Int. Ed.* **2007**, *46*, 6305–6308.
(10) Kumagai, T.; Itsuno, S. *Tetrahedron: Asymmetry* **2001**, *12*, 2509–2516.

10.1021/om701233a CCC: $40.75
Publication on Web 08/14/2008

trichlorosilane (1.40 mL, 13.2 mmol) was slowly added to the above suspension. The reaction mixture was stirred for an additional 2 h at −78 °C and then overnight while it returned to room temperature. The reaction mixture was quenched with 2 M HCl (60 mL) and extracted with ether (3 × 50 mL). The ether solution was washed with brine, dried over $MgSO_4$, and evaporated to give the oily intermediate acetal $CH_3Si(4\text{-}C_6H_4CH(OCH_3)_2)_3$, which was hydrolyzed without purification. The oil was dissolved in 100 mL of THF/2 M HCl (1:1 v/v) and the mixture refluxed for 2 h. After cooling to room temperature, the reaction mixture was poured into saturated $NaHCO_3$(aq) (50 mL) and extracted with ether (3 × 50 mL). The combined extract was washed with brine, dried with $MgSO_4$, filtered, and concentrated under reduced pressure, giving an oil. The crude product was purified by column chromatography (hexane/ethyl acetate, 3:1) to give tris(4-formylphenyl)methylsilane as a colorless liquid, 2.67 g (56%). ^{1}H NMR: δ 10.07 (s, 3H, CHO); 7.90, 7.68 (AB, 12H, aromatic CH); 0.97 (s, 3H, $SiCH_3$). ^{13}C NMR: δ 192.6, 142.63, 137.4, 135.9, 129.2, −3.7. ^{29}Si NMR: −11.3. FTIR: 3030, 2831, 1698, 1595, 1209, 838 cm^{-1}. Anal. Calcd for $C_{22}H_{18}O_3Si$ (M = 358.46): C, 73.71; H, 5.06. Found: C, 73.45; H, 5.11.

Tetrakis(4-formylphenyl)silane ($Si(4\text{-}C_6H_4CHO)_4$). 4-Bromobenzaldehyde dimethyl acetal (12.02 g, 52.0 mmol) was dissolved in dry THF (150 mL) under nitrogen. n-BuLi solution in hexane (1.6 M, 32.5 mL, 52 mmol) was added slowly at −78 °C over 45 min. After stirring the mixture for 2 h at −78 °C, tetrachlorosilane (1.14 mL, 10 mmol) was slowly added to the above suspension. The remainder of the procedure up to the isolation of the crude product was the same as that for $CH_3Si(4\text{-}C_6H_4CHO)_3$, except that the crude $Si(4\text{-}C_6H_4CHO)_4$ was obtained as an off-white solid. This was recrystallized from hexane/ethyl acetate (3:1) to give ($Si(4\text{-}C_6H_4CHO)_4$) as a white solid, 3.40 g (75%), mp 200−204 °C. ^{1}H NMR: δ 10.09 (s, 4H, C*H*O); 7.94, 7.73 (*AB*, 16H, aromatic C*H*). ^{13}C NMR: δ 192.3, 139.7, 137.9, 137.0, 129.3. ^{29}Si NMR: −16.9. FTIR: 3057, 2830, 1701, 1597, 1208, 837 cm^{-1}. Anal. Calcd for $C_{28}H_{20}O_4Si$ (M = 448.54): C, 74.98; H, 4.49. Found: C, 74.72; H, 4.60.

3,3′-[Dimethylsilylenebis(1,4-phenylene)]bis(2,4-pentanedione), $(CH_3)_2Si(phacH)_2$ (1). A mixture of bis(4-formylphenyl)dimethylsilane (2.19 g, 8.16 mmol) and 2,2,2-trimethoxy-4,5-dimethyl-1,3,2-dioxaphospholene (4.29 g, 20.4 mmol) was stirred at room temperature under argon. After 24 h, 50 mL of methanol was added, and the mixture was refluxed under nitrogen for 2 h. The solvent was removed under reduced pressure, and the residue was recrystallized from methanol to give **1** as a white solid, 1.95 g (58%), mp 155−157 °C. ^{1}H NMR: δ 16.70 (s, 2H, O*H*); 7.55, 7.18 (*AB*, 8H, aromatic C*H*); 1.92 (s, 12H, CH_3); 0.60 (s, 6H, $SiCH_3$). ^{13}C NMR: δ 191.1, 137.9, 137.8, 134.8, 130.7, 115.3, 24.5, −2.0. ^{29}Si NMR: δ 10.0. Anal. Calcd for $C_{24}H_{28}O_4Si$ (M = 408.55): C, 70.55; H, 6.91. Found: C, 70.70; H, 7.02.

4,4′-[Dimethylsilylenebis(1,4-phenylene)]bis(3,5-heptanedione), $(CH_3)_2Si(phprH)_2$ (2). A mixture of bis(4-formylphenyl)dimethylsilane (1.00 g, 3.73 mmol) and 2,2,2-trimethoxy-4,5-diethyl-1,3,2-dioxaphospholene (2.66 g, 11.2 mmol) was stirred at room temperature under argon. After 18 h, 20 mL of methanol was added, and the mixture was refluxed under nitrogen for 3 h. The solvent was removed under reduced pressure, and the residue was recrystallized from methanol to give **2** as a white solid, 0.71 g (41%), mp 98−99 °C. ^{1}H NMR: δ 16.72 (s, 2H, O*H*); 7.52, 7.15 (*AB*, 8H, aromatic C*H*); 2.11 (m, 8H, CH_2) 1.01 (t, 12H, CH_3); 0.56 (s, 6H, $SiCH_3$). ^{13}C NMR: δ 194.1, 137.2, 137.0, 134.5, 130.7, 113.8, 29.9, 9.6, −2.2. ^{29}Si NMR: δ 13.1. Anal. Calcd for $C_{28}H_{36}O_4Si$ (M = 464.66): C, 72.37; H, 7.81. Found: C, 72.21; H, 7.64.

3,3′,3″-[Methylsilylidynetris(1,4-phenylene)]tris(2,4-pentanedione), $CH_3Si(phacH)_3$ (3). A mixture of tris(4-formylphenyl)methylsilane (1.76 g, 4.91 mmol) and 2,2,2-trimethoxy-4,5-dimethyl-1,3,2-dioxaphospholene (4.60 g, 21.9 mmol) was stirred at room temperature under argon. After 20 h, 60 mL of methanol was added, and the mixture was refluxed under nitrogen for 3 h. During this time a white solid formed. It was collected and air-dried. The filtrate was concentrated under reduced pressure to about 10 mL and filtered, giving a second crop of product. The combined product was recrystallized from methanol to give **3** as a white solid, 1.56 g (56%), mp 212−215 °C. ^{1}H NMR: δ 16.71 (s, 3H, O*H*); 7.55, 7.21 (*AB*, 12H, aromatic C*H*); 1.93 (s, 18H, CH_3); 0.91 (s, 3H, $SiCH_3$). ^{13}C NMR: δ 191.1, 138.4, 135.8, 135.1, 130.9, 115.3, 24.5, −2.9. ^{29}Si NMR: δ 12.5. Anal. Calcd for $C_{34}H_{36}O_6Si$ (M = 568.72): C, 71.80; H, 6.38. Found: C, 72.00; H, 6.47.

4,4′,4″-[Methylsilylidynetris(1,4-phenylene)]tris(3,5-heptanedione), $CH_3Si(phprH)_3$ (4). A mixture of tris(4-formylphenyl)methylsilane (0.390 g, 1.09 mmol) and 2,2,2-trimethoxy-4,5-diethyl-1,3,2-dioxaphospholene (1.00 g, 4.20 mmol) was stirred at room temperature under argon. After 20 h, 10 mL of methanol was added, and the mixture was refluxed under nitrogen for 3 h. Then solvent was removed under reduced pressure, and the residue was recrystallized from methanol to give **4** as a white solid, 0.385 g (54%), mp 130−132 °C. ^{1}H NMR: δ 16.76 (s, 3H, O*H*); 7.55, 7.21 (*AB*, 12H, aromatic C*H*); 2.16 (m, 12H, CH_2) 1.05 (t, 18H, CH_3), 0.91 (s, 3H, $SiCH_3$). ^{13}C NMR: δ 194.0, 137.7, 135.6, 134.8, 130.8, 113.7, 30.0, 9.6, −3.0. ^{29}Si NMR: δ 12.4. Anal. Calcd for $C_{40}H_{48}O_6Si$ (M = 652.87): C, 73.58; H, 7.41. Found: C, 73.47; H, 7.37.

3,3′,3″,3‴-[Silanetetrayltetrakis(1,4-phenylene)]tetrakis(2,4-pentanedione), $Si(phacH)_4$ (5). A mixture of tetrakis(4-formylphenyl)silane (2.00 g, 4.46 mmol) and 2,2,2-trimethoxy-4,5-dimethyl-1,3,2-dioxaphospholene (5.60 g, 26.8 mmol) was stirred at room temperature under argon. After 20 h, 60 mL of methanol was added, and the mixture was refluxed under nitrogen for 3 h. During this time a white solid appeared. After cooling, the mixture was filtered, giving solid **5** as a pure white solid compound, 1.91 g (59%), mp >220 °C. ^{1}H NMR: δ 16.72 (s, 4H, O*H*); 7.61, 7.26 (*AB*, 16H, aromatic C*H*), 1.94 (s, 24H, CH_3). ^{13}C NMR: δ 191.0, 138.8, 136.9, 133.1, 131.0, 115.2, 24.5. ^{29}Si NMR: δ 16.6. Anal. Calcd for $C_{44}H_{44}O_8Si$ (M = 728.90): C, 72.50; H, 6.08. Found: C, 72.36; H, 6.25.

4,4′,4″,4‴-[Silanetetrayltetrakis(1,4-phenylene)]tetrakis(3,5-heptanedione), $Si(phprH)_4$ (6). A mixture of tetrakis(4-formylphenyl)silane (0.80 g, 1.78 mmol) and 2,2,2-trimethoxy-4,5-diethyl-1,3,2-dioxaphospholene (3.20 g, 13.43 mmol) was stirred at room temperature under argon. After 20 h, 20 mL of methanol was added, and the mixture was refluxed under nitrogen for 3 h. During this time a white solid appeared, which was collected and dried under vacuum. Yield: 0.925 g (62%), mp 152−155 °C. ^{1}H NMR: δ 16.74 (s, 4H, O*H*); 7.57, 7.25 (m, 16H, aromatic C*H*); 2.14 (m, 16H, CH_2); 1.04 (m, 24H, CH_3). ^{13}C NMR: δ 194.2, 138.4, 136.1, 133.0, 130.4, 113.9, 30.2, 9.1. ^{29}Si NMR: δ 16.9. Anal. Calcd for $C_{52}H_{60}O_8Si$ (M = 841.11): C, 74.25; H, 7.19. Found: C, 73.89; H, 6.99.

General Synthesis of the Complexes 7−18. The required $[M(COD)(\mu\text{-}Cl)]_2$ (M = Rh or Ir) (0.200 mmol) and a stoichiometric amount of β-diketone (chosen from **1**−**6**) were combined under N_2 in diethyl ether (20 mL), and aqueous KOH (1 mL, 1 M) was then added. The solution was stirred for 25−45 min. During this time a yellow solid precipitated. It was collected and washed with 2-propanol and pentane and dried. The crude product was recrystallized either from diethyl ether or a diethyl ether/$CHCl_3$ mixture.

Bis(1,5-cyclooctadiene)[μ-[3,3′-[dimethylsilylenebis(1,4-phenylene)]bis(2,4-pentanedionato)]dirhodium, $(CH_3)_2Si(phac\text{-}Rh(COD))_2$ (7). Yield: 0.135 g (81%); dec 240 °C. ^{1}H NMR: δ 7.48, 7.12 (*AB*, 8H, aromatic C*H*), 4.13 (s, 8H, =C*H*), 2.50 (m, 8H, CH_2), 1.87 (m, 8H, CH_2), 1.72 (s, 12H, CH_3), 0.55 (s, 6H,

Scheme 1. Synthesis of Aldehydes

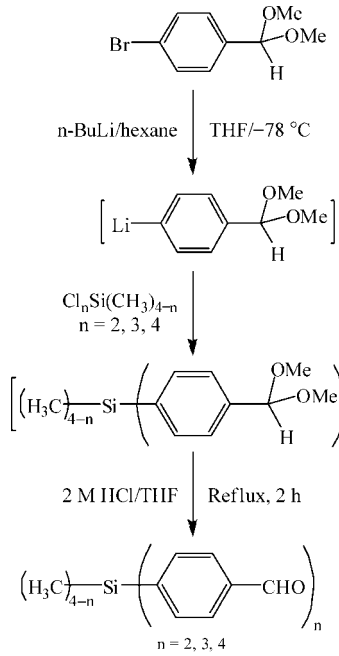

Scheme 2. Synthesis of β-Diketones 1−6

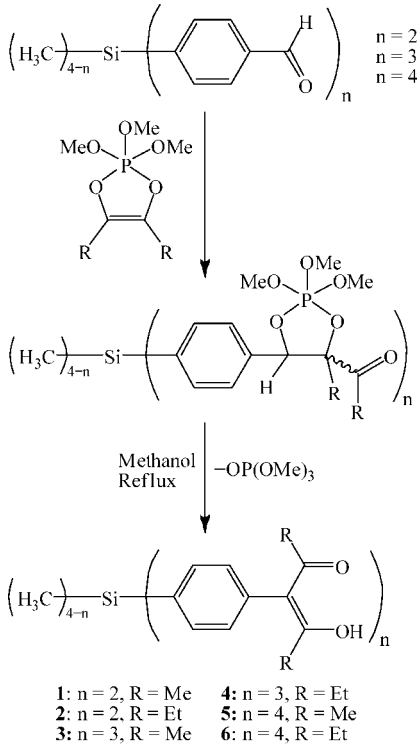

SiCH_3). ^{13}C NMR: δ 185.8, 142.8, 136.4, 134.7, 131.2, 114.4, 76.8, 30.5, 28.6, −1.9. ^{29}Si NMR: δ 8.8. Anal. Calcd for $C_{40}H_{50}O_4Rh_2Si$ (M = 828.72): C, 57.97; H, 6.08. Found: C, 58.06; H, 5.96.

Bis(1,5-cyclooctadiene)[μ-[3,3′-[dimethylsilylenebis(1,4-phenylene)]bis(2,4-pentanedionato)]diiridium, $(CH_3)_2$Si(phac-Ir(COD))$_2$ (8). Yield: 0.117 g (58%); dec 280 °C. ^{1}H NMR: δ 7.52, 7.13 (*AB*, 8H, aromatic C*H*), 4.04 (s, 8H, =C*H*), 2.31 (m, 8H, CH_2), 1.78 (s, 12H, CH_3), 1.70 (m, 8H, CH_2), 0.56 (s, 6H, SiCH_3). ^{13}C NMR: δ 185.7, 141.8, 136.9, 134.9, 131.0, 116.1, 59.9, 31.4, 28.6, −1.9. ^{29}Si NMR: δ 10.0. Anal. Calcd for $C_{40}H_{50}O_4Ir_2Si$ (M = 1007.30): C, 47.69; H, 5.00. Found: C, 47.90; H, 4.99.

Bis(1,5-cyclooctadiene)[μ-[4,4′-[dimethylsilylenebis(1,4-phenylene)]bis(3,5-heptanedionato)]dirhodium, $(CH_3)_2$Si(phpr-Rh(COD))$_2$ (9). Yield: 0.135 g (76%); dec 198 °C. ^{1}H NMR: δ 7.48, 7.12 (*AB*, 8H, aromatic C*H*); 4.13 (s, 8H, =C*H*), 2.50 (m, 8H, CH_2), 1.92 (m, 16H, CH_2 and CH_2CH$_3$); 0.85 (t, 12H, CH_3); 0.56 (s, 6H, SiCH_3). ^{13}C NMR: δ 188.6, 142.1, 135.7, 134.4, 131.6, 113.2, 76.9, 33.2, 30.5, 10.4, −2.6. ^{29}Si NMR: δ 13.8. Anal. Calcd for $C_{44}H_{58}O_4Rh_2Si$ (M = 884.83): C, 59.73; H, 6.61. Found: C, 59.52; H, 6.70.

Bis(1,5-cyclooctadiene)[μ-[4,4′-[dimethylsilylenebis(1,4-phenylene)]bis(3,5-heptanedionato)]diiridium, $(CH_3)_2$Si(phpr-Ir(COD))$_2$ (10). Yield: 0.120 g (56%); dec 190 °C. ^{1}H NMR: δ 7.48, 7.12 (*AB*, 8H, aromatic C*H*); 4.04 (s, 8H, =C*H*), 2.31 (m, 8H, CH_2), 1.99 (q, 8H, CH_2CH$_3$), 1.70 (d, 8H, CH_2), 0.93 (t, 12H, CH_3); 0.57 (s, 6H, SiCH_3). ^{13}C NMR: δ 188.5, 141.3, 136.6, 135.1, 132.2, 115.0, 60.8, 33.3, 31.4, 10.9, −3.1. ^{29}Si NMR: δ 12.3. Anal. Calcd for $C_{44}H_{58}O_4Ir_2Si$ (M = 1063.45): C, 49.69; H, 5.50. Found: C, 49.90; H, 5.49.

Tris(1,5-cyclooctadiene)[μ-[3,3′,3″-[methylsilylidynetris(1,4-phenylene)]tris(2,4-pentanedionato)]trirhodium, CH_3Si(phac-Rh(COD))$_3$ (11). Yield: 0.147 g (92%); dec 288 °C. ^{1}H NMR: δ 7.46, 7.14 (*AB*, 12H, aromatic C*H*), 4.14 (s, 12H, =C*H*), 2.49 (m, 12H, CH_2), 1.87 (m, 12H, CH_2), 1.73 (s, 18H, CH_3), 0.83 (s, 3H, SiCH_3). ^{13}C NMR: δ 185.7, 143.1, 135.8, 134.3, 131.3, 114.3, 76.8, 30.5, 28.6, −2.7. ^{29}Si NMR: δ 13.3. Anal. Calcd for $C_{58}H_{69}O_6Rh_3Si$ (M = 1198.97): C, 58.10; H, 5.80. Found: C, 57.92; H, 5.81.

Tris(1,5-cyclooctadiene)[μ-[3,3′,3″-[methylsilylidynetris(1,4-phenylene)]tris(2,4-pentanedionato)]triiridium, CH_3Si(phac-Ir(COD))$_3$ (12). Yield: 0.141 g (72%); dec 276 °C. ^{1}H NMR: δ 7.50, 7.15 (*AB*, 12H, aromatic C*H*), 4.04 (s, 12H, =C*H*), 2.31 (m, 12H, CH_2), 1.80 (s, 18H, CH_3), 1.70 (m, 12H, CH_2), 0.85 (s, 3H, SiCH_3). ^{13}C NMR: δ 185.7, 142.2, 136.0, 134.8, 131.2, 116.1, 60.0, 31.4, 28.7, −2.7. ^{29}Si NMR: δ 13.6. Anal. Calcd for $C_{58}H_{69}Ir_3O_6Si$ (M = 1466.88): C, 47.49; H, 4.74. Found: C, 47.39; H, 4.70.

Tris(1,5-cyclooctadiene)[μ-[4,4′,4″-[methylsilylidynetris(1,4-phenylene)]tris(3,5-heptanedionato)]trirhodium, CH_3Si(phpr-Rh(COD))$_3$ (13). Yield: 0.164 g (95%); dec 220 °C. ^{1}H NMR: δ 7.47, 7.14 (*AB*, 12H, aromatic C*H*); 4.11 (s, 12H, =C*H*), 2.50 (m,

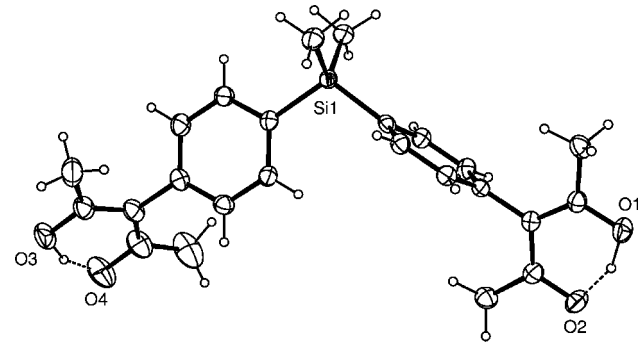

Figure 2. Molecular structure of $(CH_3)_2$Si(phacH)$_2$ (**1**) (ellipsoids shown at the 50% probability level).

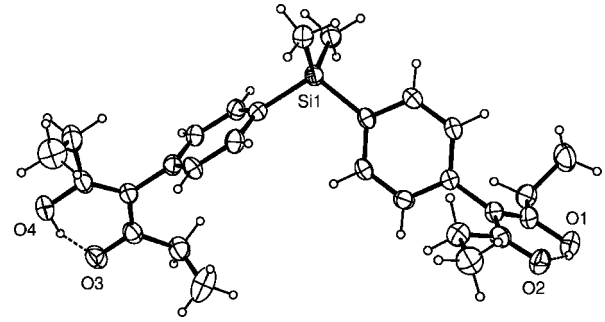

Figure 3. Molecular structure of $(CH_3)_2$Si(phprH)$_2$ (**2**) (ellipsoids shown at the 50% probability level). One of two crystallographically independent molecules in the asymmetric unit is shown.

12H, CH_2), 1.92 (m, 24H, CH_2 and CH_2CH$_3$); 0.85 (m, 21H, CH_3 and SiCH_3). ^{13}C NMR: δ 188.6, 142.1, 135.7, 134.3, 131.6, 113.2, 76.8, 33.2, 30.5, 10.4, −2.6. ^{29}Si NMR: δ 12.6. Anal. Calcd for $C_{64}H_{81}Rh_3O_6Si$ (M = 1283.13): C, 59.91; H, 6.36. Found: C, 59.73; H, 6.33.

Tris(1,5-cyclooctadiene)[μ-[4,4′,4″-[methylsilylidynetris(1,4-phenylene)]tris(3,5-heptanedionato)]triiridium, $CH_3Si(phpr\text{-}Ir(COD))_3$ (14). Yield: 0.141 g (68%); dec 290 °C. ^{1}H NMR: δ 7.51, 7.15 (*AB*, 12H, aromatic C*H*); 4.05 (s, 12H, =C*H*), 2.31 (m, 12H, CH_2), 2.00 (m, 12H, CH_2CH$_3$) 1.68 (m, 12H, CH_2); 0.91 (m, 21H, CH_3 and SiCH_3). ^{13}C NMR: δ 188.6, 136.7, 135.1, 132.3, 130.8, 115.0, 60.8, 33.4, 31.4, 11.0. ^{29}Si NMR: δ 13.0. Anal. Calcd for $C_{64}H_{81}Ir_3O_6Si$ (M = 1551.06): C, 49.56; H, 5.26. Found: C, 49.70; H, 5.49.

Tetrakis(1,5-cyclooctadiene)[μ-[3,3′,3″,3‴-[silanetetrayltetrakis(1,4-phenylene)]tetrakis(2,4-pentanedionato)]tetrarhodium, $Si(phac\text{-}Rh(COD))_4$ (15). Yield: 0.071 g (45%); mp 168−174 °C. ^{1}H NMR: δ 7.51, 7.16 (*AB*, 16H, aromatic C*H*), 4.13 (s, 16H, =C*H*), 2.48 (m, 16H, CH_2), 1.88 (m, 16H, CH_2), 1.74 (s, 24H, CH_3). This compound was not sufficiently stable in $CDCl_3$ solution for recording a high-quality ^{13}C NMR spectrum. ^{29}Si NMR: δ 16.0. Anal. Calcd for $C_{76}H_{88}O_8Rh_4Si$ (M = 1569.21): C, 58.17; H, 5.65. Found: C, 57.88; H, 5.76.

Tetrakis(1,5-cyclooctadiene)[μ-[3,3′,3″,3‴-[silanetetrayltetrakis(1,4-phenylene)]tetrakis(2,4-pentanedionato)]tetrairidium, $Si(phac\text{-}Ir(COD))_4$ (16). Yield: 0.113 g (58%). ^{1}H NMR: δ 7.55, 7.18 (*AB*, 16H, aromatic C*H*), 4.04 (s, 16H, =C*H*), 2.31 (m, 16H, CH_2), 1.82 (s, 24H, CH_3), 1.71 (m, 16H, CH_2). This compound was not sufficiently stable in $CDCl_3$ solution for recording high-quality ^{13}C or ^{29}Si NMR spectra. Anal. Calcd for $C_{76}H_{88}Ir_4O_8Si$ (M = 1926.46): C, 47.38; H, 4.60. Found: C, 47.01; H, 4.73.

Tetrakis(1,5-cyclooctadiene)[μ-[4,4′,4″,4‴-[silanetetrayltetrakis(1,4-phenylene)]tetrakis(3,5-heptanedionato)]tetrarhodium, $Si(phpr\text{-}Rh(COD))_4$ (17). Yield: 0.148 g (88%); dec 246 °C. ^{1}H NMR: δ 7.52, 7.17 (*AB*, 16H, aromatic C*H*), 4.14 (s, 16H, =C*H*), 2.50 (m, 16H, CH_2), 2.00 (m, 16H, CH_2), 1.90 (q, 16H, CH_2CH$_3$), 0.86 (t, 24H, CH_3). ^{13}C NMR: δ 188.5, 142.5, 136.8, 132.6, 131.8, 113.2, 76.1, 33.2, 30.5, 10.4. ^{29}Si NMR: δ 17.2. Anal. Calcd for $C_{84}H_{104}O_8Rh_4Si$ (M = 1681.43): C, 60.00; H, 6.23. Found: C, 60.33; H, 6.45.

Tetrakis(1,5-cyclooctadiene)[μ-[4,4′,4″,4‴-[silanetetrayltetrakis(1,4-phenylene)]tetrakis(3,5-heptanedionato)]tetrairidium, $Si(phpr\text{-}Ir(COD))_4$ (18). Yield: 0.108 g (53%); dec 204 °C. ^{1}H NMR: δ 7.53, 7.17 (*AB*, 16H, aromatic C*H*), 4.04 (s, 16H, =C*H*), 2.33 (m, 16H, CH_2), 2.04 (q, 16H, CH_2CH$_3$), 1.72 (m, 16H, CH_2), 0.93 (t, 24H, CH_3). ^{13}C NMR: δ 188.4, 141.6, 138.3, 136.9,

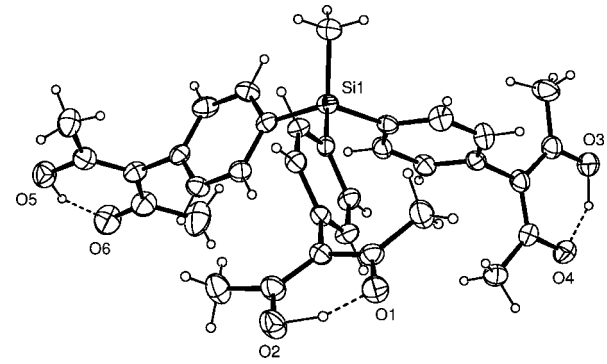

Figure 4. Molecular structure of $CH_3Si(phacH)_3$ (**3**) (ellipsoids shown at the 50% probability level).

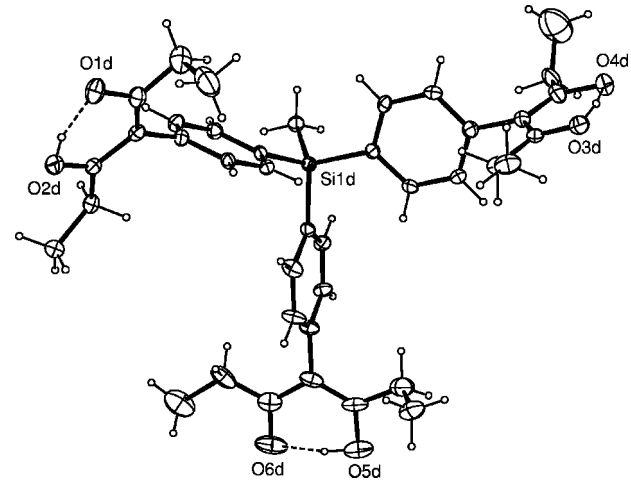

Figure 5. Molecular structure of $CH_3Si(phprH)_3$ (**4**) (ellipsoids shown at the 20% probability level). One of four crystallographically independent molecules in the asymmetric unit is shown.

Table 1. Crystal Data and Structure Refinement for Multifunctional β-Diketones 1−4

	1	2	3	4
formula	$C_{24}H_{28}O_4Si$	$C_{28}H_{36}O_4Si$	$C_{34}H_{36}O_6Si$	$C_{40}H_{48}O_6Si$
fw	408.55	464.66	568.72	652.87
cryst size, mm	0.30 × 0.27 × 0.25	0.25 × 0.11 × 0.10	0.25 × 0.10 × 0.07	0.27 × 0.22 × 0.07
cryst syst	triclinic	triclinic	monoclinic	triclinic
space group	$P\bar{1}$	$P\bar{1}$	$P2_1/n$	$P\bar{1}$
a, Å	8.016(2)	9.845(2)	7.3493(10)	13.336(2)
b, Å	8.044(2)	16.663(3)	22.774(5)	22.955(3)
c, Å	17.791(4)	17.247(4)	18.640(5)	25.885(4)
α, deg	87.401(8)	68.294(10)	90	70.796(8)
β, deg	83.350(8)	89.725(8)	91.177(7)	78.854(8)
γ, deg	81.920(11)	83.072(9)	90	89.768(9)
V, Å^3	1127.7(5)	2607.1(10)	3119.2(12)	7326.8(18)
Z	2	4	4	8
D_{calc}, Mg/m^3	1.203	1.184	1.211	1.184
T, K	105	110	105	110
θ range, deg	2.5−27.9	2.5−24.4	2.5−27.5	2.5−23.0
μ, mm^{-1}	0.130	0.120	0.118	0.109
no. of measd reflns	33 395	16 020	59 143	86 197
no. of indep reflns	5394	8538	7145	20 205
no. of reflns $I > 2\sigma(I)$	4157	4921	3753	9984
no. of params	275	623	387	1726
goodness of fit	1.034	1.022	1.003	1.028
R ($I > 2\sigma(I)$)	0.042	0.060	0.056	0.095
wR_2	0.111	0.134	0.134	0.287
lgst diff, e Å^{-3}	0.29	0.22	0.30	0.93

Scheme 3. Synthesis of Rhodium(I) and Iridium(I) Complexes 7−18

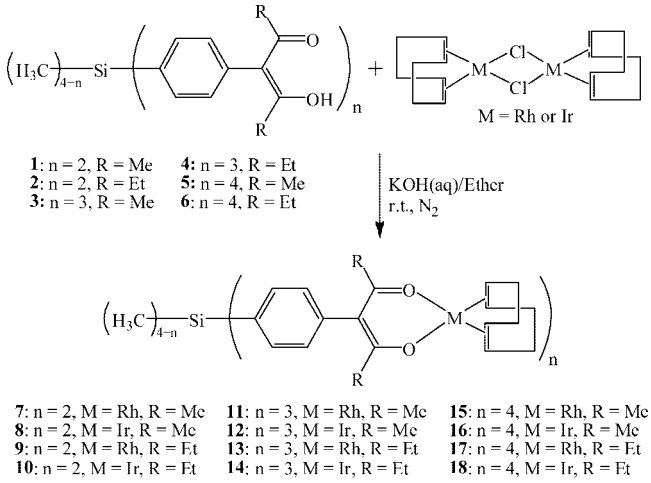

1: n = 2, R = Me **4**: n = 3, R = Et
2: n = 2, R = Et **5**: n = 4, R = Me
3: n = 3, R = Me **6**: n = 4, R = Et

7: n = 2, M = Rh, R = Me **11**: n = 3, M = Rh, R = Me **15**: n = 4, M = Rh, R = Me
8: n = 2, M = Ir, R = Me **12**: n = 3, M = Ir, R = Me **16**: n = 4, M = Ir, R = Me
9: n = 2, M = Rh, R = Et **13**: n = 3, M = Rh, R = Et **17**: n = 4, M = Rh, R = Et
10: n = 2, M = Ir, R = Et **14**: n = 3, M = Ir, R = Et **18**: n = 4, M = Ir, R = Et

131.6, 114.9, 60.0, 33.4, 30.2, 10.2. ^{29}Si NMR: δ 15.9. Anal. Calcd for $C_{84}H_{104}Ir_4O_8Si$ (M = 2038.67): C, 49.49; H, 5.14. Found: C, 49.25; H, 4.95.

X-ray Analyses. Single crystals suitable for X-ray analysis were obtained from methanol (**1**−**4**), chloroform (**7**), toluene (**11**), or diethyl ether (**13**). All X-ray data were collected on a Nonius KappaCCD instrument with Mo Kα source; crystals were mounted and then cooled to ca. 100 K in the gas stream from an Oxford Cryosystems Cryostream temperature-control device. Additional details concerning X-ray data collection and analysis are in the CIF file (see Supporting Information).

Results and Discussion

Multifunctional ligands with approximately tetrahedral angles between the ligand moieties can be derived from di-, tri-, and tetraphenylmethane. However, the Si analogues (i.e., di-, tri-, and tetraphenylsilanes; see Figure 1) are generally easier to synthesize, because of the availability of coupling reactions between aryllithium compounds and chlorosilanes.[11−22] Thus, tetraphenylsilane is considerably easier to prepare than tetraphenylmethane. Still, even among the oligoarylsilanes, some derivatives have presented synthetic challenges: for example, Wuest et al. reported that tetrakis(4-formylphenyl)silane was difficult to prepare in pure form.[11] We recently used[9] the method of Ramirez et al.[23−25] to prepare new aromatic bis(β-diketones) from the analogous aldehydes. For the present work, we wished to prepare a family of bis-, tris-, and tetrakis(β-diketones) with approximately tetrahedral angles, for reaction with metal ions. To do this, we needed the corresponding di-, tri-, and tetraaldehydes (i.e., bis-, tris-, and tetrakis(formylphenyl)silanes) as starting materials.

Synthesis of Aldehydes. Lithiation of 4-bromobenzaldehyde dimethyl acetal, followed by treatment with $(CH_3)_2SiCl_2$, produces a bis(acetal) that yields bis(4-formylphenyl)dimethylsilane ($(CH_3)_2Si(4\text{-}C_6H_4CHO)_2$) on hydrolysis.[10] We carried out analogous reactions with CH_3SiCl_3 and $SiCl_4$ and obtained the other needed aldehydes, tris(4-formylphenyl)methylsilane ($CH_3Si(4\text{-}C_6H_4CHO)_3$, liquid) and tetrakis(4-formylphenyl)silane ($Si(4\text{-}C_6H_4CHO)_4$, crystalline solid). This synthesis is summarized in Scheme 1.

Synthesis of β-Diketones. The aldehydes prepared here react with 2,2,2-trimethoxy-4,5-dimethyl-1,3,2-dioxaphospholene or 2,2,2-trimethoxy-4,5-diethyl-1,3,2-dioxaphospholene at ambient temperature under N_2 to produce dioxaphospholanes, which on refluxing in methanol yield the new β-diketones (**1**−**6**), as shown in Scheme 2. These compounds contain either two ($Me_2Si(phacH)_2$, **1**; $Me_2Si(phprH)_2$, **2**), three ($MeSi(phacH)_3$, **3**; $MeSi(phprH)_3$, **4**), or four ($Si(phacH)_4$, **5**; $Si(phprH)_4$, **6**) β-diketone substituents; in the abbreviations, "ac" and "pr" represent the β-diketone moieties acetylacetone and dipropionylmethane (3,5-heptanedione), respectively.

Crystal Structure Analyses of β-Diketones. Compounds **1**−**4** were also structurally characterized by single-crystal X-ray diffraction. Selected data from these studies are given in Table 1. ORTEP diagrams for **1**−**4** are shown in Figures 2−5.

All of the β-diketones **1**−**4** are in the enol form in their crystals, in agreement with the results of ^{1}H NMR spectral measurements in solution. In all of these structures, the refined positions for the enol H atoms are closer to one O atom than the other, and there is also slight alternation of bond lengths in

Table 2. Crystal Data and Structure Refinement for Rh Complexes 7, 11, and 13

	7·2CHCl$_3$	**11**·C$_7$H$_8$	**13**·Et$_2$O
formula	$C_{40}H_{50}O_4Rh_2Si\cdot 2CHCl_3$	$C_{58}H_{69}O_6Rh_3Si\cdot C_7H_8$	$C_{64}H_{81}O_6Rh_3Si\cdot Et_2O$
fw	1067.45	1291.09	1357.23
cryst size, mm	0.30 × 0.20 × 0.12	0.35 × 0.04 × 0.03	0.40 × 0.22 × 0.10
cryst syst	triclinic	triclinic	triclinic
space group	$P\bar{1}$	$P\bar{1}$	$P\bar{1}$
a, Å	13.507(1)	6.8596(10)	7.1909(15)
b, Å	15.562(1)	16.044(3)	16.858(2)
c, Å	22.7090(15)	27.200(5)	25.998(3)
α, deg	70.463(4)	98.156(7)	85.689(4)
β, deg	86.892(3)	96.646(9)	84.728(4)
γ, deg	87.139(3)	97.498(9)	84.439(4)
V, Å^3	4489.3(5)	2910.3(9)	3116.5(8)
Z	4	2	2
D_{calc}, Mg/m^3	1.579	1.473	1.446
T, K	100	90	90
θ range, deg	2.6−30.0	2.5−25.0	2.5−28.7
μ, mm^{-1}	1.159	0.912	0.856
no. of measd reflns	41 327	34 484	109 435
no. of indep reflns	26 062	10 169	15 301
no. of reflns $I > 2\sigma(I)$	14 921	6446	11 670
no. of params	1018	639	776
goodness of fit	0.977	1.022	1.028
R ($I > 2\sigma(I)$)	0.052	0.060	0.061
wR_2	0.142	0.138	0.152
lgst diff, e Å^{-3}	1.75	1.01	2.55

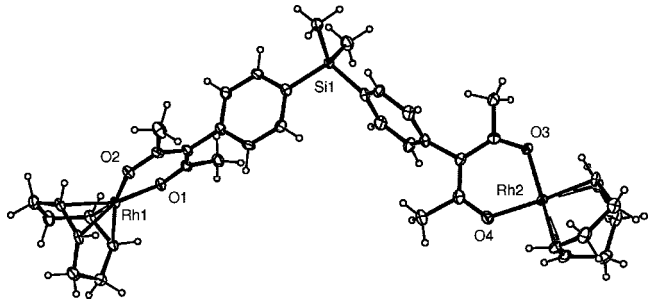

Figure 6. Molecular structure of $(CH_3)_2Si(phac\text{-}Rh(COD))_2$ (**7**) (ellipsoids shown at the 50% probability level). One of two crystallographically independent molecules in the asymmetric unit is shown. Selected interatomic distances (Å): Rh1−O1 2.042(2); Rh1−O2 2.040(3); Rh2−O3 2.025(2); Rh2−O4 2.031(3).

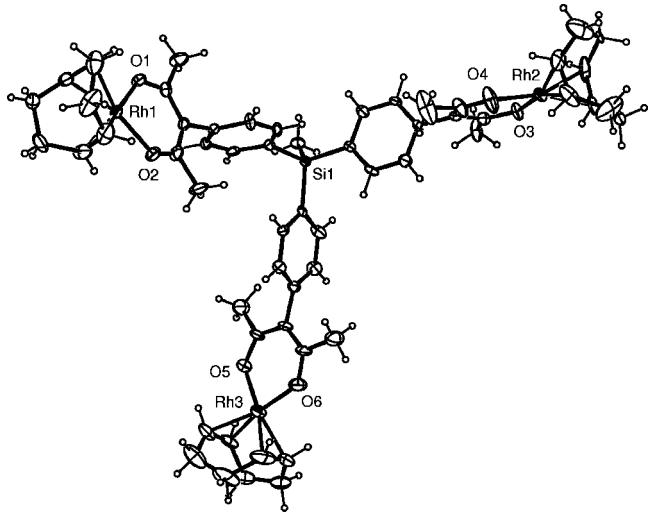

Figure 7. Molecular structure of $CH_3Si(phac\text{-}Rh(COD))_3$ (**11**) (ellipsoids shown at the 50% probability level). Selected interatomic distances (Å): Rh1−O1 2.040(5); Rh1−O2 2.038(5); Rh2−O3 2.043(4); Rh2−O4 2.031(5); Rh3−O5 2.020(5); Rh3−O6 2.029(5).

the O−C−C−C−O chelate rings. Only intramolecular O−H···O hydrogen bonds, and no unusual intermolecular contacts, were observed in these structures.

A search of the Cambridge Structural Database[26] [database version 5.29, updated to November 2007] revealed 13 compounds in which one or more β-diketone moieties are directly attached to aromatic rings.[27] Like the present compounds, all of the previous examples are in the enol form. Enolic β-diketones typically show some alternation among C−O and C−C bond lengths around the rings: average values for all structures (including those reported here) are C−O, 1.321 ± 0.019; C−C, 1.383 ± 0.012; C−C, 1.425 ± 0.019; and C−O, 1.274 ± 0.015 Å. These values represent relatively small differences in length between the formal single and double bonds of the enol structure. This effect has been discussed in terms of resonance-assisted hydrogen bonding: for β-diketones in the enol form, which have O···O distances between 2.4 and 2.5 Å, the strength of the OH···O hydrogen bond and the resulting amount of resonance are large, leading to a high degree of delocalization and a small amount of bond length alternation.[28,29]

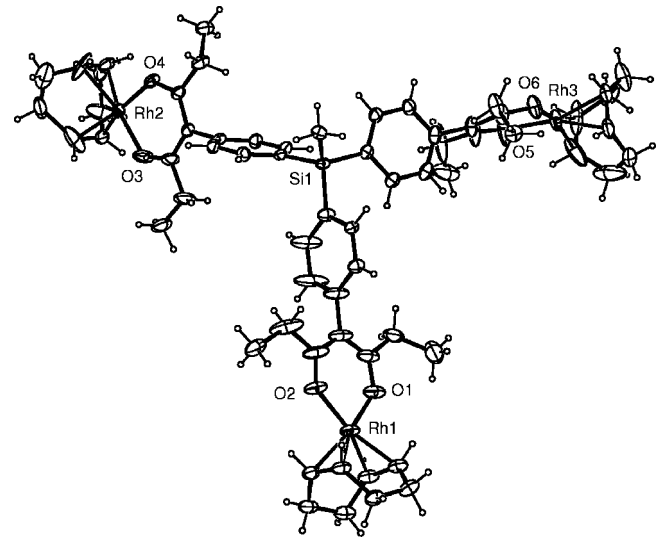

Figure 8. Molecular structure of $CH_3Si(phpr\text{-}Rh(COD))_3$ (**13**) (ellipsoids shown at the 40% probability level). Selected interatomic distances (Å): Rh1−O1 2.032(4); Rh1−O2 2.042(4); Rh2−O3 2.013(4); Rh2−O4 2.026(3); Rh3−O5 2.032(4); Rh3−O6 2.033(4).

Rhodium(I) and Iridium(I) Complexes. Early preparations of (acac)M(COD) were reported by Chatt and Venanzi[30] and by Bonati and Wilkinson[31] (M = Rh), and by Platzer et al.[32] (M = Ir). The reaction of $[M(COD)(\mu\text{-}Cl)]_2$ (M = Rh and Ir) with simple bis(β-diketones) to form binuclear complexes was reported by Whitmore and Eisenberg.[33] (Among more recent studies of related complexes is that of Tokitoh et al., who

(11) Fournier, J. H.; Wang, X.; Wuest, J. D. *Can. J. Chem.* **2003**, *81*, 376–380.
(12) Saied, O.; Maris, T.; Simard, M.; Wuest, J. D. *Acta Crystallogr., Sect. E: Struct. Rep. Online* **2005**, *61*, O2563−O2566.
(13) Laliberté, D.; Maris, T.; Wuest, J. D. *Can. J. Chem.* **2004**, *82*, 386–398.
(14) Fournier, J. H.; Maris, T.; Simard, M.; Wuest, J. D. *Cryst. Growth Des.* **2003**, *3*, 535–540.
(15) Fournier, J. H.; Maris, T.; Wuest, J. D.; Guo, W. Z.; Galoppini, E. *J. Am. Chem. Soc.* **2003**, *125*, 1002–1006.
(16) Chan, L. H.; Lee, R. H.; Hsieh, C. F.; Yeh, H. C.; Chen, C. T. *J. Am. Chem. Soc.* **2002**, *124*, 6469–6479.
(17) Minge, O.; Mitzel, N. W.; Schmidbaur, H. *Organometallics* **2002**, *21*, 680–684.
(18) Chan, L. H.; Yeh, H. C.; Chen, C. T. *Adv. Mater. (Weinheim, Ger.)* **2001**, *13*, 1637–1641.
(19) Broadus, K. M.; Kass, S. R.; Osswald, T.; Prinzbach, H. *J. Am. Chem. Soc.* **2000**, *122*, 10964–10968.
(20) Wang, S. J.; Oldham, W. J.; Hudack, R. A.; Bazan, G. C. *J. Am. Chem. Soc.* **2000**, *122*, 5695–5709.
(21) Jung, S. H.; Kim, H. K. *J. Lumin.* **2000**, *879*, 51–55.
(22) Togo, H.; Matsubayashi, S.; Yamazaki, O.; Yokoyama, M. *J. Org. Chem.* **2000**, *65*, 2816–2819.
(23) Ramirez, F.; Patwardhan, A. V.; Ramanathan, N.; Desai, N. B.; Greco, C. V.; Heller, S. R. *J. Am. Chem. Soc.* **1965**, *87*, 543–548.
(24) Ramirez, F.; Bhatia, S. B.; Patwardhan, A. V.; Smith, C. P. *J. Org. Chem.* **1967**, *32*, 2194–2199.
(25) Ramirez, F.; Bhatia, S. B.; Patwardhan, A. V.; Smith, C. P. *J. Org. Chem.* **1967**, *32*, 3547–3553.
(26) Allen, F. H. *Acta Crystallogr., Sect. B: Struct. Sci.* **2002**, *58*, 380–388.
(27) Refcodes: GASKIU, ISUHIN, JIRKAW, PUXNIF, QEJFOA, SAPYAJ, SAPYEN, SAPYIR, SEYLUD, TUFQOA, and XEWFUB. Data for two additional aromatic β-diketones from ref 9 were also included.
(28) Gilli, G.; Bellucci, F.; Ferretti, V.; Bertolasi, V. *J. Am. Chem. Soc.* **1989**, *111*, 1023–1028.
(29) Bertolasi, V.; Gilli, P.; Ferretti, V.; Gilli, G. *J. Chem. Soc., Perkin Trans. 2* **1997**, 945–952.
(30) Chatt, J.; Venanzi, L. M. *J. Chem. Soc.* **1957**, 4735–4741.
(31) Bonati, F.; Wilkinson, G. *J. Chem. Soc.* **1964**, 3156–3160.
(32) Pannetier, G.; Bonnaire, R.; Fougeroux, P.; Davignon, L.; Platzer, N. *J. Organomet. Chem.* **1973**, *54*, 313–324.
(33) Whitmore, B. C.; Eisenberg, R. *Inorg. Chem.* **1984**, *23*, 1697–1703.
(34) Sasamori, T.; Matsumoto, T.; Takeda, N.; Tokitoh, N. *Organometallics* **2007**, *26*, 3621–3623.

Table 3. Selected Distances (Å) and Angles (deg) for Compounds 1−4, 7, 11, and 13

	1	2	3	4		7	11	13
Oc[a]···Si	8.221	8.216	8.221	8.224	8.223			
	8.234	8.224	8.219	8.196	8.241			
			8.221	8.229	8.196			
		8.216						
		8.225		8.216	8.217			
				8.217	8.212			
				8.189	8.230			
Oc···Oc	13.667	13.684	13.027	13.072	13.173			
		13.407	13.065	13.999	13.751			
			13.080	13.349	13.096			
				13.591	13.498			
				13.393	13.141			
				13.068	13.340			
Si···Rh						9.5717(12)	9.541(3)	9.563(2)
						9.5242(13)	9.556(3)	9.577(2)
							9.575(3)	9.594(2)
						9.5586(12)		
						9.5759(13)		
Rh···Rh						16.0281(9)	13.889(2)	14.661(2)
						16.2330(9)	15.591(2)	16.015(2)
							16.098(3)	16.088(2)
Oc···Si···Oc	112.3	112.68	104.82	111.77	105.49			
		109.27	105.26	105.52	109.14			
			105.41	108.74	111.28			
				106.57	110.49			
				113.90	108.41			
				105.93	106.11			
Rh···Si···Rh						113.79(1)	93.32(2)	99.99(1)
						116.44(1)	109.30(2)	113.44(2)
							114.58(2)	114.11(1)

[a] "Oc" = O centroid of β-diketones.

prepared Rh β-ketophosphenates and β-ketoiminates.[34]) We used a similar procedure to prepare Rh and Ir complexes of the new silicon-based multifunctional β-diketones. Compounds **1**−**6** react with $[M(COD)(\mu\text{-}Cl)]_2$ (M = Rh and Ir) in the presence of added base to form multimetallic silicon-bridged Rh and Ir complexes (Scheme 3, which are soluble in common organic solvents. The spectral properties of the new multinuclear metal complexes are similar to those of the simpler Rh and Ir complexes, with (for example) both aromatic and aliphatic ^{1}H resonances showing slight upfield shifts compared to the uncomplexed β-diketones.

Crystal Structure Analyses of Rhodium Complexes. Compounds **7**, **11**, and **13** were also structurally characterized by single-crystal X-ray diffraction; see summary in Table 2). The molecular structures of **7**, **11**, and **13** are shown in Figures 6, 7, and 8.

The structures of the (diketonato)Rh(COD) moieties in these crystals are similar to those in six previously published structures.[35] In the COD moieties in the present structures, the C═C bonds are not quite perpendicular to the Rh−diketonate plane: in each case, both are twisted away from perpendicularity in the same direction. This situation is also found in all of the previously published (diketonato)Rh(COD) and (diketonato)Ir(COD) structures, and it is likely due to the fact that the most stable conformation of the COD molecule itself is similarly twisted. No unusual intermolecular contacts were observed in these structures.

(35) Refcodes: BFACRH ((benzoyltrifluoroacetonato)Rh(COD)); COCACR ((acac)Rh(COD)); LABLIJ ((ferrocenyl-1,3-butanedionato)Rh(COD)); LEVCEU ((trifluoroacetylacetonato)Rh(COD)); QOZZAG ((hexafluoroacetylacetonato)Ir(COD)).

Intramolecular distances and angles involving the Si atoms, the Rh atoms, and the β-diketone O atom centroids ("Oc"), as derived from the X-ray analyses, are presented in Table 3. These values show that the β-diketone moieties in **1**−**4** are ca. 13.3 Å apart, and the Rh···Rh distances in the complexes are ca. 15.6 Å. The complexes can also be viewed as composed of "rods" ca. 9.56 Å long (Si···Rh) that make approximately tetrahedral angles at Si (average 109.4°). These data will assist in designing and synthesizing supramolecular structures with arylsilane-based building blocks.

Conclusions

The aim of this study was to prepare multifunctional β-diketones and to investigate their coordination properties. Hence, we have developed a simple method for the synthesis of new organosilicon-based tri- and tetraaldehydes as well as bis-, tris-, and tetrakis(β-diketones). The simple, general, clean, and convenient method presented here has led to desirable tetrahedral building blocks for metal-organic frameworks. Crystal structure analyses were performed for β-diketones **1**−**4** and for three of their polynuclear Rh complexes (**7**, **11**, and **13**). At present, we are exploring the reactivity of the polytopic β-diketones **1**−**6** with other metal salts.

Acknowledgment. This work was supported by the Department of Energy (DE-FG02-01ER15267).

Supporting Information Available: X-ray crystallography data for **1**−**4**, **7**, **11**, and **13** as a CIF file. This material is available free of charge via the Internet at http://pubs.acs.org.

OM701233A

10512 *Inorg. Chem.* **2009**, *48*, 10512–10518
DOI: 10.1021/ic900202e

Inorganic Chemistry
Article

Preparation of an Isocyano-β-diketone via its Metal Complexes, by Use of Metal Ions as Protecting Groups

Yixun Zhang[†] and Andrew W. Maverick*

Department of Chemistry, Louisiana State University, Baton Rouge, Louisiana 70803. [†] Present address: Department of Physical Sciences, University of Texas of the Permian Basin, Odessa, Texas 79762.

Received February 1, 2009

A ligand containing isocyanide and β-diketone functional groups, 3-(4-isocyanophenyl)-2,4-pentanedione (HacphNC), and several of its metal complexes have been prepared. The free isocyano-β-diketone could not be prepared by dehydration of the analogous formamide, HacphNHCHO, because of the reactivity of its β-diketone moiety. Instead, the metal complexes Al(acphNC)$_3$, Fe(acphNC)$_3$, Cu(acphNC)$_2$, and Zn(acphNC)$_2$ were synthesized by dehydration of the formamido-β-diketonate complexes Al(acphNHCHO)$_3$, Fe(acphNHCHO)$_3$, Cu(acphNHCHO)$_2$, and Zn(acphNHCHO)$_2$. The free isocyano-β-diketone, HacphNC, can be liberated from its Al and Fe complexes by treatment with oxalate ($C_2O_4^{2-}$) and $HC_2O_4^-$. In addition to these *O*-bound complexes, *C*(N)-bound complexes can be prepared by the reaction of either Al(acphNC)$_3$ or HacphNC with Au(I). X-ray analyses of HacphNC, Al(acphNC)$_3$, (HacphNC)AuCl, Cu(acphNHCHO)$_2$, *trans*-Zn(acphNHCHO)$_2$(H$_2$O)$_2$, and two other intermediates are also reported.

Introduction

Heterofunctional ligands are of interest because of their ability to bind to different types of metal ions. This is important in the construction of metal−organic frameworks (MOFs). MOFs have attracted scientists because the various coordination geometries and abilities of metal ions together with different types of ligands provide many possible open framework structures. Rational design of ligands can lead to predictable extended solid frameworks with potential applications in separation, gas storage, molecular recognition, and catalysis.[1−5]

Several porous frameworks have been prepared from the heterofunctional ligand pyridylacetylacetone (pyacH) by Domasevitch et al.[6,7] and by our group.[8,9] For example, a porous 1D ladder structure prepared from Fe(pyac)$_3$ and AgNO$_3$ is of interest because the solvent guests in its pores can be exchanged in single-crystal-to-single-crystal transformations.[9]

Although the above 1D Fe(pyac)$_3$−AgNO$_3$ porous framework is stable under solvent exchange, the others are not, and all are unstable in a vacuum. This limited stability is likely due to the weakness of the interactions between layers in these networks. Our goal is to develop ligands that are suitable for the construction of porous 3D frameworks, because they are expected to show greatly enhanced stability. The most promising route to 3D structures is to use conditions that favor the assembly of six ligands coordinated octahedrally around one metal. Although a few M(py)$_6^{n+}$ complexes are known, they generally form only in the presence of excess pyridine.[10−12] Thus, pyridine-based ligands, such as pyac$^-$, are unlikely to be useful in preparing 3D supramolecular materials. One common method for stabilizing metal complexes is choosing chelating ligands. However, in our case, a chelating ligand (e.g., a 2,2-bipyridine derivative) is difficult to functionalize so that it will also bind to two other metal atoms. Therefore, in order to improve the prospects for 3D materials, we need to use building blocks based on strongly coordinating monodentate ligands. Nitriles, such as 3-(4-cyanophenyl)acetylacetone, have been studied as

*To whom correspondence should be addressed. E-mail: maverick@lsu.edu.

(1) Davis, M. E. *Nature* **2002**, *417*, 813–821.
(2) Eddaoudi, M.; Kim, J.; Rosi, N.; Vodak, D.; Wachter, J.; O'Keeffe, M.; Yaghi, O. M. *Science* **2002**, *295*, 469–472.
(3) Pan, L.; Adams, K. M.; Hernandez, H. E.; Wang, X. T.; Zheng, C.; Hattori, Y.; Kaneko, K. *J. Am. Chem. Soc.* **2003**, *125*, 3062–3067.
(4) Rosi, N. L.; Eckert, J.; Eddaoudi, M.; Vodak, D. T.; Kim, J.; O'Keeffe, M.; Yaghi, O. M. *Science* **2003**, *300*, 1127–1129.
(5) Ward, M. D. *Science* **2003**, *300*, 1104–1105.
(6) Vreshch, V. D.; Chernega, A. N.; Howard, J. A. K.; Sieler, J.; Domasevitch, K. V. *Dalton Trans.* **2003**, 1707–1711.
(7) Vreshch, V. D.; Lysenko, A. B.; Chernega, A. N.; Howard, J. A. K.; Krautscheid, H.; Sieler, J.; Domasevitch, K. V. *Dalton Trans.* **2004**, 2899–2903.
(8) Chen, B.; Fronczek, F. R.; Maverick, A. W. *Inorg. Chem.* **2004**, *43*, 8209–8211.
(9) Zhang, Y.; Chen, B.; Fronczek, F. R.; Maverick, A. W. *Inorg. Chem.* **2008**, *47*, 4433–4435.
(10) Jones, W. C.; Bull, W. E. *J. Chem. Soc. A* **1968**, 1849–1852.
(11) Fletcher, R. J.; Gans, P.; Gill, J. B.; Geyer, C. *J. Mol. Liq.* **1997**, *73−4*, 99–106.
(12) Templeton, J. L. *J. Am. Chem. Soc.* **1979**, *101*, 4906–4917.

Published on Web 10/12/2009

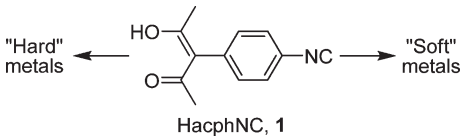

Figure 1. The bifunctional isocyano-β-diketone HacphNC.

heterofunctional ligands,[13] but nitriles tend to bind weakly to metals, making it difficult to generate six-coordinate complexes $M(NCR)_6^{n+}$. On the other hand, isocyanide ligands (CNR) are known to make stable complexes $M(CNR)_6^{n+}$ with metals such as Cr,[14−20] Mn,[21−26] Fe,[27−29] and Re.[30−34] Early on, Sacco and Naldini synthesized highly stable manganese(I) isocyanide complexes $[(RNC)_6Mn]^+$.[21−23] More recently, Barybin et al. have prepared a number of homoleptic isocyanide complexes (e.g., $Cr(CNFc)_6$ (Fc = ferrocenyl)[19]) in high yield, using only a slight excess of the isocyanide ligand.

We were interested in HacphNC (**1**, Figure 1), with one isocyanide and one β-diketone moiety, for possible conversion to 3D porous materials. This ligand's isocyanide moiety should be able to bind to "soft" metals such as Cr(0), Mn(I), or Fe(II) and its β-diketone moiety to "hard" metals such as Cu(II) or Zn(II). We report here the preparation of the HacphNC ligand and the properties of several of its metal complexes.

Results and Discussion

Synthetic Strategy. Figure 2 illustrates the overall route we chose for synthesizing the target compound, HacphNC (**1**), via 3-(4-formamidophenyl)acetylacetone (HacphNHCHO, **2**), from 4-nitrobenzaldehyde (**3**). Reduction of the nitro group of **3** and formylation of the resulting amine, and conversion of its aldehyde to a β-diketone, was expected to yield **2**. Isocyanides are normally prepared by dehydration of formamides; thus, dehydration of **2** was expected to produce **1**.

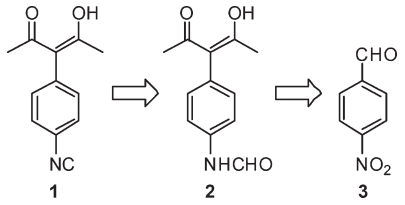

Figure 2. Synthetic strategy for the isocyano-β-diketone HacphNC (**1**).

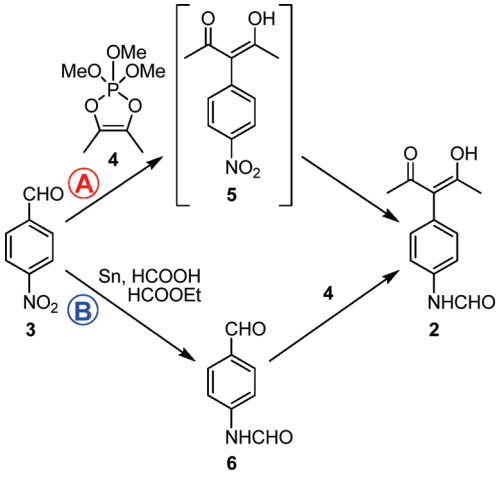

Figure 3. Two possible routes for preparing HacphNHCHO (**2**).

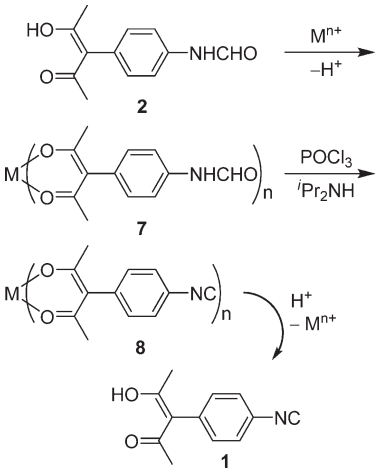

Figure 4. Protection of the β-diketone group by coordination to metal ions prior to isocyanide synthesis.

We tested two possible routes starting from 4-nitrobenzaldehyde (**3**) to make **2** (Figure 3). In route A, the aldehyde group is converted into a β-diketone first (making **5**), and then the nitro group is reduced to an amino group and formylated. In route B, the nitro group is reduced to an amino group and formylated first (**6**), and then the aldehyde is converted into a β-diketone.

After the aldehyde group is converted into a β-diketone, it is coordinated to metal ions, which serve as a "protecting group" (Figure 4). The metal formamido-β-diketonate complex **7** can then be dehydrated to an isocyanide complex (**8**). Free HacphNC (**1**) can be liberated

(13) Chen, B.; Fronczek, F. R.; Maverick, A. W. *Acta Crystallogr., Sect. C* **2004**, *60*, M147–M149.
(14) Ljungström, E. *Acta Chem. Scand. A* **1978**, *32*, 47–50.
(15) Bohling, D. A.; Mann, K. R. *Inorg. Chem.* **1984**, *23*, 1426–1432.
(16) Lentz, D. *J. Organomet. Chem.* **1990**, *381*, 205–212.
(17) Anderson, K. A.; Scott, B.; Wherland, S.; Willett, R. D. *Acta Crystallogr., Sect. C* **1991**, *47*, 2337–2339.
(18) Acho, J. A.; Lippard, S. J. *Organometallics* **1994**, *13*, 1294–1299.
(19) Barybin, M. V.; Holovics, T. C.; Deplazes, S. F.; Lushington, G. H.; Powell, D. R.; Toriyama, M. *J. Am. Chem. Soc.* **2002**, *124*, 13668–13669.
(20) Robinson, R. E.; Holovics, T. C.; Deplazes, S. F.; Lushington, G. H.; Powell, D. R.; Barybin, M. V. *J. Am. Chem. Soc.* **2003**, *125*, 4432–4433.
(21) Sacco, A. *Recl. Trav. Chim. Pays-Bas* **1956**, *75*, 646.
(22) Sacco, A. *Gazz. Chim. Ital.* **1956**, *86*, 201–206.
(23) Sacco, A.; Naldini, L. *Gazz. Chim. Ital.* **1956**, *86*, 207–210.
(24) Ericsson, M. S.; Jagner, S.; Ljungström, E. *Acta Chem. Scand. A* **1979**, *33*, 371–374.
(25) Ericsson, M. S.; Jagner, S.; Ljungström, E. *Acta Chem. Scand. A* **1980**, *34*, 535–540.
(26) Godfrey, S. M.; Li, G. Q.; McAuliffe, C. A.; Ndifon, P. T.; Pritchard, R. G. *Inorg. Chim. Acta* **1992**, *200*, 23–30.
(27) Powell, H. M.; Bartindale, G. W. R. *J. Chem. Soc.* **1945**, 799–803.
(28) Constant, G.; Daran, J. C.; Jeannin, Y. *J. Inorg. Nucl. Chem.* **1973**, *35*, 4083–4091.
(29) Schaal, M.; Weigand, W.; Nagel, U.; Beck, W. *Chem. Ber.* **1985**, *118*, 2186–2197.
(30) Malatesta, L.; Freni, M.; Valenti, V.; Bossi, E. *Angew. Chem.* **1960**, *72*, 323.
(31) Treichel, P. M.; Williams, J. P. *J. Organomet. Chem.* **1977**, *135*, 39–51.
(32) Allison, J. D.; Wood, T. E.; Wild, R. E.; Walton, R. A. *Inorg. Chem.* **1982**, *21*, 3540–3546.
(33) Girolami, G. S.; Andersen, R. A. *Inorg. Chem.* **1981**, *20*, 2040–2044.
(34) Schaffer, P.; Britten, J. F.; Davison, A.; Jones, A. G.; Valliant, J. F. *J. Organomet. Chem.* **2003**, *680*, 323–328.

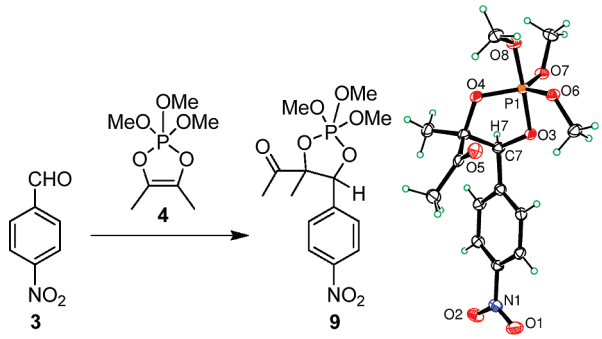

Figure 5. Synthesis and ellipsoid plot of (4-nitrophenyl)phospholane intermediate **9**.

by treatment of the metal isocyano-β-diketonate complex with a suitable metal-complexing agent or with dilute acid.

Synthesis of HacphNHCHO (2). We attempted to prepare 3-(4-nitrophenyl)acetylacetone (**5**) by route A. 4-Nitrobenzaldehyde (**3**) was mixed with 2,2,2-trimethoxy-4,5-dimethyl-1,3,2-dioxaphospholene (**4**) in dichloromethane for one day, and then the mixture was refluxed in anhydrous methanol for three days. (The conversion of aromatic aldehydes to 3-arylacetylacetones by reaction with **4** was first explored by Ramirez et al.[35]) The first stage of this reaction proceeds cleanly, producing **9** (4-acetyl-4-methyl-5-(4-nitrophenyl)-2,2,2-trimethoxy1,3,2-dioxaphospholane; Figure 5). We identified **9** by NMR spectroscopy and by X-ray analysis (see the Supporting Information). However, our attempts to convert **9** to the desired (4-nitrophenyl)acetylacetone **5**, under several different conditions, were unsuccessful. (This may be due to the electron-withdrawing effect of the nitro group in **9**.)

Because route A was not successful (see Figure 3), we turned to route B for the synthesis of **2**. Conversion of **3** to **6** proceeds by initial reduction to produce 4-aminobenzaldehyde, followed by rapid formylation to make **6**. The intermediate 4-aminobenzaldehyde self-condenses to yield insoluble polymeric products; thus, it should be formylated as quickly as possible to give a good yield of 4-formamidobenzaldehyde (**6**). Hrvatin and Sykes[36] reported the conversion of **3** to **6** using tin metal and formic acid in toluene. We modified their procedure by replacing toluene (as solvent) with a mixture of ethyl formate and ethyl acetate, increasing the amount of formic acid, and adding the tin metal in smaller portions. Our modifications in the procedure were designed to keep all of the liquid components of the reaction mixture miscible, generate 4-aminobenzaldehyde more slowly, and formylate it faster to make **6**; the resulting yield was higher (66%, vs lit.[36] 47%).

Compound **6** reacts with phospholene **4** in dichloromethane to generate β-diketone **2** (HacphNHCHO, Figure 3), which was purified by column chromatography and isolated as yellow crystals. Both *E* and *Z* forms of **2** and **6** were characterized (see the Supporting Information). The new β-diketone **2** also exhibits keto−enol

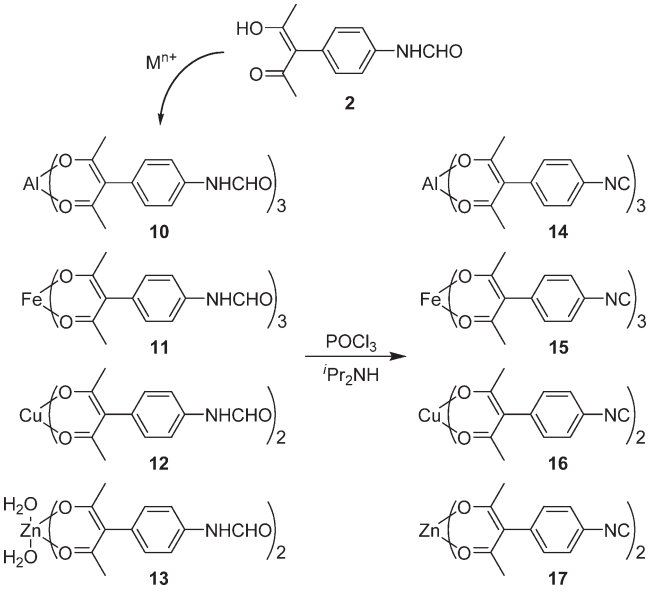

Figure 6. Preparation of formamido-β-diketonate complexes **10**−**13** and their conversion to isocyano-β-diketonate complexes **14**−**17**.

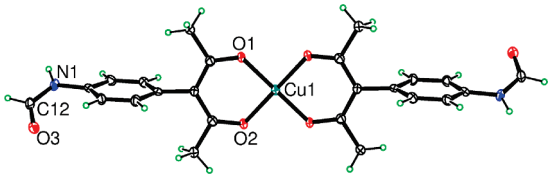

Figure 7. Crystal structure of Cu(*Z*-acphNHCHO)$_2$ (**12**).

tautomerism (in $CDCl_3$, 94% enol: 6% keto by ^{1}H NMR).

Syntheses of M(acphNHCHO)$_n$. The β-diketone moiety of **2** required protection before dehydration of the formamido group to an isocyanide. (Attempts to prepare **1** directly by the dehydration of **2** were unsuccessful; see below.) We chose metal ions as "protecting groups" for the β-diketone because there are numerous procedures available for preparing metal β-diketonates. Also, dehydration of the resulting metal formamido-β-diketonates (M(acphNHCHO)$_n$) should yield metal isocyano-β-diketonates (M(acphNC)$_n$), which may be useful in building supramolecular structures even without isolation of free HacphNC (**1**). We chose the metal ions Al^{3+}, Fe^{3+}, Cu^{2+}, and Zn^{2+}, to react with **2** (Figure 6).

We prepared Al(acphNHCHO)$_3$ (**10**) and Fe(acphNHCHO)$_3$ (**11**) by the reaction of $Al(NO_3)_3$ and $Fe(NO_3)_3$, respectively, with HacphNHCHO (**2**) in the presence of $NaHCO_3$. This is similar to previously published procedures for Al(pyac)$_3$ and Fe(pyac)$_3$.[7,9,37] The products are soluble in DMSO and acetone, and slightly soluble in chloroform and dichloromethane.

Bluish-green Cu(acphNHCHO)$_2$ (**12**) precipitates immediately when **2** and copper(II) acetate are mixed together in water/methanol solution. Compound **12** (see Figure 7) is slightly soluble in DMSO and soluble in pyridine, but insoluble in almost all other common

(35) Ramirez, F.; Bhatia, S. B.; Patwardhan, A. V.; Smith, C. P. *J. Org. Chem.* **1967**, *32*, 3547–3553.
(36) Hrvatin, P.; Sykes, A. G. *Synlett* **1997**, 1069–1070.
(37) Mackay, L. G.; Anderson, H. L.; Sanders, J. K. M. *J. Chem. Soc., Perkin Trans. 1* **1995**, 2269–2273.

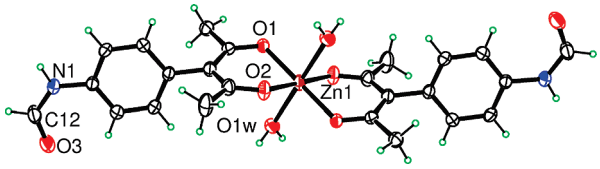

Figure 8. Ellipsoid plot of *trans*-Zn(*Z*-acphNHCHO)$_2$(H$_2$O)$_2$ (**13**), from the crystal structure of its dihydrate.

solvents. The structure of **12** also contains intermolecular contacts (Cu1···O3, 2.838(2) Å), which make the structure polymeric and give the Cu atoms an approximately octahedral coordination geometry overall.

trans-Zn(acphNHCHO)$_2$(H$_2$O)$_2$ (**13**) is made from zinc acetate and **2**, with added NaHCO$_3$. Crystals grown during the synthesis were suitable for single-crystal X-ray analysis. In the structure of **13** (see Figure 8), the two β-diketonate groups form a stepped arrangement about Zn^{2+}. This contrasts with the structure of **12**, in which the two acac moieties are coplanar. Compound **13** is readily soluble in DMSO and pyridine, and slightly soluble in chloroform and dichloromethane.

M(acphNC)$_n$ Complexes. All four metal formamido-β-diketonate complexes (**10**−**13**) can be dehydrated by POCl$_3$ in the presence of diisopropylamine (Figure 6), in a dichloromethane solution. The starting materials are not very soluble in CH$_2$Cl$_2$, whereas the products dissolve readily. The Al, Fe, and Zn starting materials (**10**, **11**, and **13**) all react within 2 h. In contrast, most of the copper starting material (**12**) still remains as unreacted solid even after five days. This slow reaction may be due to the fact that **12** is polymeric in the solid state (see Figure 7). Such polymerization would explain the low solubility of **12** and also interfere sterically with the dehydration reaction. A similar phenomenon is observed with Cu(pyac)$_2$: its crystals are also polymeric, which leads to low solubility in a variety of solvents.[38]

The IR absorptions ($\nu_{C\equiv N}$) for the isocyano-β-diketonate complexes Al(acphNC)$_3$ (**14**), Fe(acphNC)$_3$ (**15**), Cu(acphNC)$_2$ (**16**), and Zn(acphNC)$_2$ (**17**) appear at 2121, 2126, 2147, and 2124 cm^{-1}, respectively. The values for **14**, **15**, and **17** are very close to those for free aryl isocyanide ligands[39−42] and for the free ligand HacphNC (2122 cm^{-1}; see below). The higher frequency for the Cu complex (**16**) may again indicate coordination of the isocyanide groups to adjacent Cu atoms, but it could be obtained only in impure form. The yield for **17** was low (13%); this may be due to the fact that the Zn complex reactant, **13**, was hydrated, and its water of hydration could react readily with POCl$_3$. However, an attempt using an excess of POCl$_3$ still gave a low yield of **17**. Preparation of Al(acphNC)$_3$ and Fe(acphNC)$_3$ (**14** and **15**), on the other hand, proceeded in 75% and 90% yield, respectively, relatively high values for the transformation of three identical functional groups in the same molecule.

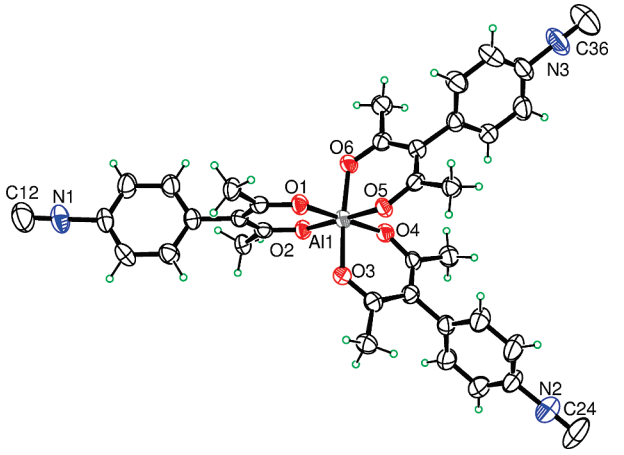

Figure 9. Ellipsoid plot of Al(acphNC)$_3$ (**14**), from the crystal structure of its hexane solvate.

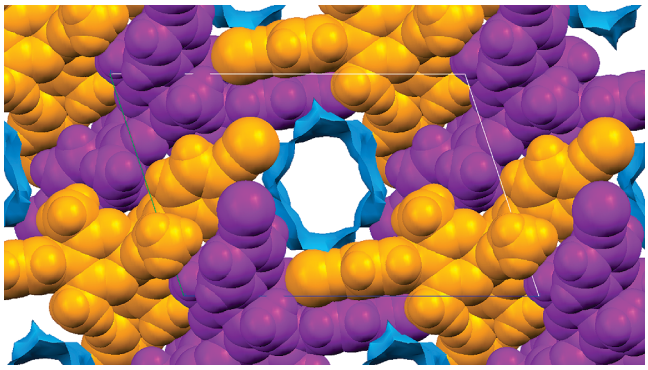

Figure 10. Illustration of the crystal structure of Al(acphNC)$_3$, viewed parallel to the *a* axis. One orientation of the Al(acphNC)$_3$ molecules is shown in purple, and the inversion-related orientation is in gold. The blue surfaces, calculated with a 0.9 Å probe radius and a 0.7 Å grid, enclose voids of ca. 400 Å^3, or 21% of the unit cell volume.

The crystal structure of Al(acphNC)$_3$ (**14**) is shown in Figure 9. Molecules of Al(acphNC)$_3$ in the crystal are crudely trigonal in shape, but their CN···Al···NC angles (137.7°, 81.9°, and 140.3°) show large deviations from the ideal 120°. Similarly large distortions have been observed in the structures of Al(pyac)$_3$[43] and Fe(pyac)$_3$.[7,9]

Initial solution of the crystal structure of Al(acphNC)$_3$ revealed molecules of **14**, but also a region with poorly defined electron density attributable to solvent molecules. Several approximately evenly spaced difference electron density peaks of similar intensity were observed in the solvent region, which suggested a hydrocarbon. Because hexane had been used in the crystallization process, our first model included disordered partially occupied hexane molecules in this region, with an overall formula of Al(acphNC)$_3$·0.5C$_6$H$_{14}$. For the final refinement, however, the solvent contribution to the data was removed using SQUEEZE[44] (in PLATON[45]): approximately 58 electrons were removed per unit cell (corresponding to ca. 0.58 molecule of hexane per formula unit), and a void of

(38) Chen, B. L.; Fronczek, F. R.; Maverick, A. W. *Chem. Commun.* **2003**, 2166–2167.
(39) Ecken, H.; Olmstead, M. M.; Noll, B. C.; Attar, S.; Schlyer, B.; Balch, A. L. *J. Chem. Soc., Dalton Trans.* **1998**, 3715–3720.
(40) Singleton, E.; Oosthuizen, H. E. *Adv. Organomet. Chem.* **1983**, *22*, 209–310.
(41) Uson, R.; Laguna, A.; Vicente, J.; Garcia, J.; Bergareche, B.; Brun, P. *Inorg. Chim. Acta* **1978**, *28*, 237–243.
(42) Treichel, P. M. *Adv. Organomet. Chem.* **1973**, *11*, 21–86.
(43) Zhang, Y. Ph. D. Dissertation, Louisiana State University, Baton Rouge, LA, **2006**.
(44) van der Sluis, P.; Spek, A. L. *Acta Crystallogr., Sect. A* **1990**, *A46*, 194–201.
(45) Spek, A. L. *PLATON*; Utrecht University: Utrecht, The Netherlands, 2008. See also: Spek, A. L. *J. Appl. Crystallogr.* **2003**, *36*, 7–13.

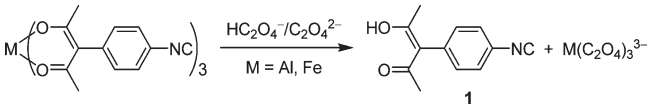

Figure 11. Displacement of metal ions from Al(acphNC)$_3$ (**14**) and Fe(acphNC)$_3$ (**15**) to produce the free isocyano-β-diketone ligand HacphNC (**1**).

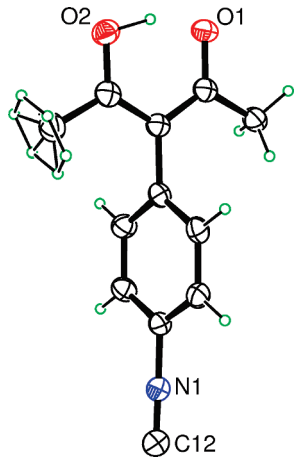

Figure 12. Crystal structure of HacphNC (**1**).

ca. 400 Å^3 per unit cell was left behind, see Figure 10. This void has approximately the right volume for two hexane molecules (on the basis of the density of liquid hexane at 25 °C, 0.655 g cm^{-3}, the volume of one molecule of hexane is approximately 219 Å^3). Thus, it is possible that the crystals formed as Al(acphNC)$_3$·C$_6$H$_{14}$ ($Z = 2$), but some hexane was lost during selection and mounting. This propensity for solvent loss is consistent with the microanalysis for **14** (see the Experimental Section), which fits well with the ansolvous compound.

Synthesis of HacphNC. We attempted to prepare the free HacphNC ligand (**1**) directly from **2** by treatment with POCl$_3$. Spectra of this reaction mixture indicated that the formamide moieties were consumed (NMR) and isocyanide was formed (IR). However, the NMR spectra indicated that the β-diketone group was destroyed under the reaction conditions. Instead, we isolated HacphNC from its Al, Fe, and Zn complexes (**14**, **15**, and **17**).

We explored two strategies for obtaining HacphNC (**1**) from its complexes. First, we treated **14**, **15**, and **17** with dilute acetic acid; this produced the desired HacphNC, but only in low yields (ca. 10%). Second, we treated CH$_2$Cl$_2$ solutions of Al(acphNC)$_3$ (**14**) and Fe(acphNC)$_3$ (**15**) with aqueous solutions prepared from oxalic acid and oxalate salts as extractants. In this scheme (Figure 11), the H$^+$ from the acid is designed to protonate the coordinated β-diketonate ligand, and the oxalate is designed to complex the liberated Fe^{3+}. The procedure with Fe(III) has the advantage that the colors of Fe(acphNC)$_3$ and Fe(C$_2$O$_4$)$_3^{3-}$ make it easy to determine visually when the extraction of the metal ion into the aqueous layer is complete. With an excess of oxalate, we obtained HacphNC in 37% yield from Fe(acphNC)$_3$; yields from Al(acphNC)$_3$ were lower. The crystal structure of **1** (IR $\nu_{C\equiv N}$ 2122 cm^{-1}) is shown in Figure 12.

To explore the reactivity of the isocyanide moiety of HacphNC, we treated both the free ligand (**1**) and its Al complex (**14**) with (Me$_2$S)AuCl, giving HacphNCAuCl (**18**) and Al(acphNCAuCl)$_3$ (**19**), respectively. These products were characterized by NMR and IR, and crystals of **18** suitable for X-ray analysis were also obtained (Figure 13). The $\nu_{C\equiv N}$ values are higher in the products compared to HacphNC (2122 cm^{-1}), as expected: 2223 and 2222 cm^{-1} for **18** and **19**, respectively. These values are very close to that observed by Uson et al. for PhNCAuCl (2230 cm^{-1}).[41] The Al−Au complex **19** is an example in which both the soft (isocyanide) and hard (β-diketonate) moieties of HacphNC are coordinated to metal ions.

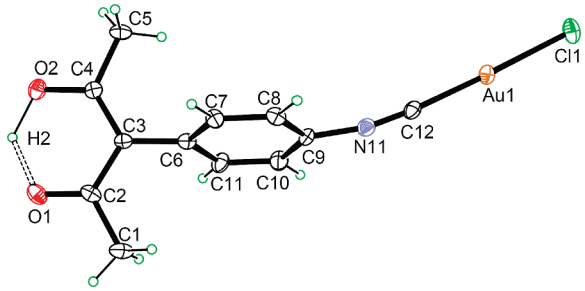

Figure 13. Crystal structure of HacphNCAuCl (**18**). Adjacent molecules in the crystal are arranged to form zigzag chains of weak Au···Au interactions (3.466 Å), similar to those previously reported for (2,6-Me$_2$C$_6$H$_3$NC)AuX (X = Br, I).[39]

Conclusion

The first ligand combining isocyanide and β-diketone groups, 3-(4-isocyanophenyl)-2,4-pentanedione (HacphNC), has been synthesized. The ligand was first prepared in the form of its Al, Fe(III), Cu(II), and Zn complexes. Treatment of the Al and Zn complexes with dilute acid, or of the Al and Fe complexes with $C_2O_4^{2-}/HC_2O_4^-$, liberates the target ligand HacphNC. The isocyanide moieties in both the free ligand HacphNC and its Al complex Al(acphNC)$_3$ can also bind to Au(I). We are now extending the chemistry of HacphNC to metals that will yield higher coordination numbers, for the construction of 3D supramolecular structures.

Experimental Section

A Bruker DPX-250 instrument (250 MHz) was used for NMR spectroscopy. All IR spectra were performed on thin films with the use of a Bruker Tensor 27 spectrometer. Single-crystal X-ray diffraction data were collected with use of a Nonius KappaCCD instrument; the results are summarized in Tables 1 and 2. All experimental procedures were carried out in the air unless otherwise noted. Crystal-structure illustrations were prepared using CSD Mercury, version 2.2 (Figure 10) and Ortep-3 for Windows.

4-Formamidobenzaldehyde (OHC-4-C$_6$H$_4$NHCHO, 6). 4-Formamidobenzaldehyde was first synthesized by Hrvatin and Sykes[36] in formic acid/toluene. We obtained a higher yield of the product by using a mixture of ethyl formate and ethyl acetate as the reactant/solvent, and by adding the tin metal in two portions. 4-Nitrobenzaldehyde (6.04 g, 40 mmol) was dissolved in a mixture of formic acid (90%, 60 mL), ethyl formate (50 mL), and ethyl acetate (150 mL). The solution was refluxed under nitrogen with stirring. Tin metal (9.0 g, 76 mmol) was added in two equal portions: one immediately and the other after 24 h. The reaction was complete after three days, as judged by TLC. The solution was filtered hot and evaporated nearly to dryness. Toluene (300 mL) was added to the residue and the mixture refluxed with a Dean−Stark trap for about 2 h to remove the

Table 1. Crystal Data and Refinement Parameters for the Isocyano-β-diketone **1** and Related Compounds

compd	**1**	(*E*)-**2**	(*Z*)-**2**	(*E*)-**6**	**9**
formula	$C_{12}H_{11}NO_2$	$C_{12}H_{13}NO_3$	$C_{12}H_{13}NO_3$	$C_8H_7NO_2$	$C_{14}H_{20}NO_8P$
fw	201.22	219.23	219.23	149.15	361.28
space group	$P2_1/c$	$C2/c$	$P2_1/c$	$P2_1$	$Pca2_1$
a, Å	7.0820(15)	14.379(3)	13.289(2)	4.3910(15)	13.383(2)
b, Å	11.606(3)	10.339(2)	7.5180(15)	6.917(2)	17.884(2)
c, Å	12.427(3)	14.974(4)	11.561(2)	11.793(3)	13.509(3)
α	90	90	90	90	90
β	93.666(13)	91.296(15)	111.153(8)	97.81(2)	90
γ	90	90	90	90	90
V, Å^3	1019.3(4)	2225.5(9)	1077.2(3)	354.86(18)	3233.3(9)
Z	4	8	4	2	8
T, K	110	110	110	110	110
D_{calcd}, g cm^{-3}	1.311	1.309	1.352	1.396	1.484
μ, mm^{-1}	0.090	0.095	0.098	0.102	0.214
R ($I > 2\sigma(I)$)	0.0539	0.0473	0.0424	0.0396	0.0233
R_w (all data)	0.1572	0.1194	0.1109	0.0995	0.0629

Table 2. Crystal Data and Refinement Parameters for Metal Complexes

compd	**12** $Cu(acphNH\text{-}CHO)_2$	**13**·$2H_2O$ [*trans*-$Zn(acphNHCHO)_2(H_2O)_2$]·$2H_2O$	**14**·$0.58C_6H_{14}$[a] $Al(acphNC)_3$·$0.58C_6H_{14}$	**18** HacphNCAuCl
formula	$C_{24}H_{24}CuN_2O_6$	$C_{24}H_{28}N_2O_8Zn\cdot 2H_2O$	$C_{36}H_{30}AlN_3O_6\cdot 0.58C_6H_{14}$	$C_{12}H_{11}AuClNO_2$
fw	500.00	573.89	677.59	433.63
space group	$P2_1/n$	$P2_1/c$	$P\bar{1}$	$P2_1/n$
a, Å	8.136(2)	12.442(5)	7.433(5)	14.638(3)
b, Å	7.480(2)	9.637(4)	13.510(10)	6.4219(12)
c, Å	17.771(4)	11.947(5)	20.66(2)	14.919(2)
α	90	90	107.65(3)	90
β	103.166(7)	114.60(2)	97.53(3)	117.761(6)
γ	90	90	94.57(3)	90
V, Å^3	1053.1(5)	1302.5(10)	1944(3)	1241.0(4)
Z	2	2	2	4
T, K	110	110	110	90
D_{calcd}, g cm^{-3}	1.577	1.463	1.158	2.321
μ, mm^{-1}	1.084	1.001	0.099	12.057
R ($I > 2\sigma(I)$)	0.0543	0.0537	0.069	0.043
R_w (all data)	0.1385	0.1385	0.185	0.128

[a] $0.58C_6H_{14}$ was included in fw, *D*, and μ; it represents the approximate amount of electron density removed by SQUEEZE[44] before final refinement. See text for details.

remaining water and formic acid. The mixture was filtered when it was still hot, and the filtrate was evaporated to dryness. The residue was chromatographed on silica gel with 2:1 ethyl acetate/hexane. Colorless crystals of the *E* conformer of **6** grew easily from the eluate by evaporation. Yield: 3.91 g (66%). MP: 134−136 °C (lit. 139 °C[36]). ^{1}H NMR spectra of **6** show a mixture of *E* and *Z* conformers immediately on mixing. In $CDCl_3$, *E*: 7.24, 7.91 (E3−4, 4H, *AB*), 8.30 (E1, 1H, d), 8.91 (NH, 1H, d), 9.95 (E5, 1H, s). *Z*: 7.60 (Z1, 1H, s), 7.75, 7.88 (Z3−4, 4H, *AB*), 8.47 (NH, 1H, s), 9.94 (Z5, 1H, s). In DMSO-d_6, *E*: 7.40, 7.86 (E3−4, 4H, *AB*), 9.03 (NH, 1H, d), 9.89 (E5, 1H, s), 10.56 (E1, 1H, d). *Z*: 7.79, 7.89 (Z3−4, 4H, *AB*), 8.37 (NH, 1H, s), 9.89 (Z5, 1H, s), 10.64 (Z1, 1H, s).

3-(4-Formamidophenyl)pentane-2,4-dione (HacphNHCHO, 2). Compound **6** (2.56 g, 17.2 mmol) and phospholene **4** (2,2,2-trimethoxy-4,5-dimethyl-1,3,2-dioxaphospholene; 4.02 g, 19.2 mmol) were dissolved in 15 mL of dichloromethane under argon. The reaction was complete after 3 days, as judged by the disappearance of the aldehyde resonance in ^{1}H NMR. The solvent was removed, and the residue was chromatographed on silica gel with 2:1 ethyl acetate/hexane. Yield: 1.95 g (52%). MP (*Z*): 124 °C. Anal. Calcd for $C_{12}H_{13}NO_3$: C, 65.74; H, 5.98; N, 6.39. Found: C, 65.59; H, 6.14; N, 6.48. Slow evaporation of solutions of **2** yields crystals. In most of our experiments, the crystals were of the *Z* conformer; in one case, we also obtained a small amount of the *E* conformer in crystalline form. However, solutions of either conformer quickly develop a second set of ^{1}H NMR resonances attributable to the other conformer. In $CDCl_3$, *E*: 7.12, 7.18 (E3−4, 4H, *AB*), 8.19 (E1, 1H, d), 8.74 (E2, 1H, d). *Z*: 7.15, 7.58 (Z3−4, 4H, *AB*), 7.45 (Z1, 1H, s), 8.41 (Z2, 1H, s). Enol: 1.88 (CH_3, 6H, s), 16.66 (OH, 1H, s). Keto: 2.20 (CH_3, 6H, s), 4.83 (CH, 1H, s). In DMSO-d_6, *E*: 7.16, 7.23 (E3−4, 4H, *AB*), 8.84 (E2, 1H, d), 10.20 (E1, 1H, d). *Z*: 7.20, 7.62 (Z3−4, 4H, *AB*), 8.29 (Z2, 1H, s), 10.26 (Z1, 1H, s). Enol: 1.85 (CH_3, 6H, s), 16.79 (OH, 1H, s). Keto: 2.13 (CH_3, 6H, s), 5.30 (CH, 1H, s).

Al(acphNHCHO)$_3$ (10). A solution of $Al(NO_3)_3\cdot 9H_2O$ (1.125 g, 3.00 mmol) in 15 mL of H_2O was added to a solution of HacphNHCHO (2.19 g, 10.0 mmol) in 15 mL of CH_3OH with stirring. Then, $NaHCO_3$ (0.756 g, 9.0 mmol) in 5 mL of H_2O was added. A light yellow precipitate formed, which was collected, triturated with H_2O (2 × 15 mL) and methanol (10 mL), and air-dried. Yield: 1.89 g (92%). Anal. Calcd for $C_{36}H_{36}AlN_3O_9$: C, 63.43; H, 5.32; N, 6.16. Found: C, 63.47; H, 5.33; N, 6.24. ^{1}H NMR (DMSO-d_6): 1.77 (s, Me, 18H). *E*: 7.18, 7.22 (E3−4, 12H, *AB*), 8.81 (E2, 3H, d), 10.18 (E1, 3H, d). *Z*: 7.14, 7.61 (Z3−4, 12H, *AB*), 8.28 (Z2, 3H, s), 10.23 (Z1, 3H, s).

Fe(acphNHCHO)$_3$ (11). A solution of $Fe(NO_3)_3\cdot 9H_2O$ (3.43 g, 8.5 mmol) in 15 mL of H_2O was added to a solution of HacphNHCHO (6.65 g, 30.4 mmol) in 40 mL of CH_3OH with stirring. Then, $NaHCO_3$ (2.14 g, 25.5 mmol) in 25 mL of H_2O was added. A deep red precipitate formed, which was collected; washed with H_2O (2 × 15 mL), methanol (2 × 15 mL), and acetone (2 × 15 mL); and dried at 100 °C. Yield: 3.77 g (62%).

Cu(acphNHCHO)$_2$ (12). $Cu(OAc)_2\cdot H_2O$ (0.363 g, 1.82 mmol) in 7 mL of H_2O was added to a solution of HacphNHCHO

(0.92 g, 4.2 mmol) in 8 mL of methanol, with stirring. A blue-green precipitate formed, which was collected, washed with H_2O and methanol, and air-dried. Yield: 0.90 g (99%). Anal. Calcd for $C_{24}H_{24}CuN_2O_6$: C, 57.64; H, 4.84; N, 5.60. Found: C, 57.49; H, 4.63; N, 5.58. Crystals suitable for X-ray analysis were grown from DMSO/water.

***trans*-Zn(acphNHCHO)$_2$(H$_2$O)$_2$ (13).** Solutions of $Zn(OAc)_2 \cdot 2H_2O$ (0.11 g, 0.50 mmol, in 5 mL of H_2O) and HacphNHCHO (0.22 g, 1.00 mmol, in 3 mL of CH_3OH) were mixed. $NaHCO_3$ (0.08 g, 1.0 mmol) in 2 mL of H_2O was added to this mixture, and a yellow precipitate formed immediately. The precipitate was collected; washed with dichloromethane, H_2O, and diethyl ether; and dried at 70 °C overnight. Yield: 0.11 g (40%). This material contained both *E* and Z conformers of its formamide moieties, as judged by its ^{1}H NMR spectrum immediately after dissolving in DMSO-d_6: 1.65 (s, Me, 12H). *E*: 7.16, 7.19 (E3−4, 8H, *AB*), 8.81 (E2, 2H, d), 10.13 (E1, 2H, d). *Z*: 7.14, 7.58 (Z3−4, 8H, *AB*), 8.28 (Z2, 2H, s), 10.18 (Z1, 2H, s). Meanwhile, light yellow single crystals of [*trans*-$Zn(acphNHCHO)_2(H_2O)_2] \cdot 2H_2O$ (i.e., **13**$\cdot 2H_2O$, with *Z*-formamides) were obtained from the H_2O/methanol filtrate the next day; this material was suitable for X-ray analysis.

Al(acphNC)$_3$ (14). To a solution of $Al(acphNHCHO)_3$ (1.023 g, 1.50 mmol) and diisopropylamine (1.50 g, 14.8 mmol) in CH_2Cl_2 (50 mL) was added $POCl_3$ (0.690 g, 4.50 mmol) at room temperature under argon. After stirring for 1 h, the whole solution became clear. It was washed with 10% $NaHCO_3$ (20 mL), and the CH_2Cl_2 layer was separated and evaporated to 10−15 mL. Hexane was added to this solution to precipitate the powdery yellow product, which was dried at 70 °C. Yield: 0.710 g (75%). Anal. Calcd. for $C_{36}H_{30}AlN_3O_6$: C, 68.89; H, 4.82; N, 6.70. Found: C, 68.69; H, 4.81; N, 6.78. IR: 2121 cm^{-1}. ^{1}H NMR(250 MHz, $CDCl_3$): 1.87 (18H, s), 7.25, 7.41 (12H, *AB*). Single crystals of the hexane solvate of **14** suitable for X-ray diffraction were grown by vapor diffusion of hexane into a dichloromethane solution of the compound.

Fe(acphNC)$_3$ (15). To a mixture of $Fe(acphNHCHO)_3$ (2.65 g, 3.73 mmol) and diisopropylamine (5.56 g, 55.0 mmol) in CH_2Cl_2 (15 mL) was added $POCl_3$ (2.61 g, 17.0 mmol) at room temperature under argon and stirred for 2 h. The above solution was then washed with 10% $NaHCO_3$ (2 × 40 mL), and the CH_2Cl_2 layer was separated and evaporated to 5 mL. The addition of hexanes (100 mL) to this solution precipitated the powdery red product, which was collected, washed with 50 mL of hexanes, and dried at 70 °C. Yield: 2.20 g (90%). IR: 2126 cm^{-1}.

Cu(acphNC)$_2$ (16). To a mixture of $Cu(acphNHCHO)_2$ (**12**; 0.350 g, 0.70 mmol) and diisopropylamine (0.446 g, 4.4 mmol) in CH_2Cl_2 (20 mL) was added $POCl_3$ (0.220 g, 1.44 mmol) at room temperature under argon. The color slowly changed from blue to green. After stirring for 5 days, not all of the $Cu(acphNHCHO)_2$ had dissolved. The mixture was filtered and the filtrate washed with water (2 × 15 mL) and with 10% $NaHCO_3$(aq). When hexane was added to the dichloromethane phase, a brown gum separated. It could not be isolated in pure form, even after trituration with several solvents, but its IR spectrum showed $\nu_{C\equiv N} = 2147$ cm^{-1}.

Zn(acphNC)$_2$ (17). $Zn(acphNHCHO)_2 \cdot 2H_2O$ (0.163 g, 0.30 mmol) and $^i Pr_2NH$ (0.217 g, 2.15 mmol) were dissolved in dichloromethane (10 mL). $POCl_3$ (0.110 g, 0.72 mmol) was added slowly to the solution, with stirring. The whole solution became clear in 30 min. The solution was washed with 10 mL of 10% $NaHCO_3$(aq). The CH_2Cl_2 layer was separated, dried (Na_2SO_4), and evaporated to 10−15 mL, and hexane was added to precipitate the product as a yellow powder. Yield: 0.018 g (13%). IR: 2124 cm^{-1}. ^{1}H NMR (250 MHz, $CDCl_3$): 1.87 (12H, s), 7.23, 7.42 (8H, *AB*).

3-(4-Isocyanophenyl)pentane-2,4-dione (HacphNC, 1). The iron(III) isocyano-β-diketonate complex $Fe(acphNC)_3$ (**17**; 1.36 g, 2.07 mmol) was dissolved in 100 mL of dichloromethane. Oxalic acid ($H_2C_2O_4 \cdot 2H_2O$, 2.52 g, 20.0 mmol) and potassium oxalate ($K_2C_2O_4 \cdot H_2O$, 33.12 g, 180.0 mmol) were dissolved in 200 mL of distilled water. These two solutions were stirred together for 20 min, and the red color in the organic layer disappeared, indicating that the reaction was complete. The organic phase was then separated, and the aqueous layer was extracted with 50 mL of dichloromethane. The organic phases were combined, dried over Na_2SO_4, and evaporated to ca. 3 mL. This residue was chromatographed with ethyl acetate−hexane (1:1 v/v). Yield: 0.46 g (37%). Anal. Calcd for $C_{12}H_{11}NO_2$: C, 71.63; H, 5.51; N, 6.96. Found: C, 71.44; H, 5.36; N, 7.03. ^{1}H NMR (250 MHz, $CDCl_3$): 1.89 (6H, s), 7.23, 7.42 (4H, *AB*), 16.71 (1H, s). IR: 2122 cm^{-1}. Compound **1** decomposed at ca. 140 °C without melting. Crystals suitable for X-ray crystallography were grown by slow evaporation of a solution in ethyl acetate−hexane (1:2 v/v).

HacphNCAuCl (18). (Me_2S)AuCl (0.059 g, 0.20 mmol) and HacphNC (0.044 g, 0.22 mmol) were dissolved in $CHCl_3$ (3 mL) and refluxed for 1 h. The solution was evaporated at 45 °C to remove the solvent and Me_2S. The residue was dissolved in 0.6 mL of $CHCl_3$ and precipitated with 3 mL of hexanes. The precipitate was air-dried. Yield: 0.028 g (32%). ^{1}H NMR (250 MHz, $CDCl_3$): 1.88 (6H, s), 7.37, 7.60 (4H, *AB*), 16.75 (1H, s). IR: 2223 cm^{-1}. Crystals suitable for X-ray crystallography were grown from $CHCl_3$ by layering with hexanes.

Al(acphNCAuCl)$_3$ (19). $Al(acphNC)_3$ (**14**; 0.0314 g, 0.050 mmol) and (Me_2S)AuCl (0.0441 g, 0.150 mmol) were dissolved in 10 mL of CH_2Cl_2 and refluxed under nitrogen for 2 h. The solution was then evaporated to dryness. ^{1}H NMR (250 MHz, $CDCl_3$): 1.86 (18H, s), 7.34, 7.60 (12H, *AB*). IR: 2222 cm^{-1}.

Acknowledgment. We thank Drs. Frank R. Fronczek and Emily F. Maverick for assistance with the X-ray analyses. This work was supported by the Department of Energy (DE-FG02-01ER15267).

Supporting Information Available: X-ray data for compounds **1**, (*E*)- and (*Z*)-**2**, (*E*)-**6**, **9**, **12**, **13**$\cdot 2H_2O$, **14**$\cdot 0.58C_6H_{14}$, and **18**, in CIF format. This material is available free of charge via the Internet at http://pubs.acs.org.

Inorganic Chemistry

ARTICLE

pubs.acs.org/IC

Bis(*o*-phenylenebis(acetylacetonato))dicopper(II): A Strained Copper(II) Dimer Exhibiting a Wide Range of Colors in the Solid State

Chandi Pariya,*,† Frank R. Fronczek, and Andrew W. Maverick*

Department of Chemistry, Louisiana State University, Baton Rouge, Louisiana 70803, United States

Supporting Information

ABSTRACT: The bis(β-diketone) *o*-pbaH$_2$ (*o*-phenylenebis(acetylacetone), **1**) reacts readily with Cu^{2+}. Although this reaction was expected to yield a trimeric product (**2**) on geometric grounds, the binuclear complex Cu_2(*o*-pba)$_2$ (**3**) is obtained instead. Materials containing Cu_2(*o*-pba)$_2$ adopt a variety of colors, depending on the solvents used in preparation: dark green (microcrystalline, **3a**), golden-brown (ansolvous, **3b**), green-brown ($CHCl_3$—C_6H_6 solvate, **4**), dark blue (nitrobenzene solvate, **5**), or violet (toluene solvate, **6**). Complexes **5** and **6** contain 1D chains of Cu_2(*o*-pba)$_2$ molecules joined by weak Cu···O interactions. Crystalline adducts [Cu_2(*o*-pba)$_2$L]$_n$ (**7** and **8**) containing 1D polymeric chains are also obtained upon reaction of **3** with bridging ligands (L = 1,2-bis(4-pyridyl)ethane or 4,4′-bipyridine, respectively). All of the new metal complexes except for **3a** have been characterized by X-ray analysis.

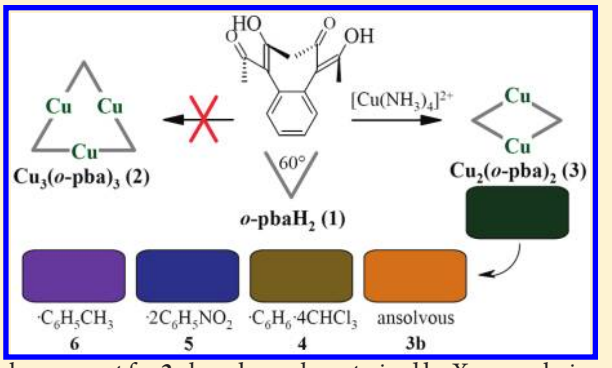

INTRODUCTION

Metal—organic supramolecules constructed from Cu^{2+} and organic linkers continue to be developed at a rapid rate owing to their diverse structures and range of applications.[1] Our group and others have been interested in using β-diketones as organic linkers.[2] We recently described the bis(β-diketone) *meta*-phenylenebis(acetylacetone) (*m*-pbaH$_2$), whose β-diketone moieties make an angle of 120°. Although this linker appeared to be well suited for the construction of a "molecular hexagon", Cu$_6$(*m*-pba)$_6$, we found no evidence for this product, obtaining instead the square Cu$_4$(*m*-pba)$_4$ in high yield (Scheme 1).[3]

We now report the chemistry of the ortho isomer, *o*-pbaH$_2$, with Cu^{2+}. On the basis of the ∼60° angle between the β-diketone moieties in *o*-pbaH$_2$, we expected a trinuclear product, Cu$_3$(*o*-pba)$_3$ (**2**). Other linkers with donor groups at 60° angles, and related multidentate ligands, have been used successfully to prepare trinuclear species.[4] However, the sole product in the Cu^{2+}—*o*-pba^{2-} reaction is the cyclic *dimer*, Cu$_2$(*o*-pba)$_2$ (**3**).

Other investigators have reported the formation of unexpectedly small cyclic metal—organic structures. For example, right-angle "corners" such as *cis*-disubstituted Pd(II) complexes usually react with a linear linker such as 4,4′-bpy to produce the square [Pd$_4$(4,4′-bpy)$_4$], but a number of examples of trinuclear products [Pd$_3$(4,4′-bpy)$_3$] have been observed.[5] The formation of a triangle instead of the expected square requires a distortion of ca. 30° at each metal ion, just like the formation of a square instead of the expected hexagon (as we saw in the formation of Cu$_4$(*m*-pba)$_4$[3]). In contrast, the amount of distortion required to assemble Cu$_2$(*o*-pba)$_2$ is twice as large, ca. 60° at each metal ion. In the present work, we show that this dimer forms solids of a variety of colors, ranging from blue to green to golden-brown, depending on the solvents used in preparation.

Scheme 1. Preparation of Supramolecular Cu Complexes from the Meta (a) and Ortho (b) Isomers of the Bis(β-diketone) pbaH$_2$

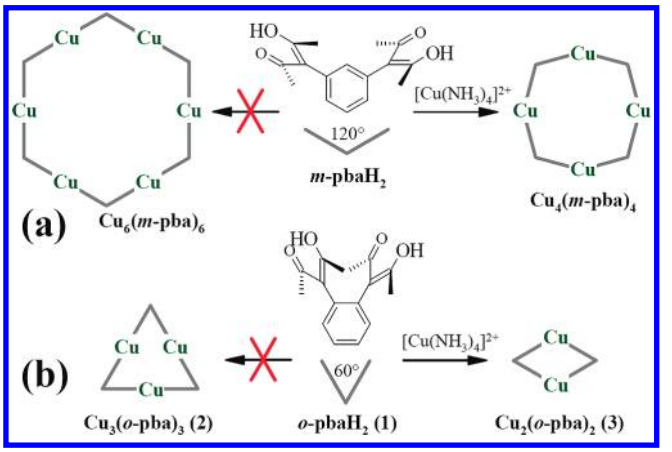

EXPERIMENTAL SECTION

All reagents were used as received. Elemental analyses were performed by M-H-W Laboratories, Phoenix, Arizona.

Received: August 12, 2010
Published: March 09, 2011

Table 1. X-Ray Crystallographic and Structure Refinement Data for 3b, 4−8

Compound	3b	4	5
empirical formula	$C_{32}H_{32}Cu_2O_8$	$C_{32}H_{32}Cu_2O_8 \cdot C_6H_6 \cdot 4CHCl_3$	$C_{32}H_{32}Cu_2O_8 \cdot 2C_6H_5NO_2$
fw	671.66	1227.24	917.88
cryst syst	triclinic	monoclinic	triclinic
space group	$P\bar{1}$ (No. 2)	$P2_1/n$ (No. 14)	$P\bar{1}$ (No. 2)
a, Å	7.5200(14)	11.7288(10)	7.7190(5)
b, Å	9.200(3)	20.790(2)	11.6921(9)
c, Å	10.728(3)	12.0788(11)	12.1682(10)
α, deg	90.484(13)	90	79.475(4)
β, deg	91.742(16)	119.005(4)	80.666(5)
γ, deg	105.265(16)	90	72.687(6)
V, Å^3	715.6(3)	2575.9(4)	1023.98(13)
Z	1	2	1
T, K	115	115	90
D_{calcd}, g cm^{-3}	1.559	1.582	1.488
cryst dimenions, mm	0.12 × 0.02 × 0.02	0.40 × 0.30 × 0.18	0.42 × 0.15 × 0.12
θ limits, deg	2.8 < θ < 25.1	2.7 < θ < 35.0	2.7 < θ < 36.4
reflns, measd/unique/obsd	9333/2423/1056	62001/10919/8596	33966/9553/8515
data/param	2423/194	10 919/294	9553/276
μ, mm^{-1}	1.538	1.496	1.106
R ($I > 2\sigma(I)$)	0.117	0.036	0.034
R_w (all data)	0.282	0.094	0.092
GOF	1.074	1.029	1.046
compound	6	7	8
empirical formula	$C_{32}H_{32}Cu_2O_8 \cdot C_7H_8$	$C_{32}H_{32}Cu_2O_8 \cdot C_{12}H_{12}N_2 \cdot 1.5C_7H_8$	$C_{32}H_{32}Cu_2O_8 \cdot C_{10}H_8N_2 \cdot C_7H_8$
fw	763.79	994.09	919.97
cryst syst	triclinic	triclinic	orthorhombic
space group	$P\bar{1}$ (No. 2)	$P\bar{1}$ (No. 2)	*Cmma* (No. 67)
a, Å	7.5492(10)	8.670(3)	20.978(9)
b, Å	11.4219(15)	11.963(5)	11.525(4)
c, Å	11.9423(15)	12.116(8)	16.980(6)
α, deg	116.990(6)	101.86(2)	90
β, deg	93.970(8)	110.69(2)	90
γ, deg	105.046(8)	101.23(2)	90
V, Å^3	864.94(19)	1100.4(9)	4105(3)
Z	1	1	4
T, K	115	115	115
D_{calcd}, g cm^{-3}	1.466	1.500	1.488
cryst dimensions, mm	0.43 × 0.10 × 0.02	0.20 × 0.15 × 0.05	0.45 × 0.08 × 0.07
θ limits, deg	2.8 < θ < 30.0	2.5 < θ < 24.3	3.0 < θ < 22.1
reflns, measd/unique/obsd	18674/5043/4420	19243/6513/4847	16670/1392/939
data/param	5043/245	6513/143	1392/158
μ, mm^{-1}	1.283	1.029	1.096
R ($I > 2\sigma(I)$)	0.032	0.123	0.097
R_w (all data)	0.079	0.350	0.286
GOF	1.057	1.341	1.589

Preparation of Compounds. *Cu_2(o-pba)$_2$ (**3a**).* $CuSO_4 \cdot 5H_2O$ (0.500 g, 2.00 mmol) was dissolved in 10 mL of H_2O and converted to $[Cu(NH_3)_4]SO_4$(aq) by the dropwise addition of conc. NH_3(aq). To this blue-violet solution, a solution of *o*-pbaH_2 (0.275 g, 1.00 mmol) in 20 mL of CH_2Cl_2 was added slowly, and the mixture was stirred for 6 h. CH_2Cl_2 (20 mL) was added, and the organic layer was separated, dried over $MgSO_4$, and evaporated to give a dark green powder. This residue was washed with hexane (2 × 10 mL) and dried in the air. Yield: 0.325 g (96%), mp > 210 °C. Anal. Calcd for $C_{32}H_{32}Cu_2O_8$: C, 57.22; H, 4.80. Found: C, 57.11; H, 4.93.

*Cu_2(o-pba)$_2$ (**3b**).* A solution of Cu_2(*o*-pba)$_2$ (**3a**, 0.050 g, 0.074 mmol) in 1.5 mL of $CHCl_3$ was layered with acetone. Small golden-brown crystals of **3b** were obtained after ca. 48 h. This product was collected and dried in the air. Yield: 0.039 g (78%). Anal. Calcd for $C_{32}H_{32}Cu_2O_8$: C, 57.22; H, 4.80. Found: C, 57.46; H, 4.56.

*Cu_2(o-pba)$_2 \cdot C_6H_6 \cdot 4CHCl_3$ (**4**).* A solution of Cu_2(*o*-pba)$_2$ (**3a**, 0.050 g) in 1.5 mL of $CHCl_3$ was layered with benzene. Green-brown dichroic crystals of **4** were obtained after ca. 72 h. Yield: 0.053 g (58%). These crystals slowly become opaque on standing, suggesting a loss of

dx.doi.org/10.1021/ic101641r |*Inorg. Chem.* 2011, 50, 2748–2753

solvent; microanalysis results were in agreement with the ansolvous material. Anal. Calcd for $Cu_2(o\text{-pba})_2$ ($C_{32}H_{32}Cu_2O_8$): C, 57.22; H, 4.80. Found: C, 57.12; H, 4.65.

$Cu_2(o\text{-pba})_2 \cdot 2C_6H_5NO_2$ (**5**). A solution of $Cu_2(o\text{-pba})_2$ (**3a**, 0.050 g) in 1.5 mL of $CHCl_3$ was layered with nitrobenzene. Dark blue crystals of **5** were obtained in ca. 4 days. This product was collected and dried in the air. Yield: 0.047 g (65%). Anal. Calcd for $C_{44}H_{42}Cu_2N_2O_{12}$: C, 57.57; H, 4.61, N, 3.05. Found: C, 57.48; H, 4.72; N, 3.11.

$Cu_2(o\text{-pba})_2 \cdot C_6H_5CH_3$ (**6**). A solution of $Cu_2(o\text{-pba})_2$ (**3a**, 0.050 g) in 1.5 mL of $CHCl_3$ was layered with toluene. Violet crystals of **6** were obtained in ca. 4 days. This product was collected and dried in the air. Yield: 0.042 g (74%). Anal. Calcd for $C_{39}H_{40}Cu_2O_8$: C, 61.32; H, 5.29. Found: C, 61.50; H, 5.50.

Coordination Polymers of $Cu_2(o\text{-pba})_2$. *$[Cu_2(o\text{-pba})_2(dpea)] \cdot 1.5C_6H_5CH_3$* (**7**). A solution of $Cu_2(o\text{-pba})_2$ (**3a**, 0.025 g, 0.037 mmol) in 1.0 mL of $CHCl_3$ turned bluish-green when 1,2-bis(4-pyridyl)ethane (dpea; 0.010 g, 0.054 mmol, in 0.5 mL $CHCl_3$) was added; the resulting mixture was layered with toluene. Bluish-green crystals of **7** were obtained in 2 days. These crystals slowly become opaque on standing, suggesting a loss of solvent; microanalysis results were in agreement with the ansolvous material. Yield: 0.026 g (82%). Anal. Calcd for $Cu_2(o\text{-pba})_2(dpea)$ ($C_{44}H_{44}N_2Cu_2O_8$): C, 61.69; H, 5.18, N, 3.27. Found: C, 61.99; H, 5.23; N, 3.43.

$[Cu_2(o\text{-pba})_2(4,4'\text{-bpy})] \cdot C_6H_5CH_3$ (**8**). A solution of $Cu_2(o\text{-pba})_2$ (**3a**, 0.025 g, 0.037 mmol) in 1.0 mL of $CHCl_3$ turned bluish-green when 4,4′-bipyridine (0.009 g, 0.058 mmol, in 0.5 mL $CHCl_3$) was added; the resulting mixture was layered with toluene. Bluish-green crystals of **8** were obtained in 2 days. These crystals slowly become opaque on standing, suggesting a loss of solvent; microanalysis results were in agreement with the ansolvous material. Yield: 0.027 g (88%). Anal. Calcd for $Cu_2(o\text{-pba})_2(4,4'\text{-bpy})$ ($C_{42}H_{40}N_2Cu_2O_8$): C, 60.88; H, 4.87, N, 3.38. Found: C, 60.75; H, 4.90; N, 3.44.

X-Ray Structure Determinations. Intensity data were collected at low temperatures on a Nonius KappaCCD diffractometer equipped with an Oxford Cryosystems Cryostream sample cooler and a graphite monochromated Mo Kα X-ray source (λ = 0.71073 Å). Data were corrected for absorption using the multiscan method using DENZO and SCALEPACK.[6] Structures were solved by direct methods using SIR[7] and refined on F^2 using SHELXL.[8] Crystal quality for **4**, **5**, and **6** was excellent, less so for **3b**, **7**, and **8**. The toluene solvent in **6** was disordered about an inversion center. The toluene solvent in **8** was also disordered into two orientations, and a common isotropic displacement parameter was refined for its C atoms. Contribution from disordered solvent in **7**, assumed to be toluene, was removed using SQUEEZE.[9] For **7**, only Cu and O were treated as anisotropic. For all structures, hydrogen atoms were frequently visible in difference maps but were placed in idealized positions, and torsional parameters were refined for methyl groups. Crystal data and refinement details are given in Table 1.

Powder diffraction data were collected by using a Bruker D8 Advance instrument.

RESULTS AND DISCUSSION

The bis(β-diketone) *o*-pbaH$_2$ was synthesized according to the literature procedure[10] and converted to dark green $Cu_2(o\text{-pba})_2$ (**3**) in a CH_2Cl_2 solution by treatment with $[Cu(NH_3)_4]^{2+}$ (aq). The transformations of **3** are illustrated in Scheme 2. The initial product is a dark green powder (**3a**) which dissolves readily in $CHCl_3$ or CH_2Cl_2 but not in most other solvents. For example, **3a** dissolves in acetone to give a green solution, but this solution deposits a golden-brown powder within a few seconds. Slow evaporation of a $CHCl_3$/acetone solution yields crystalline golden-brown $Cu_2(o\text{-pba})_2$ (**3b**; Figure 1) over a period of several days. Complex **3a** is microcrystalline, as determined by powder X-ray diffraction,

Scheme 2. Transformations of $Cu_2(o\text{-pba})_2$

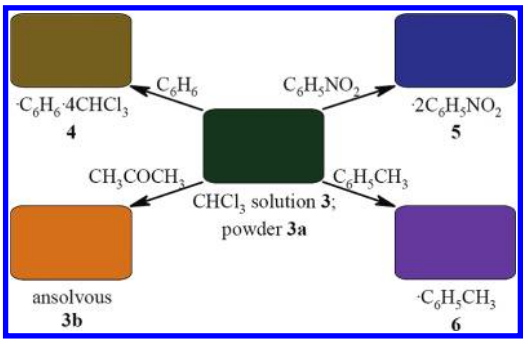

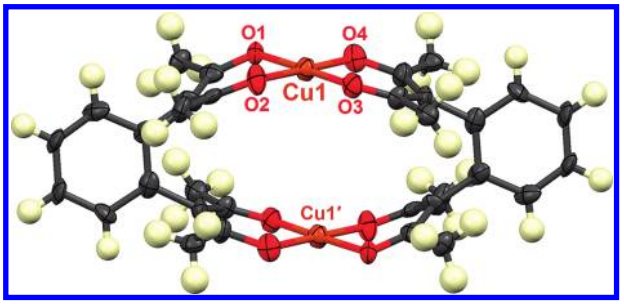

Figure 1. Crystal structure of $Cu_2(o\text{-pba})_2$ (**3b**) (Cu1···Cu1′ = 4.551(2) Å), with 50% ellipsoids for non-hydrogen atoms.

and its diffraction pattern is quite different from that of **3b** (see Figure S1, Supporting Information).

The other crystalline materials described here were all prepared from $CHCl_3$ solutions of **3** by layering and have been characterized by X-ray analysis: with benzene, green-brown $Cu_2(o\text{-pba})_2 \cdot C_6H_6 \cdot 4CHCl_3$ (**4**; Figure 2); with nitrobenzene, dark blue $Cu_2(o\text{-pba})_2 \cdot 2C_6H_5NO_2$ (**5**; Figure 3); with toluene, violet $Cu_2(o\text{-pba})_2 \cdot C_6H_5CH_3$ (**6**; Figure 4). All of the crystalline materials (**3b**, **4**, **5**, and **6**) dissolve in $CHCl_3$ or CH_2Cl_2 to give green solutions which are indistinguishable from those prepared using **3a**. (Complex **3b** dissolves less readily than the other materials; this may be for thermodynamic reasons, as suggested by the fact that solid **3a** spontaneously converts to solid **3b** in solvents such as acetone.)

Compounds **3a** and **3b** have the same composition but different colors. The absorption spectrum of dark green solid **3a** is nearly identical to that of its $CHCl_3$ solution, as illustrated by the spectra in Figure 5 (for the solid) and in Figure S2 (for the solution), with maxima at 690−700 and 580−590 nm and a rising absorbance below 500 nm. (The spectra in Figure 5 were recorded for Nujol mulls of the solids, because their solutions are all dark green.) These spectra are similar to those of Cu complexes of other 3-substituted acetylacetonates (d−d bands above 500 nm, and CT and intraligand transitions at shorter wavelengths), suggesting that **3a** contains isolated molecules.

Ansolvous crystalline **3b**, on the other hand, is golden-brown, with intense absorption at shorter wavelengths in addition to the features in the 550−700 nm region. The CuO_4 coordination environment in **3b** is nearly planar (the Cu atom is 0.005 Å from the O_4 plane), and the CuO_4 and two crystallographically independent β-diketonate planes make angles of 15.9° and 30.3° with the CuO_4 coordination plane.

dx.doi.org/10.1021/ic101641r |*Inorg. Chem.* 2011, 50, 2748–2753

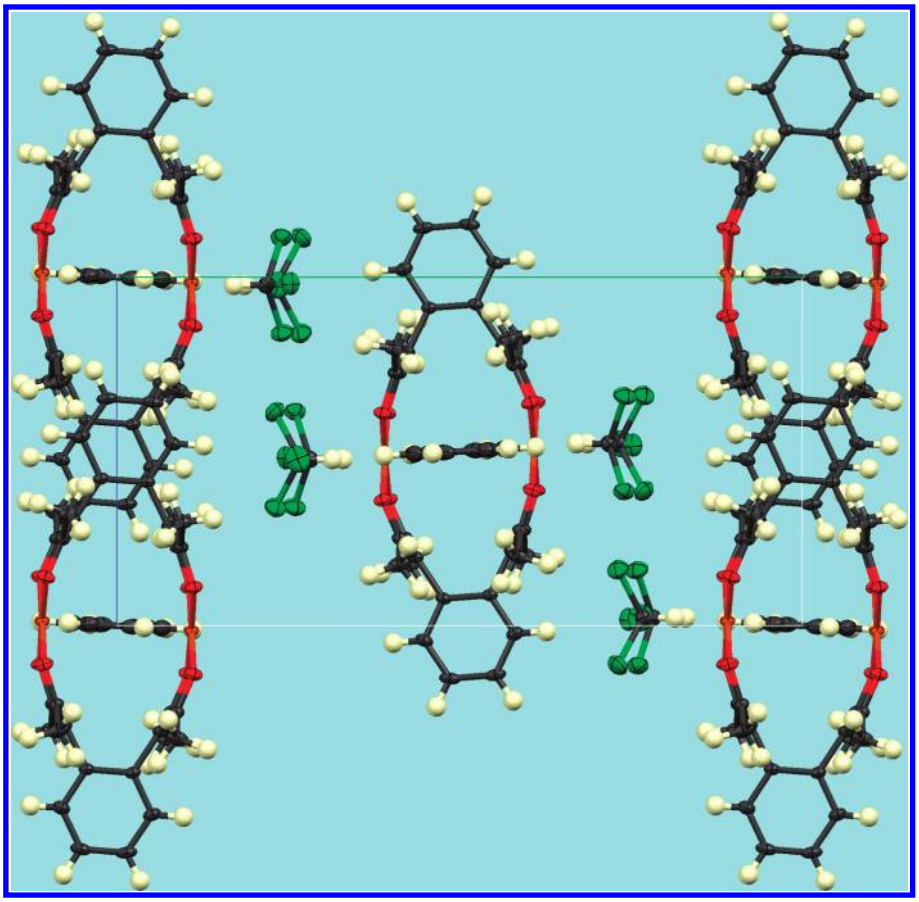

Figure 2. Crystal structure of $Cu_2(o\text{-pba})_2 \cdot C_6H_6 \cdot 4CHCl_3$ (**4**; Cu1···Cu1′ 4.5482(5) Å), showing one unit cell, viewed along the crystallographic *a* direction; *b* is horizontal (50% ellipsoids for non-hydrogen atoms).

The $C_6H_6-CHCl_3$ solvate **4** is green-brown, and individual crystals frequently show a well-developed dichroic face, with green and brown colors in polarized light (Figure 6). These green and brown colors are similar to those of **3a** and **3b**, respectively. We could not obtain spectra of this material in the two polarizations for a more quantitative comparison, owing to a rapid loss of solvent from the crystals. X-ray analysis of **4** (Figure 2) reveals molecules that are almost identical to those in **3b** (Cu···Cu = 4.5482(5) Å; Cu atom 0.012 Å from O_4 plane; 26.0° and 20.7° between the CuO_4 and β-diketonate planes). The Bruker Apex2 face-indexing software[11] identified the prominent face in crystals of **4** as (100), as illustrated in Figure 7. The location of the *b* axis enabled us to assign the polarizations in Figure 6.

The brown colors in **3b** and **4** are similar, but their cause remains puzzling. We considered the severe structural distortions that occur in the $Cu_2(o\text{-pba})_2$ molecules as a possible cause for the unusual colors. If **3a** contained polymeric $[Cu(o\text{-pba})]_n$, for example, it might be unstrained and show the "normal" dark green color. However, this is unlikely, because it would require that the polymer and dimer interconvert rapidly as the solids are dissolved and precipitated. Such an interconversion could only occur by dissociation of the chelating ligands, which is unfavorable in nonpolar solvents. Also, **3a** and **3b** interconvert to some extent even in the solid state: dark green **3a** slowly turns brownish-green on standing, and grinding golden-brown crystalline **3b** gives it a slight green color. Thus, **3a**, like **3b**, consists of discrete $Cu_2(o\text{-pba})_2$ molecules.

The orientation of the molecules in crystals of **4** is shown in Figure 2. The $Cu_2(o\text{-pba})_2$ molecules are aligned so that their

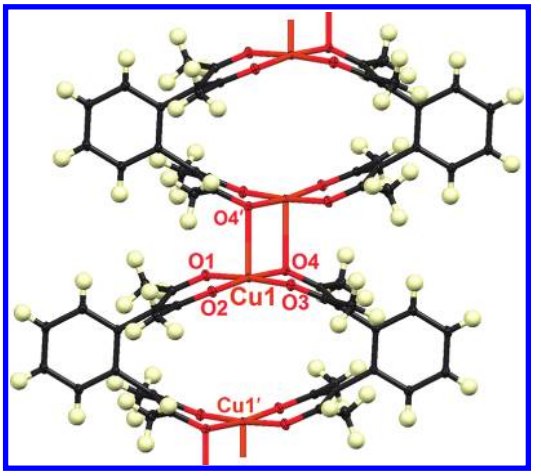

Figure 3. Crystal structure of $Cu_2(o\text{-pba})_2 \cdot 2C_6H_5NO_2$ (**5**), showing a portion of the 1D chain of $Cu_2(o\text{-pba})_2$ units: Cu1···Cu1′ = 4.9636(4) Å; Cu1···O4′ = 2.422(1) Å. Solvent molecules omitted for clarity; 50% ellipsoids for non-hydrogen atoms.

Cu···Cu vectors are almost exactly along the *b* axis. The intense brown color in the micrographs in Figure 6 appears only in polarization perpendicular to *b*. This information limits the transitions that could be responsible: the intensity of the color suggests a charge-transfer assignment, and LMCT transitions originating in the π system of the β-diketonate ligands are possible. These transitions normally lie in the ultraviolet region.

dx.doi.org/10.1021/ic101641r |*Inorg. Chem.* 2011, 50, 2748–2753

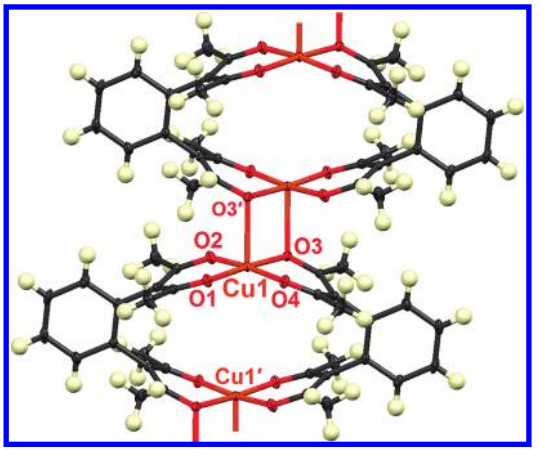

Figure 4. Crystal structure of $Cu_2(o\text{-pba})_2 \cdot C_6H_5CH_3$ (**6**), showing a portion of the 1D chain of $Cu_2(o\text{-pba})_2$ units: Cu1···Cu1′ = 4.7575(7), Cu1···O3′ = 2.443(1) Å. Solvent molecules omitted for clarity; 50% ellipsoids for non-hydrogen atoms.

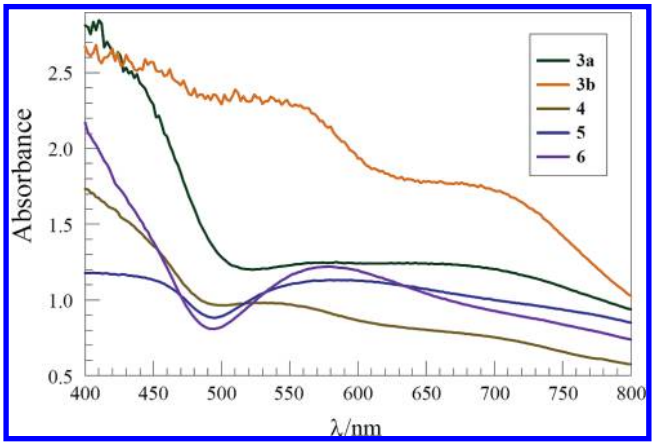

Figure 5. Absorption spectra of the five forms of $Cu_2(o\text{-pba})_2$ (**3a**, **3b**, **4**, **5**, and **6**) in the solid state, recorded as Nujol mulls.

The β-diketonates in $Cu_2(o\text{-pba})_2$ are noticeably distorted from planarity, and this distortion could lead to a red-shift in the LMCT transition(s) and the observed brown color. However, the structure of the $Cu_2(o\text{-pba})_2$ unit is almost identical in all of the crystalline solids studied here, so we would expect to see similar intense transitions in the other materials as well; but only **3b** and **4** show them. Intermolecular interactions in **3b** and **4** could produce the brown color, but no unusual interactions were apparent in their crystal structures.[12] Thus, we do not have a complete explanation of the origin of the brown color.

The solvated compounds **5** and **6** both contain separate one-dimensional stacks of $Cu_2(o\text{-pba})_2$ molecules and solvent molecules. In the $Cu_2(o\text{-pba})_2$ stacks, adjacent molecules make close approaches, with intermolecular Cu···O distances of 2.422(1) Å (in **5**; Figure 3) and 2.443(1) Å (in **6**; Figure 4). This close approach leads to pyramidal distortions and effective five-coordination at the Cu atoms. The dark blue and violet colors of **5** and **6**, respectively, and their spectra in Figure 5 are consistent with the change to five-coordination.

Solutions of $Cu_2(o\text{-pba})_2$ turn greenish-blue on reaction with nitrogen-donor ligands, as expected for the formation of 5-coordinate adducts at Cu. We have crystallized two such adducts,

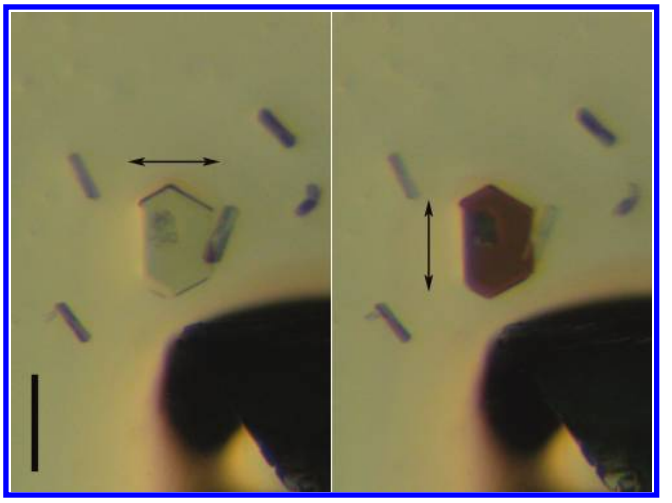

Figure 6. Photographs of the (100) face of a crystal of $Cu_2(o\text{-pba})_2 \cdot C_6H_6 \cdot 4CHCl_3$ (**4**) in polarized light. Left, horizontal polarization (parallel to *b*); right, vertical (perpendicular to *b*). Scale bar (black bar on left) = 0.25 mm. [This view is slightly different from that in Figure 2, which is along the *a* axis. However, *b* is still horizontal, and the vertical direction is approximately along *c*.]

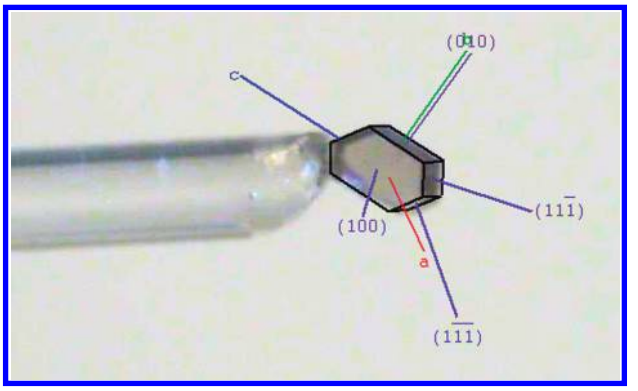

Figure 7. Face indexing performed for a crystal of $Cu_2(o\text{-pba})_2 \cdot C_6H_6 \cdot 4CHCl_3$ (**4**).

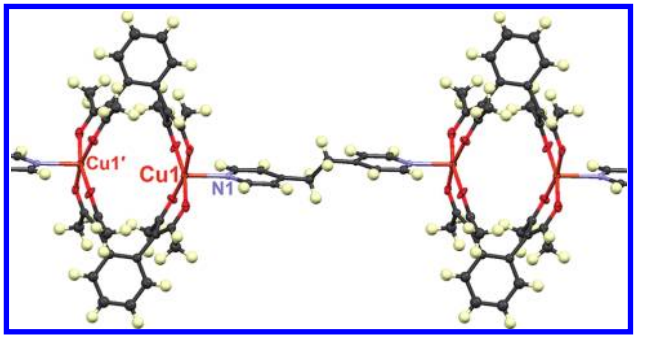

Figure 8. Crystal structure of $Cu_2(o\text{-pba})_2L \cdot 1.5C_6H_5CH_3$ (**7**; L = 1,2-bis(4-pyridyl)ethane), showing a portion of the 1D polymeric chain of $Cu_2(o\text{-pba})_2L$ units: Cu1···Cu1′ = 5.287(1) Å; Cu1···N1 = 2.292(6) Å (50% ellipsoids for non-hydrogen atoms).

with 1,2-bis(4-pyridyl)ethane (**7**, Figure 8) and 4,4′-bipyridine (**8**, Figure 9), both of which are 1-D coordination polymers.

Binding of adjacent O or N atoms to $Cu_2(o\text{-pba})_2$ leads to pyramidal environments about Cu and increased Cu···Cu distances: 4.9636(4), 4.7575(7), 5.287(1), and 5.318(3) Å in

dx.doi.org/10.1021/ic101641r |*Inorg. Chem.* 2011, 50, 2748–2753

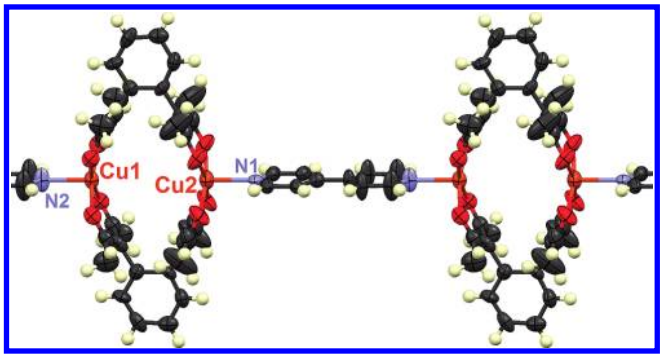

Figure 9. Crystal structure of $Cu_2(o\text{-pba})_2L\cdot 1.5C_6H_5CH_3$ (**8**; L = 4,4′-bipyridine), showing a portion of the 1D polymeric chain of $Cu_2(o\text{-pba})_2L$ units: Cu1···Cu2 = 5.318(3) Å (50% ellipsoids for non-hydrogen atoms).

5, **6**, **7**, and **8**, respectively. The greater elongation in **7** and **8** is also accompanied by greater displacements of the Cu atoms away from the O4 planes (0.096, 0.087, 0.194, and 0.179 and 0.217 Å in **5**, **6**, **7**, and **8**, respectively); both of these trends reflect the stronger coordination of N donors to the Cu centers. Formation of square pyramidal adducts may be favored in the $Cu_2(o\text{-pba})_2$ system, because the orientation of the β-diketone moieties is more compatible with pyramidal geometry at the Cu atom than with planar geometry.

CONCLUSIONS

The reaction of the bis(β-diketone) *o*-pbaH$_2$ with Cu^{2+} yields the cyclic dimer $Cu_2(o\text{-pba})_2$, rather than the trimer that was expected on the basis of ligand geometry. This reaction proceeds in high yield despite the severe distortion required in the product; the distortion occurs primarily in the dihedral angles between the β-diketonate and CuO_4 planes. $Cu_2(o\text{-pba})_2$ forms solids with a wide range of colors, depending on the solvents used in preparation, and it also binds to bidentate N donors to give 1-D coordination polymers.

ASSOCIATED CONTENT

Supporting Information. Powder X-ray diffraction results for **3a** and **3b** (Figure S1). Absorption spectrum of **3** in solution (Figure S2). X-ray crystallographic data for **3b**, **4**, **5**, **6**, **7**, and **8**, in CIF format. This material is available free of charge via the Internet at http://pubs.acs.org.

AUTHOR INFORMATION

Corresponding Author

*E-mail: cpariya@cas.org (C.P.); maverick@lsu.edu (A.W.M.).

Present Address

[†]Synthetic and Polymer Chemistry, CAS, a division of the American Chemical Society, 2540 Olentangy River Road, Columbus, Ohio 43202, United States

ACKNOWLEDGMENT

Acknowledgment is made to the U.S. Department of Energy (Grant DE-FG02-01ER15267) for support of this work. We thank Gregory McCandless and Dr. Julia Chan for assistance with the powder X-ray diffraction experiments.

REFERENCES

(1) (a) Ma, L.; Mihalcik, D. J.; Lin, W. *J. Am. Chem. Soc.* **2009**, *131*, 4610. (b) Yan, Y.; Lin, X.; Yang, S. H.; Blake, A. J.; Dailly, A.; Champness, N. R.; Hubberstey, P.; Schröder, M. *Chem. Commun.* **2009**, 1025. (c) Prakash, M. J.; Zou, Y.; Hong, S.; Park, M.; Bui, M. P. N.; Seong, G. H.; Lah, M. S. *Inorg. Chem.* **2009**, *48*, 1281. (d) Tranchemontagne, D. J.; Ni, Z.; O'Keeffe, M.; Yaghi, O. M. *Angew. Chem., Int. Ed.* **2008**, *47*, 5136. (e) Jung, M.; Kim, H.; Baek, K.; Kim, K. *Angew. Chem., Int. Ed.* **2008**, *47*, 5755. (f) Furukawa, H.; Kim, J.; Ockwig, N. W.; O'Keeffe, M.; Yaghi, O. M. *J. Am. Chem. Soc.* **2008**, *130*, 11650. (g) Hamilton, T. D.; Papaefstathiou, G. S.; Friščič, T.; Bučar, D. K.; MacGillivray, L. R. *J. Am. Chem. Soc.* **2008**, *130*, 14366. (h) Dalgarno, S. J.; Power, N. P.; Atwood, J. L. *Coord. Chem. Rev.* **2008**, *252*, 825. (i) Larsen, R. W. *J. Am. Chem. Soc.* **2008**, *130*, 11246. (j) Park, J.; Hong, S.; Moon, D.; Park, M.; Lee, K.; Kang, S.; Zou, Y.; John, R. P.; Kim, G. H.; Lah, M. S. *Inorg. Chem.* **2007**, *46*, 10208. (k) Perry, J. J.; Kravtsov, V. C.; McManus, G. J.; Zaworotko, M. J. *J. Am. Chem. Soc.* **2007**, *129*, 10076. (l) Hamilton, T. D.; Papaefstathiou, G. S.; MacGillivray, L. R. *J. Solid State Chem.* **2005**, *178*, 2409. (m) Hamilton, T. D.; MacGillivray, L. R. *Cryst. Growth Des.* **2004**, *4*, 419. (n) Eddaoudi, M.; Kim, J.; Wachter, J. B.; Chae, H. K.; O'Keeffe, M.; Yaghi, O. M. *J. Am. Chem. Soc.* **2001**, *123*, 4368.

(2) (a) Bray, D. J.; Antonioli, B.; Clegg, J. K.; Gloe, K.; Jolliffe, K. A.; Lindoy, L. F.; Wei, G.; Wenzel, M. *Dalton Trans.* **2008**, 1683. (b) Clegg, J. K.; Bray, D. J.; Gloe, K.; Hayter, M. J.; Jolliffe, K. A.; Lawrance, G. A.; Meehan, G. V.; McMurtrie, J. C.; Lindoy, L. F.; Wenzel, M. *Dalton Trans.* **2007**, 1719. (c) Chen, B.; Fronczek, F. R.; Maverick, A. W. *Inorg. Chem.* **2004**, *43*, 8209. (d) Benites, M. R.; Fronczek, F. R.; Hammer, R. P.; Maverick, A. W. *Inorg. Chem.* **1997**, *36*, 5826. (e) Wrobleski, D. A.; Rauchfuss, T. B. *J. Am. Chem. Soc.* **1982**, *104*, 2314.

(3) Pariya, C.; Sparrow, C. R.; Back, C. K.; Sandí, G.; Fronczek, F. R.; Maverick, A. W. *Angew. Chem., Int. Ed.* **2007**, *46*, 6305.

(4) (a) Zangrando, E.; Casanova, M.; Alessio, E. *Chem. Rev.* **2008**, *108*, 4979. (b) Bar, A. K.; Chakrabarty, R.; Mukherjee, P. S. *Inorg. Chem.* **2009**, *48*, 10880. (c) Willison, S. A.; Krause, J. A.; Connick, W. B. *Inorg. Chem.* **2008**, *47*, 1258. (d) Derossi, S.; Casanova, M.; Iengo, E.; Zangrando, E.; Stener, M.; Alessio, E. *Inorg. Chem.* **2007**, *46*, 11243. (e) Ghosh, S.; Turner, D. R.; Batten, S. R.; Mukherjee, P. S. *Dalton Trans.* **2007**, 1869. (f) Chand, D. K.; Biradha, K.; Kawano, M.; Sakamoto, S.; Yamaguchi, K.; Fujita, M. *Chem. Asian J.* **2006**, *1*, 82. (g) Qin, Z.; Jennings, M. C.; Puddephatt, R. *J. Inorg. Chem.* **2002**, *41*, 3967. (h) Sun, S. S.; Lees, A. *J. Inorg. Chem.* **1999**, *38*, 4181. (i) Schnebeck, R. D.; Randaccio, L.; Zangrando, E.; Lippert, B. *Angew. Chem., Int. Ed.* **1998**, *37*, 119.

(5) (a) Uehara, K.; Kasai, K.; Mizuno, N. *Inorg. Chem.* **2007**, *46*, 2563. (b) Cotton, F. A.; Murillo, C. A.; Yu, R. M. *Dalton Trans.* **2006**, 3900. (c) Schweiger, M.; Seidel, S. R.; Arif, A. M.; Stang, P. *J. Inorg. Chem.* **2002**, *41*, 2556. (d) Sautter, A.; Schmid, D. G.; Jung, G.; Würthner, F. *J. Am. Chem. Soc.* **2001**, *123*, 5424.

(6) Otwinowski, Z.; Minor, W. *Methods Enzymol.* **1997**, *276*, 307.

(7) Altomare, A.; Burla, M. C.; Camalli, M.; Cascarano, G. L.; Giacovazzo, C.; Guagliardi, A.; Moliterni, A. G. G.; Polidori, G.; Spagna, R. *J. Appl. Crystallogr.* **1999**, *32*, 115.

(8) Sheldrick, G. M. *Acta Crystallogr., Sect. A* **2008**, *64*, 112.

(9) Spek, A. L. *Acta Crystallogr. Sect. D* **2009**, *65*, 148.

(10) Ramirez, F.; Bhatia, S. B.; Patwardhan, A. V.; Smith, C. P. *J. Org. Chem.* **1967**, *32*, 3547.

(11) *APEX2*; Bruker AXS Inc.: Madison, WI, 2006.

(12) The crystal structures were determined on the basis of low-temperature data, while the color observations and spectral measurements were performed at room temperature. However, we saw no evidence for phase changes upon cooling the crystals for data collection. Thus, we believe the low-temperature structures give good indications of the presence or absence of intermolecular interactions in the solids at room temperature.